UNIQUE APPLICATIONS OF CULTURED NEURONAL NETWORKS IN PHARMACOLOGY, TOXICOLOGY, AND BASIC NEUROSCIENCE

Edward W. Keefer III, B.S., M.S.

Dissertation Prepared for the Degree of

DOCTOR OF PHILOSOPHY

UNIVERSITY OF NORTH TEXAS

May 2001

APPROVED:

Guenter W. Gross, Major Professor
Warren W. Burggren, Committee Member
Kent D. Chapman, Committee Member
Jannon L. Fuchs, Committee Member
Harris D. Schwark, Committee Member
Earl Zimmerman, Chair of the Department of Biological Sciences
C. Neal Tate, Dean of the Robert B. Toulouse School of Graduate Studies

Keefer, Edward W. III, Unique applications of cultured neuronal networks in pharmacology, toxicology, and basic neuroscience. Doctor of Philosophy (Biology), May 2001, 140 pp., 3 tables, 27 illustrations, references, 111 titles.

This dissertation research explored the capabilities of neuronal networks grown on substrate integrated microelectrode arrays *in vitro* with emphasis on utilizing such preparations in three specific application domains: pharmacology and drug development, biosensors and neurotoxicology, and the study of burst and synaptic mechanisms. Chapter 1 details the testing of seven novel AChE inhibitors, demonstrating that neuronal networks rapidly detect small molecular differences in closely related compounds, and reveal information about their probable physiological effects that are not attainable through biochemical characterization alone. Chapter 2 shows how neuronal networks may be used to classify and characterize an unknown compound. The compound, trimethylol propane phosphate (TMPP) elicited changes in network activity that resembled those induced by bicuculline, a known epileptogenic. Further work determined that TMPP produces its effects on network activity through a competitive inhibition of the $GABA_A$ receptor. This demonstrates that neuronal networks can provide rapid, reliable warning of the presence of toxic substances, and from the manner in which the spontaneous activity changes provide information on the class of compound present and its potential physiological effects. Additional simple pharmacological tests can provide valuable information on primary mechanisms involved in the altered neuronal network responses.

Chapter 3 explores the effects produced by a radical simplification of synaptic driving forces. With all synaptic interactions pharmacologically limited to those mediated through the NMDA synapse, spinal cord networks exhibited an extremely regular burst oscillation characterized by a period of 2.9 ± 0.3 s, with mean coefficients of variation of 3.7, 4.7, and 4.9 % for burst rate, burst duration, and inter-burst interval, respectively (16 separate cultures). The reliability of expression of this oscillation suggests that it may represent a fundamental mechanism of importance during periods of NMDA receptor dominated activity, such as embryonic and early postnatal development. NMDA synapse mediated activity produces a precise oscillatory state that allows the study of excitatory-coupled network dynamics, burst mechanisms, emergent network properties, and structure-function relationships.

“*Mine is the first step and therefore a small one, though worked out with much thought and hard labor. You, my readers or hearers of my lectures, if you think I have done as much as can fairly be expected of an initial start. … will acknowledge what I have achieved and will pardon what I have left for others to accomplish"*

Aristotle of Stagirus

"*What I see in Nature is a magnificent structure that we can comprehend only very imperfectly, and that must fill a thinking person with a feeling of "humility." This is a genuinely religious feeling that has nothing to do with mysticism"*

Albert Einstein

“*Nothing tends so much to the advancement of knowledge as the application of a new instrument. The native intellectual powers of men in different times are not so much the causes of the different success of their labours, as the peculiar nature of the means and artificial resources in their possession."*

Sir Humphrey Davy

ACKNOWLEDGMENTS

I thank the following individuals for their valued participation and contributions to the chapters indicated.

CHAPTER 1

Scott J. Norton , Department of Biological Sciences, University of North Texas, Denton, Texas
Nicholas A.J. Boyle, Department of Chemistry, University of Sheffield, Sheffield, UK
Vincenzo Talesa, Department of Experimental Medicine and Biochemical Sciences, University of Perugia, Perugia, IT
Guenter W. Gross, Department of Biological Sciences, University of North Texas, Denton, Texas

CHAPTER 2

Alexandra Gramowski, Institute for Cell Technology, University of Rostock, GR
David A. Stenger, Center for Bio/Molecular Science and Engineering, Naval Research Laboratory, Washington, D.C.
Joseph J. Pancrazio, Center for Bio/Molecular Science and Engineering, Naval Research Laboratory, Washington, D.C.
Guenter W. Gross, Department of Biological Sciences, University of North Texas, Denton, Texas

CHAPTER 3

Alexandra Gramowski, Institute for Cell Technology, University of Rostock, GR
Guenter W. Gross, Department of Biological Sciences and Center for Network Neuroscience, University of North Texas, Denton TX

Financial support was provided by the DARPA Tissue Based Biosensor Program (TBBS), the Nannie Hogan-Boyd Trust for Mental Retardation, and the Charles Bowen endowment to the CNNS.

TABLE OF CONTENTS

LIST OF TABLES

LIST OF ILLUSTRATIONS

OVERVIEW

Growing interest in acute and chronic effects of environmental toxins, increasing awareness of the threats posed by chemical or biological terrorism, and the accelerating pace of drug discovery require the development of new tools for rapid detection and prediction of the effects of a wide range of molecular species. For example, current technologies relying on antibody, electrochemical, mass spectrometry, or nucleic acid recognition offer highly sensitive and specific detection of many compounds. The disadvantages of many of these systems lie in their very specificity. They are exquisitely sensitive for compounds they are tuned to detect, for example, antibody detection of 5-10 ng/ml of botulinum toxoid can be rapidly accomplished (Emanuel et al., 2000). However, compounds not matched to the recognition pocket in these assays are invisible. Additionally, detection of a particular compound by these methods provides no information on the potential physiological consequences of exposure to the detected agent. A toxin epitope may be recognized by an antibody-based detector, but be physiologically inactive because of prior exposure to denaturing conditions. In the development of new drugs, a novel compound may be completely characterized biochemically, but may possess secondary effects in a physiological assay that renders it unsuitable for clinical applications. Thus, a system is needed that can provide rapid, broad-spectrum, yet sensitive, detection of environmental and novel compounds with information on the physiological consequences of exposure.

Cultured neuronal networks possess these capabilities. When coupled to circuitry to enabling transduction of extracellular electrical activity, these networks provide a tissue-based sensor that responds to a wide variety of compounds (Gross, 1994; Gross et al., 1992, 1995, 1997a,b). The advantages of neuronal networks, compared systems such as the antibody based ones discussed in the previous paragraph, lie both in the ability to detect unexpected compounds and generate meaningful physiological information on the effects of those compounds.

One proposed use of cultured neuronal networks is as a tissue-based biosensor for both military and civilian applications (Gross et al., 1995, Gross et al., 1992). A tissue-based biosensor may be defined as a device that monitors changes in the physiological activity of living cells caused by exposure to environmental perturbations. The state-of-the art in portable tissue-based biosensors that can be transported outside of a laboratory environment remains, as it has for at least one hundred years, the canary in a cage. Canaries were used in the 18^{th} and 19^{th} centuries to detect methane gas in coal mines. They were the detector of choice in 1995 for Japanese police, who employed the birds in their raid of the Aum Shin Rikyo sect, members of which carried out a Sarin nerve gas attack on the Tokyo subway system. Other live animals, such as chickens, fish, and clams are used today to detect agents such as encephalitis viruses and water contaminates.

Tissue-based biosensors utilizing cultured cells instead of whole animals offer several advantages, including the ability to automate the monitoring process and a reduction in the numbers of animals required for sensing elements. Most important,

tissue-based systems utilizing mammalian cell sources can yield physiologically relevant data on the nature of a detected threat, which may be extrapolated to the anticipated effect should a human be exposed. Several research programs designed to develop tissue-based biosensors for military and civilian use, have been created. These include the current Defense Advanced Research Projects Agency (DARPA) Tissue-Based Biosensor program. Numerous cell types, including bacteria, algae, lymphocytes, hepatocytes, chromatophores, alveolar macrophages, cardiomyocytes, and neurons have been tested as substrates for biosensors under the aegis of the DARPA program.

Neurons are particularly attractive biosensor elements, as they combine an array of cell-surface receptors, which have been evolutionarily selected to respond to a broad spectrum of diverse substances, with an electrically excitable membrane. Thus, real-time information may be obtained on the consequences of receptor activation or interference with the mechanisms maintaining the neuronal membrane potential. Cultured neuronal networks grown on substrate-integrated thin-film micro-electrode arrays (MEAs) (Gross, 1979), take advantage of these characteristics. Additionally, by utilizing networks of neurons instead of single cells, the actions of unknown compounds may be interpreted in the context of physiologically behaving systems, and may provide redundancy in the detection mechanism.

The dissociation of embryonic neural tissue produces isolated neuron and glial cells. When both are seeded on electrode arrays prepared with suitable adhesion molecules, such as poly-lysine and laminin, a shallow three-dimensional tissue develops

with neuronal cell bodies growing generally on top of a flat glia carpet and with neuronal processes situated both above and below that carpet. The initial stages of organization seem to be determined by a competition between cell-cell and cell-substrate adhesion. There appears to be a correlation between morphological stabilization of the network and the initiation of bursting, which commonly occurs in the second to third week of *in vitro* development.

Neuron-electrical hybrid systems offer speed and sensitivity of detection, with robust changes in network behavior elicited by compounds such as tetrodotoxin and strychnine in the low nanomolar range (Gross et al., 1997; Harsch et al., 1997). Detection of low picomolar concentrations of compounds such as botulinum toxin is possible (unpublished observations). The use of such systems for automated monitoring of environmental threats and drug development is made more practical by the rapid increase in processing speeds and availability of personal computers. Analysis algorithms which formerly required off-line processing by dedicated computer systems now can be run in real time by laptop machines.

Several challenges remain for the realization of neuronal networks as common tools in biosensor and drug development domains. Among them are: a) the demonstration of reliability and reproducibility of responses; b) the ability to produce and distribute large numbers of cultures that possess those reliable and reproducible responses; c) the development of life support systems for maintenance of the cultures in remote locations; and d) the implementation of automatic data analysis algorithms that will provide

unskilled operators with a meaningful interpretation of changes in network activity. Progress in each of these areas is being made. However, the biosensor application may ultimately be hindered less by the limitations of the neuronal networks themselves, than by the lack of suitable technology with which to extract environmental contaminants from the air and water; and then concentrate, sterilize, and deliver those contaminants to the neuronal network for analysis.

Thus, it is anticipated that the first of large-scale use of neuronal networks will come in the area of drug development. The pharmaceutical industry has a profound need for a device to provide information on the neuroactivity of large numbers of potential drugs. The number of compounds waiting to be screened may exceed 2-3 million (H. Hammerle, University of Tubingen, personal communication). Additionally, current methods used in rational drug development require the synthesis of large numbers of closely related molecules in an effort to discover the molecular configuration that imparts a desired effect and to eliminate those configurations that yield deleterious effects. This results in huge families of novel molecules, each of which must be screened in some way. The only method currently available for testing for neuroactivity and neurotoxicity uses live animals such as mice, rats, and chickens. This is an enormously expensive methodology, in both monetary costs and animal lives. A screening procedure based upon cultured neuronal networks should result in large cost savings, as well as prove a more humane alternative in that it requires minimal numbers of animals to be sacrificed to obtain the necessary tissue.

Advances in neurobiology have enabled rapid progress on the cellular and whole animal levels. However, the fundamental processing unit within the brain may be small groups of neurons that transiently and dynamically associate, with the degree and duration of the association determined by sensory input (Edelman, G, 1987). This level of neurobiological processing is relatively well characterized for some phenomena, such as rhythmic pattern generation within the spinal cord and the respiratory center (Grillner et al., 2000, Smith et al., 1991). This processing was not characterized in other areas such as the motor cortex, however, until the availability of multielectrode technology allowed researchers to study the mechanisms of population coding (Chapin et al., 1999; Georgopoulos et al., 1986; Schwartz A, 1994).

Cultured neuronal networks offer a preparation in which group processing may be studied conveniently. Such networks are isolated from afferent input that often complicates interpretation of changes in behaving animals. Pharmacological manipulations may be performed rapidly and repeatedly, allowing isolation of particular neurotransmitter systems. Electrical stimulation is possible through the same electrodes used to record. Long-term monitoring of networks has been limited to date only by contamination and has reached 16 days in an open chamber configuration. Experiments of several months' duration are foreseeable, with only minor improvements in network environmental control necessary.

As previously mentioned, the computing capabilities necessary for handling the large data streams from multichannel recording have become widely available and

affordable only recently. With these new systems will come new data analysis and visualization techniques. Such innovations promise rapid progress in the understanding of many network ensemble properties, such as pattern generation and storage, spontaneous shifts in dynamic neuronal associations, and fault-tolerance limits of network processing. The study of network development, the contributions of different neurotransmitter systems to network behavior, and the neuropathophysiology of various diseases, such as Alzheimer's, and infectious agents like HIV, may be expedited by cultured neuronal networks. These networks bridge cellular and whole animal physiology, and will yield valuable insights into the chemical and biological processes required to facilitate the association of single neuronal elements into highly interconnected neuronal networks as well as the emergent computational abilities of such networks.

The purpose of this work is to demonstrate the use of neuronal networks cultured on multi-electrode arrays in drug development, biosensors and neurtoxicology, and the study of burst mechanisms. In Chapter 1, the acute effects of a battery of novel acetylcholinestase inhibitors and common cholinergic compounds, including physostigmine and carbachol, will be described. This study highlights the ability of neuronal networks to detect minor molecular differences in a series of compounds that possess nearly identical AChE inhibition constants. Additionally, it offers a clear example of the advantage of supplementing biochemical characterization with physiological information. Two of the seven novel compounds tested produced irreversible inhibition of neuronal activity, an effect that could not be predicted from the biochemical data. This response implies a potentially lethal side-effect if the compounds

were to be administered to living animals. With physiological information provided by the neuronal networks, compounds with undesirable consequences can be eliminated prior to expensive, time-consuming animal testing.

Chapter 2 offers an example of neuronal network detection and classification of an unidentified compound. This compound, trimethylol propane phosphate (TMPP), was supplied by the Naval Research Laboratory, (Washington D.C.) as a blind test. After four experiments over a period of three days, it was determined that TMPP had effects on the organization of network activity at concentrations as low as 2μM, and that these effects resembled those of known epileptogenic substances, such as bicuculline. These conclusions confirmed experiments performed with acute and chronically dosed rats over a two-year period at the Naval Health Research Center, Wright-Patterson Air Force Base. Further characterization of TMPP by the neuronal networks demonstrated that it functions as an antagonist at the $GABA_A$ receptor, a property that correlates with its disinhibitory effects on network activity. The methodology outlined in the detection and classification of TMPP provides a basis for future applications of neuronal networks as biosensors and demonstrates the possible utility of compiling a reference library of network response to pharmacological compounds. This library of substance "fingerprints" will facilitate classification of unknown compounds by matching the responses they elicit to those of a known compound and will expand the capabilities of neuronal network sensors beyond that of simple threat detectors.

Chapter 3 details a series of 16 experiments using spinal cord cultures in which all neuronal synaptic interactions were limited to those mediated by the N-methyl-D-aspartate (NMDA) type glutamate receptor. This pharmacological state provides a model of the excitatory-coupled networks found during brief periods of mammalian development (Habets et al., 1987; Jackson et al., 1982) during which time networks exhibit bursts of action potentials roughly synchronized across the population. These synchronous population bursts are thought to be important in pruning and sculpting neuronal circuits during development (Tosney and Landmesser, 1985). When spinal cord networks were driven solely by the NMDA receptor, the activity exhibited uniquely periodic population bursts in which virtually every neuron participated. The temporal coefficients of variation (CV), reflecting the rhythmic nature of the oscillation, were 3.7, 4.7, and 4.9 % for burst rate, burst duration, and inter-burst interval, respectively (mean CVs for all 16 cultures). In addition to unmasking a type of neuronal activity with unprecedented regularity, these experiments also demonstrate the extreme pharmacological manipulations that are possible with cultured networks. They provide clear evidence that problems in basic neurobiology can be attacked with these preparations.

Each of the three chapters has been accepted for publication as an independent research report. By including them in one document, it is hoped that the utility of multielectrode recording in diverse areas of scientific inquiry can be more fully recognized. While the data presented has contributed to the body of scientific knowledge, the true aim of this work is to provide a reference for future experimenters desiring to

take advantage of multichannel recording techniques. Thus, the methods sections in each chapter provide guidance on the cell culture procedures necessary to grow a dependable supply of networks, as well as the analysis techniques to utilize once data are generated. The hardware necessary to reproduce the experimental stations employed in this research is available from several sources. The simple experimental paradigm is the same in each of the studies, in that a period of control activity is compared to a period during which the network is under the influence of a test substance. It is hoped the information and examples provided will facilitate future research using cultured neuronal networks.

The experience of this researcher indicates that primary neuronal culture remains as much an art as it is a science. Until the science becomes more exact, experimenters will be challenged with cultures that obstinately refuse to grow, or, if they grow, fail to produce reliable activity. Hopefully, the examples presented here will show that, with perseverance, the combination of multichannel recording and cultured neuronal networks offers an unequalled means of rapidly exploring significant questions in neurobiology.

CHAPTER 1

ACUTE TOXICITY SCREENING OF NOVEL ACHE INHIBITORS USING NEURONAL NETWORKS ON MICROELECTRODE ARRAYS

Summary

Spontaneously active neuronal networks grown from embryonic murine frontal cortex on substrate integrated electrode arrays with 64 recording sites were used to assess acute neurobiological and toxic effects of a series of seven symmetrical, bifunctional alkylene-linked bis-thiocarbonate compounds designed to possess anticholinesterase activity. Acute functional neurotoxicity in the absence of cytotoxicity was defined as total collapse of spontaneous activity. All of the compounds were characterized as mixed inhibitors of AChE, with K_is in the 10^{-7}-10^{-6} M range. The neuronal network assay revealed surprisingly diverse effects in response to these closely related compounds. Six of the seven compounds produced changes in network activity at concentrations of 10-350 µM. Three of the compounds were excitatory, one was biphasic (excitatory, reversibly inhibitory), and two were irreversibly inhibitory. Responses of cortical cultures to eserine were compared to the effects produced by the test compounds, with only one of seven exhibiting a close match to the eserine profile. Matching of response patterns allows the classification of new drugs according to their similarity to well-characterized agents. Spontaneously active neuronal networks reflect the interactions of multiple neurotransmitter systems and can reveal unexpected side effects due to secondary binding. Utilizing such networks holds the promise of greater research efficiency through a more rapid recognition of primary tissue responses.

Introduction

Unexpected secondary binding by compounds designed to be specific for certain receptors or an enzyme is a problem that affects every drug development effort. A reliable method for screening novel compounds for unwanted or toxic side effects could significantly increase the efficiency of the drug development process and minimize the use of experimental animals. We have used cultured neuronal networks grown from embryonic murine frontal cortex to assess the effects on spontaneous activity of seven symmetrical, bifunctional alkylene-linked bis-thiocarbonate compounds designed and biochemically verified to interact with both the peripheral and catalytic sites of AChE. Our purpose was to explore the relative efficacies of these compounds in modulating spontaneous activity and to utilize cultured neuronal networks as rapid screening platforms for determining general neurophysiological and toxic effects of novel compounds.

The networks were grown on thin-film multielectrode arrays (MEAs) constructed with transparent indium-tin oxide (ITO) conductors allowing simultaneous monitoring of multiple neuronal spike trains and visual observation of neuronal somata and processes (Fig. 1.1). Such networks are spontaneously active in culture and are sensitive to pharmacological manipulation of the medium. This sensitivity provides an effective platform for rapidly assaying effects induced by known and novel neuroactive substances (Gross et al., 1995, 1997a,b, Morefield et al., 2000). Compounds may acutely modulate the activity of spontaneously active networks via several pathways. Among them are

receptor activation and deactivation, metabolic disturbances, modification of membrane characteristics, alteration of vesicular dynamics, and changes in ionic potentials. These effects are reflected reliably by changes in the temporal dynamics of neuron-to-neuron communication as monitored non-invasively with extracellular recording.

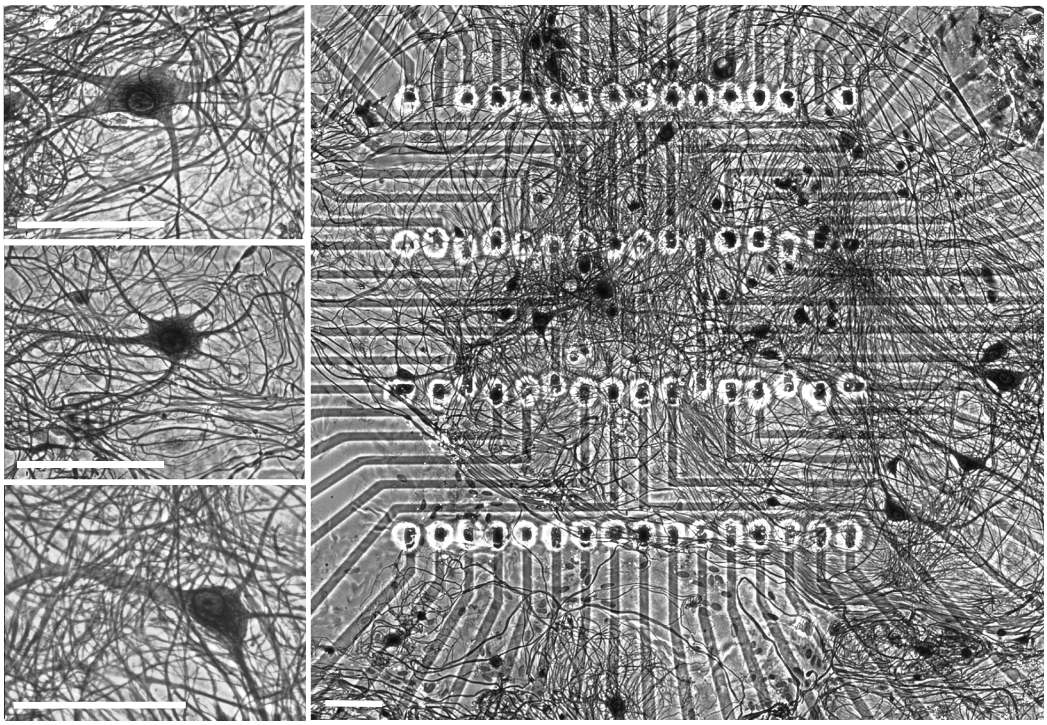

Figure 1.1: Neuronal network on recording matrix of a 64-electrode array plate. The indium-tin oxide conductors are 8 μm wide and 1,200A thick. The polysiloxane insulation is removed by a single laser shot to form a recording crater the end of the conductor. Electrolytic addition of gold lowers impedances to 1-2 megohms (at 1 kHz). Higher magnifications of neurons from this network are shown in the inserts. Mouse embryonic spinal cord; age: 52 days in vitro. (bars = 40μm)

It is evident from the literature that the cholinergic system in the CNS has a wide range of physiological influences. Although single cell data provide important insights into these domains, sequential analysis of single cell responses cannot give an accurate

picture of population response dynamics. These population responses are relatively easy to obtain with networks cultured on microelectrode arrays, at a cost, however, of disrupting the original circuitry. Nevertheless, the re-formed circuits in culture are pharmacologically histiotypic and demonstrate changes in spike patterns characteristic of the parent tissue (Gross et al., 1997a, 1997b; Morefield et al., 2000).

Methods

Techniques used to fabricate and prepare microelectrode arrays (MEAs) have been described previously (Gross, 1979; Gross et al., 1985; Gross and Kowalski, 1991). The hydrophobic surfaces of the MEAs were activated via butane flaming through a stainless steel mask, followed by application of poly-D-lysine and laminin. Cortical tissues were harvested from embryonic 15-to-18 day gestational age Hsd:ICR mice. The tissue was dissociated enzymatically (papain) and mechanically, seeded on prepared areas of the MEAs, and maintained in Dulbecco's Modified Minimal Essential Medium (DMEM) supplemented with 5% horse serum and 5% fetal calf serum in a 90% air/ 10% CO_2 atmosphere. No antibiotics/antimitotics were used. Cultures were "fed" twice a week with DMEM containing 5% horse serum. Cultures maintained under these conditions can remain spontaneously active and pharmacologically responsive for more than six months (Gross, 1994).

The recording medium consisted of a 50/50 mixture of fresh DMEM and conditioned DMEM (conditioned by culturing dissociated cortical tissue in flasks), supplemented with 5% horse serum. Osmolarity was adjusted to 320 mOsmoles. Eserine, curare and atropine (Sigma, St Louis, MO) were dissolved in sterile water. The test compounds were dissolved in 0.8% saline. All drugs were bath applied (bath volume 1.0-1.5ml). Stock concentrations were prepared so that total volume added never exceeded 1% of the total bath volume. The novel AChE inhibitors were synthesized by Vincenzo Talesa, University of Perugia, Perugia, Italy, and Nicholas Boyle, University of Sheffield,

Sheffield, England. The details of the synthesis and the AChE (purified from calf forebrain) inhibition analyses of the test compounds have been submitted for publication elsewhere (Drug Development Res.).

MEAs were placed in stainless steel recording chambers (Gross and Schwalm, 1994), and maintained at 37^{o}C on an inverted microscope stage. The pH was stabilized at 7.4 by passing a stream of humidified 10% CO_2 (flow rate of 10-15 ml/min) in air through a cap featuring a heated ITO window to prevent condensation and allow continued observation. Neuronal activity was recorded with a two-stage, 64-channel amplifier system (Plexon Inc., Dallas), and digitized simultaneously via a Dell 300 MHz computer (spike analysis) and a Masscomp 5700 computer (burst analysis). Total system gain was normally 12K. The neuronal activity was discriminated with a template-matching algorithm (Plexon Inc.) in real time to provide single unit spike rate data. Whole channel (multiple-units/ channel) data was analyzed using custom programs for burst recognition and analysis. The 16 cultures used in this study had an average electrode yield of 48%, and a mean signal-to-noise ratio (SNR) of 3.3:1 (including 1.5:1 SNRs). Maximum SNRs often exceeded 10:1. Cultures were randomly assigned to experimental groups, with the only requirement being they were at least 21 days in vitro (d.i.v.) and exhibited significant spontaneous activity. No influence of culture age on mean levels of spontaneous activity was observed.

The effects of the test compounds were interpreted in terms of two network activity variables, burst rate and spike rate. These variables are easily quantified, and

changes in mean values associated with experimental manipulations relative to a reference period provide reliable information on the functional state of the neuronal networks. The simultaneous monitoring of spike and burst rates allows detection of activity increases, decreases, and spike organization into bursts on a single unit basis, while cross-channel averaging provides information on network activity coordination. These relatively simple analysis techniques allow quantification of the data and easily visualized graphical representations of network responses to pharmacological compounds.

All analyses were done with binned data, with a bin size of 60 seconds. Single unit activity was averaged across channels yielding mean network spike and burst rates. These quantities were graphed as a function of time, providing a picture of the temporal evolution of activity and allowing a determination of stationary activity states (variations in burst and spike rates of $<15\%$). An experimental episode mean was obtained from the values comprising the stationary state. Control periods were always 30 min., whereas experimental episodes ranged from 20-30 min. because of exclusion of the transition states. Within single experiments, significance of changes induced by drug application was tested with a paired Student's t test, with $p<0.05$ accepted as significant. For pooled data (Figure 1.2d and 1.3), significance was tested with a one-way ANOVA followed by a post hoc Dunnett's test, $p<0.05$.

Results

The responses of frontal cortex cultures to a series of cholinergic agonists, antagonists, and the well-characterized AChE inhibitor eserine, were determined in order to demonstrate that these cultures were suitable assay vehicles for the series of novel AChE blockers. Figure 1.2a illustrates the results of applying curare (15 μM), an antagonist at nicotinic receptors containing the α7 subunit. An increase in both bursting and spiking occured within seven minutes and persisted until the end of the experiment. Figure 1.2b shows the response to an application of the non-specific muscarinic antagonist, atropine. Both burst and spike rates are depressed below reference period levels, (28% and 32% respectively). This depression lasted until the end of the recording. Under conditions of spontaneous activity, antagonists were especially effective in revealing functional cholinergic synapses.

Figure 1.2c shows a network in which 30 μM bicuculline, the $GABA_A$ antagonist, was applied at the beginning of recording, followed by application of 30μM carbachol at 190 minutes. The network response shows a near doubling of burst and spike rates that persist for the duration of the experiment. The bicuculline-carbachol effect could be antagonized by application of 20 μM atropine (not shown). The major potentiation of activity is reminiscent of the well-known effects of carbachol in producing epileptiform bursting in hippocampal preparations (Williams and Kauer, 1997).

Figure 1.2d summarizes the results from 4 experiments in which eserine, a well-characterized inhibitor of AChE, was titrated from 10 to 150 µM. The mean response is biphasic, with eserine increasing both bursting and spiking at 10 and 25 µM and inhibiting activity at concentrations above 50 µM. The inhibition of activity by eserine was reversible by washing (not shown). Together, these data indicate that the frontal cortex cultures used here possess both curare-sensitive nicotinic and atropine-sensitive muscarinic cholinergic receptors. Additionally, functional cholinergic synapses mediate a tonic inhibition of activity through nicotinic receptors concomitant with a tonic excitation of activity through muscarinic receptors.

Figure 1.2

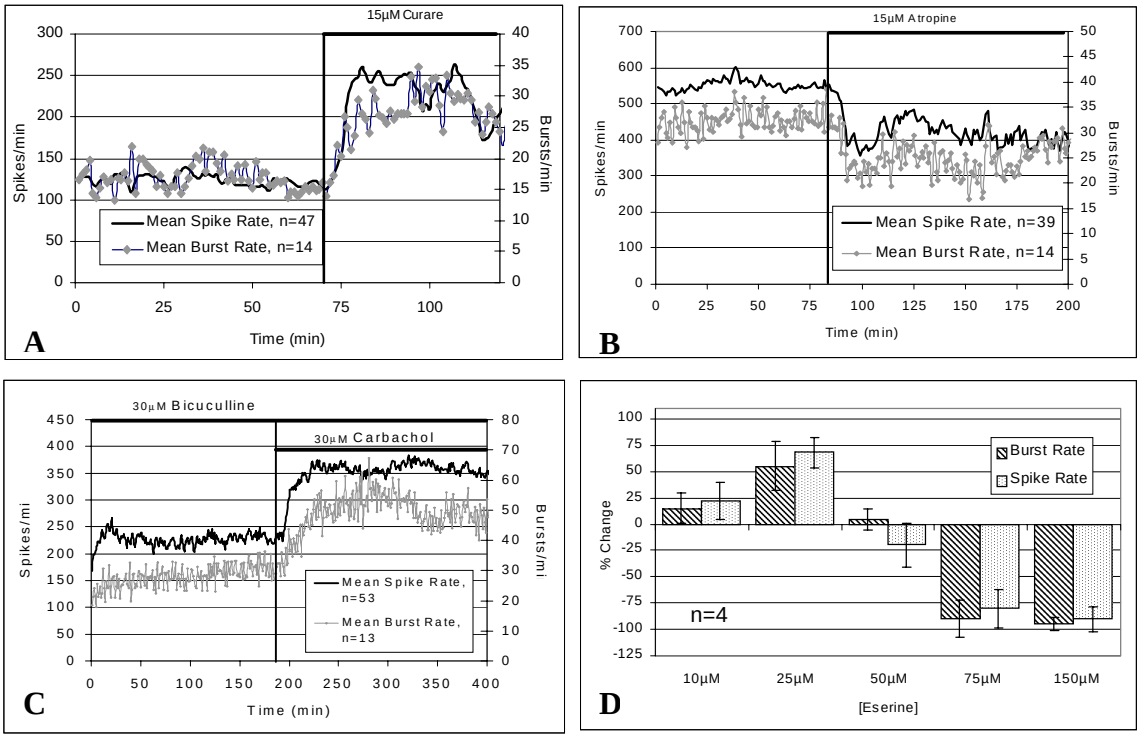

Figure 1.2: Response of frontal cortex cultures to well characterized agents affecting cholinergic neurotransmission. a) Application of the nicotinic receptor antagonist curare (15 µM) induced an increase in burst and spike rates. b) The non-specific muscarinic receptor antagonist atropine (15 µM) produced an inhibition of bursting and spiking. c) Application of carbachol 30 min after bicuculline produced large increases in the burst and spike rate activity. This effect persisted for the duration of the experiment. d) Mean responses of 4 experiments to titration of the acetylcholinesterase inhibitor eserine (10-150 µM). At low concentrations, eserine produced an increase in both burst and spike rates. The excitation was reversed by increasing concentrations, resulting in an average 95% suppression of burst rates and an average 90% inhibition of spike rates at 150 µM. The effects produced by eserine were fully reversible by washing.

Averaged (n=4) cortical network responses to eserine (Fig. 1.2d) were used to define a response profile to this known AChE inhibitor. Main features of this profile include an initial excitation at lower concentrations (10-40 µM), followed by a suppression of activity at concentrations beyond 40 µM, with almost total inhibition of bursting and spiking at 150µM. The effects were reversible with one or two complete medium exchanges. This profile served as a reference for the novel AChE inhibitors.

For testing the novel AChE inhibitors, which were identified as pure with TLC, ^{1}H NMR, and FTIR spectrophotometry by Nicholas Boyle, 16 murine frontal cortex cultures were used. The median age of the networks was 27 days *in vitro*, with a minimum of 21 and a maximum of 41 days. Cultures stabilize 3 weeks after seeding and do not change their pharmacological responses for up to 4-6 months (Gross et al., 1997a). Table 1 lists the structure and AChE inhibition constant of each compound.

TABLE 1: LIST OF TEST COMPOUNDS

INHIBITOR	STRUCTURE	AChE INHIBITION CONSTANTS, Ki (M)	INHIBITION TYPE
I1	Ch+O-CO-S(CH2)2S-CO-OCh+	1.0x10-6	Mixed
I2	Ch+O-CO-S(CH2)3S-CO-OCh+	1.4x10-6	Mixed
I3	Ch+O-CO-S(CH2)4S-CO-OCh+	1.0x10-6	Mixed
I4	Ch+O-CO-S(CH2)5S-CO-OCh+	1.4x10-6	Mixed
I5	Ch+O-CO-S(CH2)6S-CO-OCh+	1.4x10-6	Mixed
I6	DMEA+O-CO-S(CH2)4S-CO-DMEA+	3.6x10-7	Mixed
I7	DMEA+O-CO-S(CH2)6S-CO-DMEA+	5.0x10-7	Mixed

Ch+O- represents choline residues, DMEA+- represents N,N-dimethylethanolamine residues.

The network activity changes induced by the novel compounds were grouped into two categories, Excitatory and Inhibitory. These categories were further subdivided into Reversible (R), Irreversible (I), and Partially Reversible (P). Reversibility was defined as a return to near reference activity (< 20% change) after one to two complete medium changes. Partial reversibility represented recovery of activity after washing that deviated more than 20% from control period. Partial reversibility was not encountered in this data set. An effect was considered irreversible if there was no return of any activity after two or more complete medium changes and a subsequent wait of at least 2hr. Table 2 summarizes the structure, minimum effective concentration, and type of effect for each of the compounds.

TABLE 2: NETWORK RESPONSES TO TEST COMPOUNDS

INHIBITOR	SPACER	BASE	EXCITATORY [mM]	INHIBITORY [mM]	REVERSIBILITY	n
I1	2C	choline	10		R	2
I2	3C	choline	50		R	3
I3	4C	choline	10		R	2
I4	5C	choline	NE	NE	--	2
I5	6C	choline		350	I	2
I6	4C	ethanolamine	25	125	R	3
I7	6C	ethanolamine		200	I	2

n= # of cultures tested
R= reversible after one or two medium exchanges
I= irreversible after two or more medium exchanges and at least a two hour wait
NE= no effect

The results from application of novel AChE inhibitors to frontal cortex networks are summarized with dose-response graphs in Fig. 1.3. It is apparent that minor molecular differences in the structures of the inhibitors can have profound effects on the changes in network activity. Two compounds, I1 and I3, caused increases in bursting, with little effect on spike rates, but I3 was significantly more potent in its effects. Two of the compounds, I5 and I7, irreversibly inhibited network activity at relatively high concentrations. One compound, I6, increased activity at low concentrations, but reversibly inhibited bursting and spiking when the concentration was increased. Another compound (I4), elicited little effect on network activity at concentrations to 0.5 mM. Inhibitor 2 increased spiking activity, while simultaneously lowering the burst rate, reflecting changes in the organization of network spike activity. It is of interest that the three cultures used in assaying the effects of I2 were 23, 28, and 37 d.i.v. An examination of the standard error bars in the graph for I2 in Fig. 1.3 shows responses of the networks were not affected by age differences in any significant way.

Figure 1.3

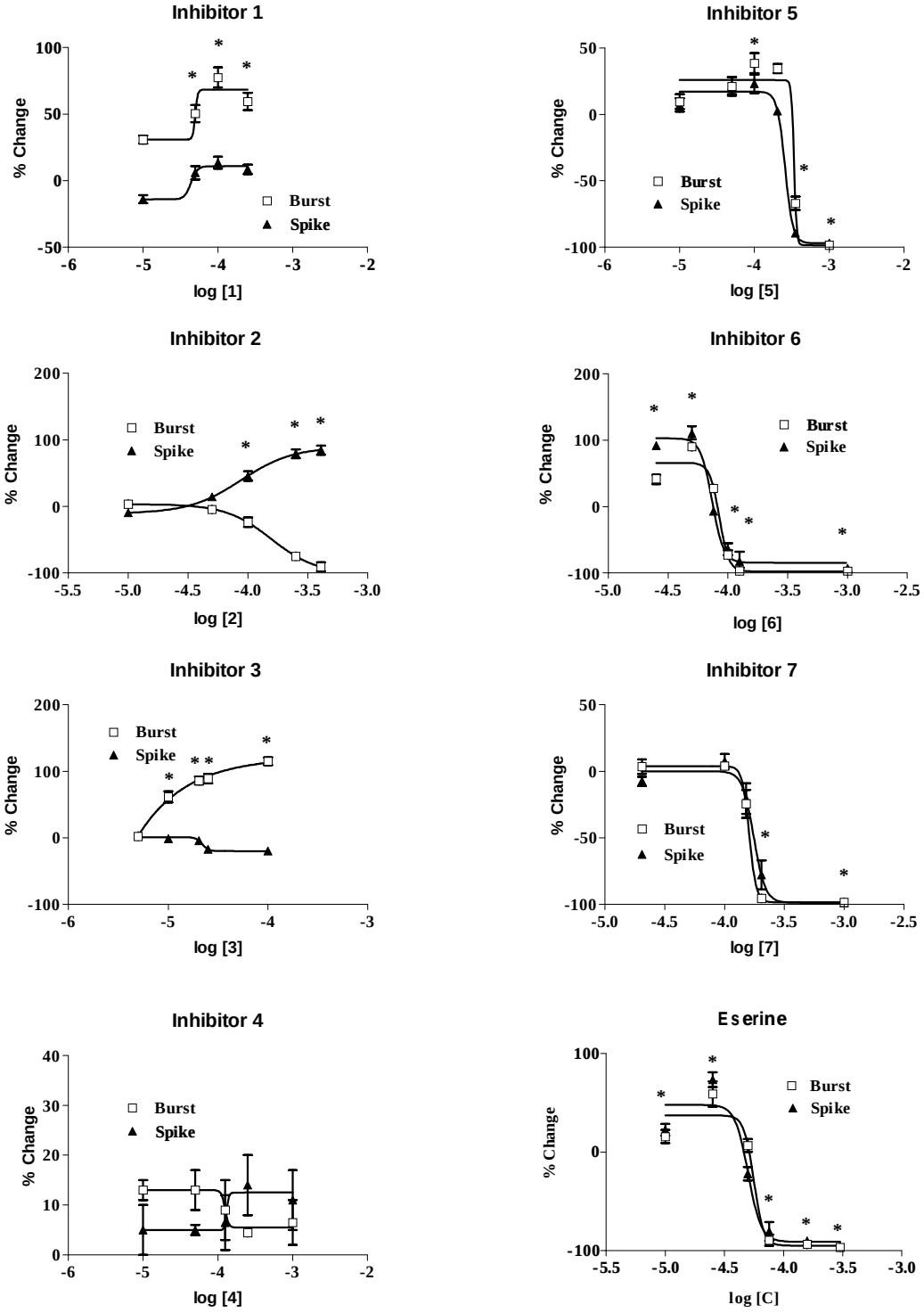
Inhibitor 1
% Change
log [1]
Burst
Spike
Inhibitor 5
% Change
log [5]
Burst
Spike
Inhibitor 2
% Change
log [2]
Burst
Spike
Inhibitor 6
% Change
log [6]
Burst
Spike
Inhibitor 3
% Change
log [3]
Burst
Spike
Inhibitor 7
% Change
log [7]
Burst
Spike
Inhibitor 4
% Change
log [4]
Burst
Spike
Eserine
% Change
log [C]
Burst
Spike

Figure 1.3: Dose-response summary for eserine and seven novel anticholinesterases using the network activity variables burst rate and spike rate. Percent change was calculated for a 20-30 minute window of activity at the concentration listed (see Methods section), relative to a 30-minute reference period of spontaneous activity. Data shown represents mean of two, or in the case of Inhibitors 2 and 6, three experiments. Eserine data originates from four experiments. Vertical bars represent the range of responses for inhibitors 1,3,4,5,7, (n=2) and standard error for inhibitors 2, 6, and eserine. I1 increased burst rate at 10µM eliciting a maximal increase of 74% at 100µM. The compound did not change spike rates significantly at any concentration tested. I2 increased spike rates at 100µM and above with a concomitant inhibition of bursting. I3 was the most efficacious of the compounds, increasing burst rates an average of 98% above baseline at 25µM. I3 was ineffective at altering spike rates in the range shown, and at concentrations up to 0.5mM (data not shown). I4 was the least effective agent tested, producing a 27% inhibition of burst rate only at concentrations of 0.5mM. I5 produced a slight increase in both bursting and spiking at 50-200µM, which was transformed into a 79% and 84% inhibition of burst and spike rates, respectively, at 350µM. This inhibition could not be reversed by washing. I6 produced a biphasic effect, increasing both bursting and spiking significantly at 25-50µM, and reversibly inhibiting both parameters at concentrations above 75µM. I7 produced effects very similar to I5, although it was more potent, with an irreversible inhibition of both bursting and spiking at concentrations above 150µM. Response to eserine was biphasic, with excitation of burst and spike rates occurring at the 10 and 25µM concentrations, and inhibition of both activity measures occurring at 75µM and above. The suppression of activity by eserine was reversible. * indicates significant difference from control period, $p<0.05$, one way ANOVA.

Figure 1.4 provides an alternative view of the data presented in Fig. 1.3 for the seven novel AChE inhibitors. The bars make the biphasic nature of the network responses more apparent for I5 and I6, and offer a better look at the opposing effects on network activity produced by I2. The dose-response presentation however, allows EC_{50}s to be calculated.

Figure 1.4

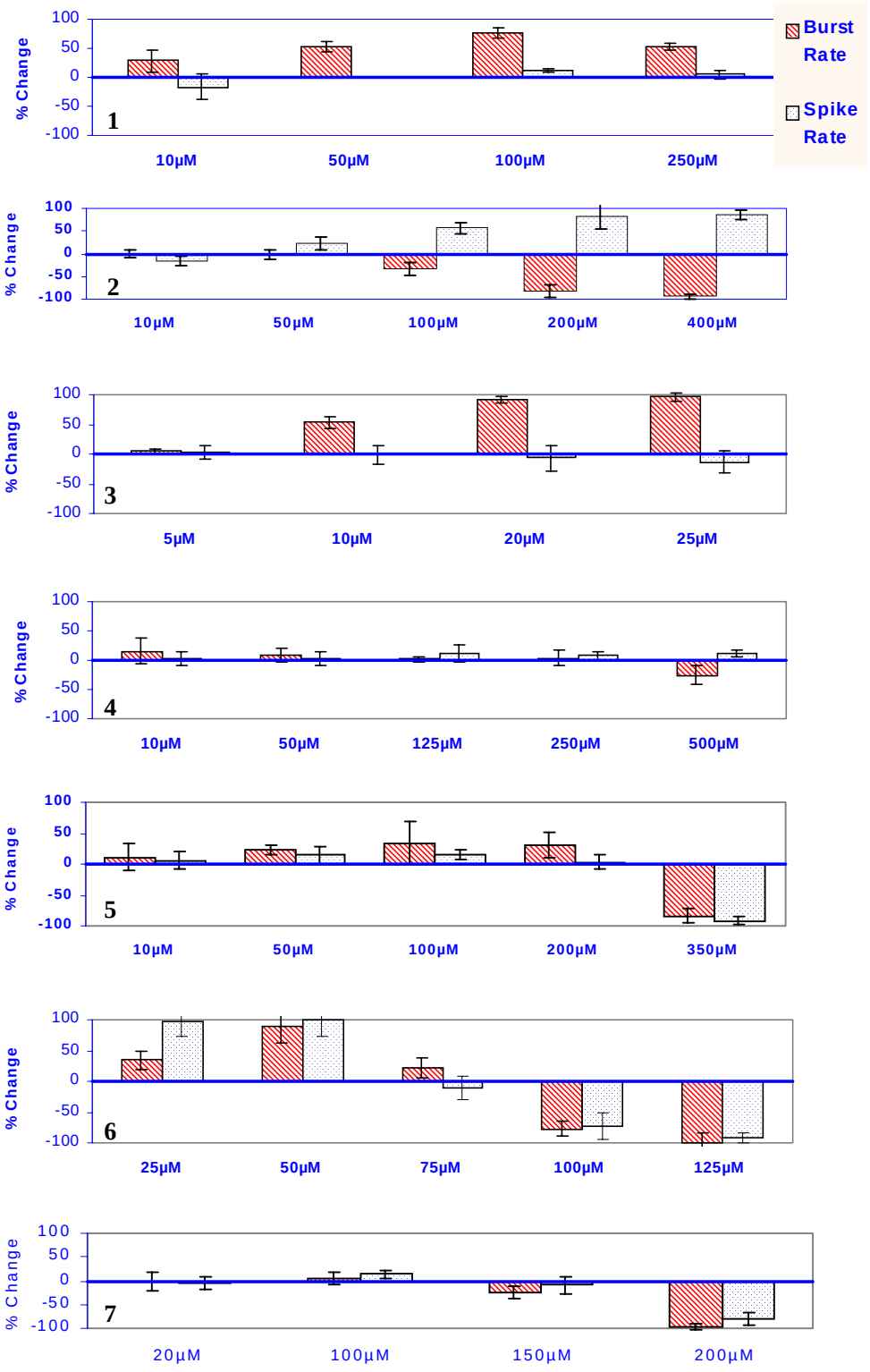
% Change
100
50
0
-50
-100
1
10µM
50µM
100µM
250µM
Burst Rate
Spike Rate
2
10µM
50µM
100µM
200µM
400µM
3
5µM
10µM
20µM
25µM
4
10µM
50µM
125µM
250µM
500µM
5
10µM
50µM
100µM
200µM
350µM
6
25µM
50µM
75µM
100µM
125µM
7
20µM
100µM
150µM
200µM

Figure 1.4: Summary of effects of novel anticholinesterases on network activity variables burst rate and spike rate. Percent change was calculated for a 20-30 minute window of activity at the concentration listed, relative to a 30-minute reference period of spontaneous activity. Data shown represents mean of two, or in the case of Inhibitors 2 and 6, three experiments. Vertical bars represent the range of responses for inhibitors 1,3,4,5,7, and the SD for inhibitors 2 and 6. Inhibitor 1 increased burst rate at 10µM, eliciting a maximal increase of 74% at 100µM. The compound did not change spike rates significantly at any concentration tested. Inhibitor 2 increased spike rates at 100µM and above with a concomitant inhibition of bursting. I3 was the most efficacious of the compounds at increasing burst rate, with a 98% increase above baseline occurring at 25µM. Inhibitor 4 was the least effective agent tested, producing a 27% inhibition of burst rate only at concentrations of 0.5mM. I5 produced a slight increase in both bursting and spiking at 50-200µM, which was transformed into a 79% and 84% inhibition of burst and spike rates, respectively, at 350µM. This inhibition was not reversed by washing. I6 produced a biphasic effect, increasing both bursting and spiking significantly at 25-50µM, and inhibiting both parameters at concentrations above 75µM. The inhibitory effects of I6 were reversible. Inhibitor 7 produced effects very similar to I5, although it was more potent, with an irreversible inhibition of both bursting and spiking at concentrations above 150µM.

Figure 1.5 illustrates the effect of I5, a choline-based compound with a 6-carbon, hexylene spacer. I5 produced small increases in burst and spike rates at 10-200 µM but produced an irreversible inhibition of activity at 350 µM. However, monitoring of the network for a 12-hour period through an inverted microscope and video display showed no visually discernible cytotoxicity associated with the loss of activity. No activity was recorded on any channel during the 12 hrs.

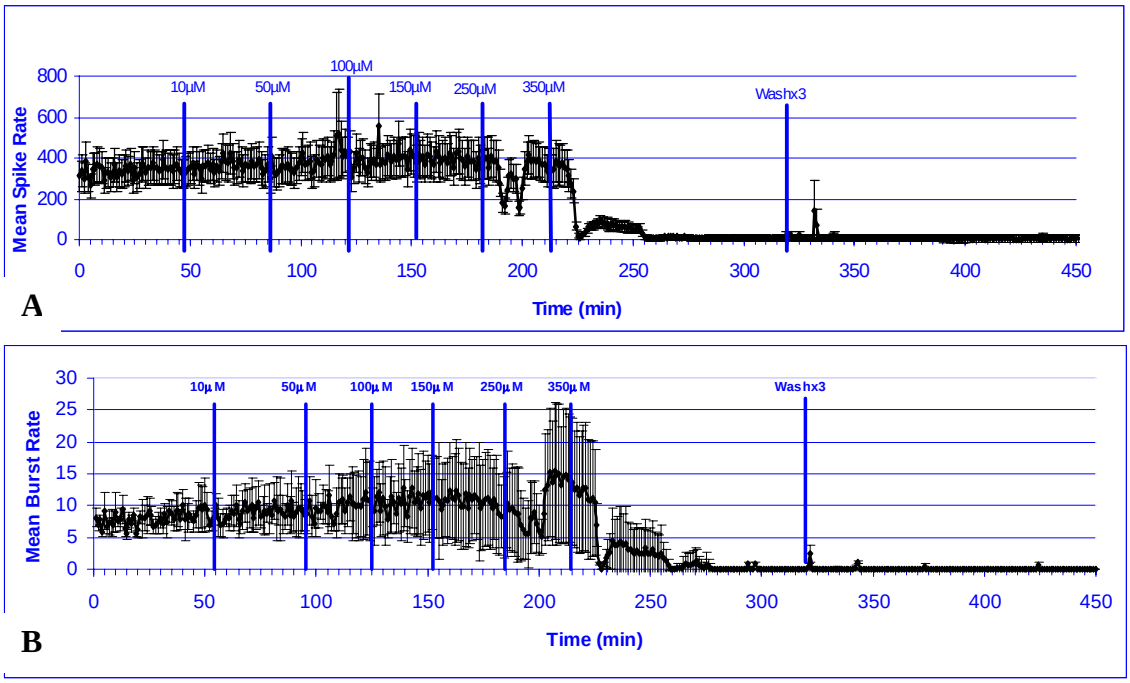

Figure 1.5: Irreversible inhibition of network activity in response to I5. (A) Mean +/- SD of 28 discriminated units. Titration to 200µM produced very little effect on spike rates, raising the concentration to 350µM caused a rapid reduction in spiking. All spike activity was abolished within approximately 30 min. (B) The effect on spike rates was paralleled by burst rate inhibition (mean+/-SD of 12 channels). However the standard deviation of the burst rates began to increase at 50µM, indicating a lessened cross-channel coordination. The inhibition was not reversible by 3 complete medium changes at 320 minutes.

Inhibitor 6, a DMEA-based compound, produced a biphasic effect on network activity (Fig. 1.6). At 25 µM, I6 caused increased spike production greater than 90%. Burst rate was increased by 80% at the same concentration. Increasing the concentration to 50 µM resulted in a spike rate increase averaging 101%, with a concomitant increase in burst rates of 73%. The excitatory window for I6 was rather narrow; at 75 µM the spike rate was inhibited by 28% while burst rates were 29% below baseline. Maximal inhibition of mean spike rate by 92% was produced by concentrations of 125 µM and

above. The burst rate was reduced to zero by concentrations exceeding 100 µM. The inhibition of network activity was reversible by washing, in contrast to that produced by Inhibitors 5 and 7.

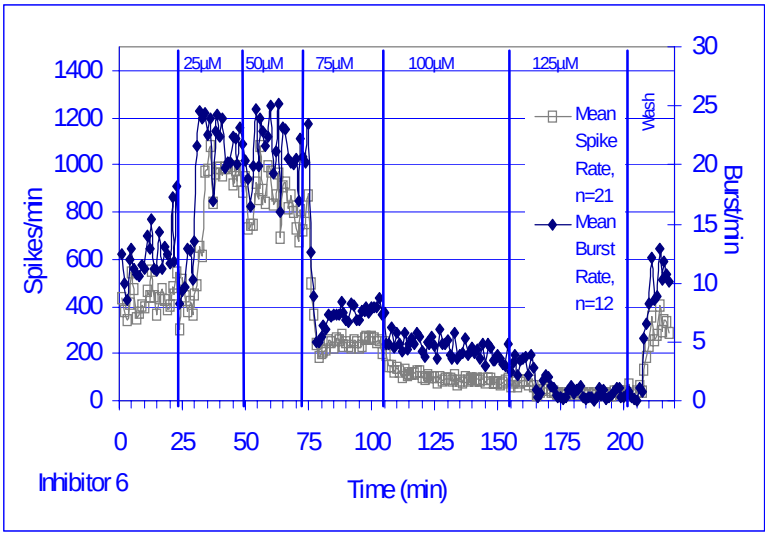

Figure 1.6: With a 4C spacer and a DMEA residue, I6 had a biphasic effect on spiking and bursting, increasing both activity measures at concentrations of 25-50 µM. This activity increase was reversed at concentrations of 75 µM and above. Only minor spiking remained at 125 µM. The inhibitory effect was reversible by washing.

The other DMEA-based compound, Inhibitor 7, produced only inhibitory effects on network activity, suppressing spike and burst rates at 150 µM by an average of 50% and 43% respectively. I7 totally stopped all activity at 200 µM (Fig. 1.7). This effect was irreversible with only transient activity recovery after 2 complete medium changes, followed by a complete cessation of activity for a 3-hour observation period. There was no overt cytotoxicity associated with this functional (electrophysiological) toxicity. Neuronal somata remained phase-bright, without cytoplasmic granularity throughout the observation period.

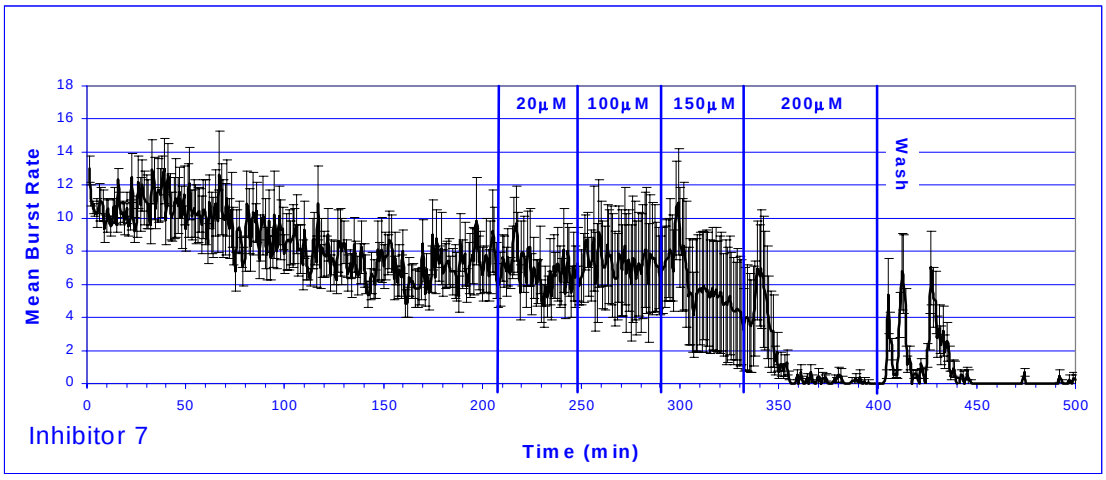

Figure 1.7: Inhibitor 7 (DMEA-based compound with a hexylene spacer) caused only moderate increases in the standard deviation of the burst rate, until the concentration was increased to 150µM, at which point the burst rate was depressed. At 200µM, Inhibitor 7 totally suppressed all network activity. The inhibition was not reversed by two complete medium changes.

Discussion

We tested the responses of murine frontal cortex networks cultured on multielectrode arrays to seven newly synthesized compounds designed to block AChE, the primary effector of ACh removal from the synaptic cleft. The presence of this enzyme in the cortical cultures was deduced from the change in activity elicited by eserine, a specific blocker of AChE. Eserine was effective in increasing network activity at a concentration range of 10-25 µM, while it suppressed network activity at higher concentrations. This biphasic activity of eserine has been seen at the neuromuscular junction at which eserine at low concentrations (1-20 µM) increased the amplitude and prolonged the decay time of endplate-currents but, at 20 µM to 2 mM, decreased the decay times (Dudel et al., 1999). The 1-20 µM effects were attributed to inhibition of AChE, while the high dose effects were thought to be a result of a direct blocking action of eserine on the open channel configuration of the nicotinic receptor**.** Blocking of nicotinic ACh receptors by eserine and 4 other AChE inhibitors was also seen by van den Beukel et al. (1998) in a variety of cell types. In the feline medulla, chemosensitive respiratory neurons also responded biphasically to eserine, with an initial augmentation of neuronal activity at low concentrations that converted to a depression in firing rates at higher concentrations in an apparently opioid-receptor dependent fashion (Trouth et al., 1993).

Although eserine is approved for clinical applications in the treatment of Alzheimer's, the therapeutic window for this drug is relatively narrow. This is also the

case for I6, the novel compound that most closely resembled eserine in its effects. Possible therapeutic windows are wider for compounds I2 and I3, which demonstrate increases in spike production and burst production respectively. Although they show no general inhibition, the compounds affect spontaneous activity differently. Whereas I2 transforms bursting into spiking, I3 is very effective at organizing existing spikes into bursts. As increased bursting generally is associated with epileptiform activity, I3 may indeed trigger epilepsy, whereas I2 may stabilize epileptic tissue. Animal experiments clearly are required to determine the final behavioral response. However, the dose-response curves of Figure 3 provide valuable data that can be used to increase the efficiency of drug screening procedures. The irreversible inhibitory effects of I5 and I7 would seem to make them unsuitable for possible clinical applications. Such inhibition of network activity should be considered acute, functional toxicity despite a lack of cytotoxicity. Tetrodotoxin would be a compound in this category.

Cholinergic neurons intrinsic to the frontal cortex have been labeled immunohistochemically with antibodies to the vesicular acetylcholine transporter (Arvidsson et al., 1997) and choline acetyltransferase (ChAT) (Johnston et al., 1981). Cossette et al. (1993) demonstrated that ChAT activity recovered to near normal levels in the fronto-parietal cortex within three months of ibotenic acid lesion of the nucleus basalis in adult rats. These results, along with the effects of eserine that we observed, imply that cholinergic neurons are intrinsic to the cortex of intact animals and that these neurons survive in our cultures and make functional synapses.

It is interesting to compare the effects on neuronal activity of the seven compounds with their inhibition of AChE (Tables 1 and 2). All the test compounds were classified as giving mixed inhibition, although double reciprocal plots suggest inhibition of a non-competitive nature. This phenomenon has been addressed by others, who contend that certain types of AChE inhibitors exhibit mixed inhibition (Krupka, et al., 1961). From Table1, it can be argued that the DMEA derivatives (compounds 6 and 7), are better AChE inhibitors than the choline derivatives, (compounds 1-5). The former have K_i values in the 10^{-7}M range, while the latter derivatives have K_i values in the 10^{-6}M range. Further, there is no apparent relationship between alkylene length separating the thiocarbonate moieties and the inhibitory potencies of the choline or the DMEA derivatives. This also suggests that inhibitory potencies of the compounds are not dependent upon binding with both the peripheral binding site and the active site of AChE, since the greater the separation between the thiocarbonate moieties the greater the anticipated binding with both sites (Pang et al., 1996).

For the choline-containing compounds, Table 2 shows that there is an apparent relationship between alkylene length and increase or inhibition of the spontaneous network activity. With linker chains having two to five carbon atoms (compounds 1-4), no inhibitory action is found, but excitatory activity does occur with demonstrated reversibility. The one exception is compound I4 (5-C spacer), which shows neither excitatory nor inhibitory activity and apparently is in a transitory position between excitatory and inhibitory behavior. When the choline-bearing bis-thiocarbonate has a

spacer length of 6 carbon atoms (compound 5), all excitatory activity is lost and irreversible inhibition of spontaneous network activity occurs. The reversible and irreversible cessation of network activity in response to three of the seven compounds could not be anticipated from the biochemical data. The fact that two of these compounds are irreversibly toxic is surprising and emphasizes the importance of tissue-based screening early in the drug development process.

For the better AChE inhibitors, the DMEA derivatives, Table 2 shows that compound I6 (4-C spacer) demonstrates both reversible excitatory and reversible inhibitory effects on neuronal networks. This contrasts with the activity of choline-containing compound I3 (4-C spacer), which has only reversible excitatory activity. The DMEA-containing compound 7 (6-C spacer) has only irreversible inhibitory effects, similar to that of the choline-containing compound 5 (6-C spacer). A logical conclusion from these data is that the effects of the inhibitory bis-thiocarbonates on the neuronal networks reflect varying combinations of their actions on AChE activity and their unexpected interaction with neuronal ionotropic receptor sites.

Acetylcholine in the frontal cortex is primarily a neuromodulator that has been implicated in arousal, attention, learning and memory. The effects of ACh are exerted pre- and post-synaptically and have been shown to regulate release of neurotransmitters and post-synaptic excitability (McGehee and Role, 1996). The therapeutic strategy of increasing cholinergic activity by inhibiting the enzymatic hydrolysis of ACh, thereby increasing the constitutive amount of neurotransmitter available, can have multiple

outcomes depending upon the receptor subsequently activated. Increased ACh levels that result in an activation of certain presynaptic nicotinic receptors, such as the $\alpha 7$ and $\alpha 4\beta 2$ subtypes, could lead to increased release of ACh from the cell stimulated, especially in conditions of impaired cholinergic function as exists in Alzheimers (Marchi and Raiteri, 1996). On the other hand, increasing the activation of presynaptic m2 muscarinic receptors could result in lower levels of ACh release (Vizi et al., 1989; Rouse et al., 1997). Such antagonistic responses make it difficult to predict physiological effects from biochemical or even single cell data. However, a spontaneously active network reflects the interactions of all transmitter systems present. The use of such networks as an intermediate step between biochemical analyses and animal experiments holds the promise of greater research efficiency through a rapid recognition and quantification of physiological tissue responses.

Additional Considerations for the Use of Cultured Neuronal Networks in Pharmacology

This work demonstrates the utility of neuronal networks in testing novel drug candidates that can affect neural activity. The compounds described had a known biochemical effect, the inhibition of AChE. However, the biochemical assay examines only one aspect of a drug. The neuronal networks consist of living cells expressing a wide variety of neurotransmitter receptors, ion channels, and transport proteins on the surface of their plasma membranes. There are continual intracellular biochemical processes, the sum of which produces a characteristic behavior that can be monitored optically and electrically. Novel drugs potentially can interact at any of these points, producing changes in neuronal activity that cannot be predicted from the biochemical activity of the drug.

Thus, neuronal networks, when used in a drug development environment, can provide valuable information that may be used to guide the drug developer in discriminating between molecules that are potentially acceptable for further testing and those that produce neurotoxicity or changes in network activity not representative of the known biochemical effects. Implementation of neuronal network screening of novel drugs as a standard methodology could offer large cost savings to pharmaceutical companies, by allowing the drug development effort to focus on candidate compounds that possess both a desired biochemical activity and effects on neuronal interactions that are compatible with that activity. Most important, such screening can provide information

on undesired binding or interactions that are extremely difficult to discover with purely biochemical assays and are expensive to elucidate in whole-animal experiments.

Additional information can be gained from the neuronal networks. As shown here, titration of drugs can produce reliable dose-response curves. These curves may be used to compare the effects of different compounds that putatively interact at the same binding site, allowing characterization of drugs by rank order potency. Rank order potencies can give a qualitative estimate of the selectivity of the binding site for different compounds. A quantitative evaluation of selectivity may be gathered by the use of potency ratios. The ratio of the EC_{50}s for two compounds is related linearly to the relative binding strengths of the compounds at a specific site.

Determination of the binding strengths for agonists ($1/Kd_A$) at specific receptors is possible if a specific irreversible antagonist is available. Constructing dose response curves in the absence and in the presence of increasing concentrations of the antagonist will allow comparison of the concentration of agonist required to elicit equal functional responses as the antagonist concentration is increased. The Kd_A may be determined from a plot of the agonist concentrations in the presence of the antagonist against the ratio of the agonist concentration in the presence of the antagonist ([A']) to the agonist concentration in the absence of the antagonist ([A]).

The binding strength of reversible antagonists (Kd_B) may be found by constructing dose response curves for an agonist effect as the concentration of the

antagonist is increased. The values for the EC_{50} of the agonist at different concentrations of antagonist may be used to find a dose ratio. This number is the ratio of the EC_{50} with antagonist to the EC_{50} without antagonist ([A']/[A]). A plot of log (([A']/ [A])-1) against the log of the concentration of antagonist is called a Schild plot. The intercept of a line fitted to the data with the X-axis is the Kd of the antagonist.

Determination of binding strengths using neuronal networks is susceptible to several problems. A particular response is elicited by a unique concentration of drug at a binding site. Therefore, maintenance of drug concentrations at a constant level at the receptor of interest is necessary. Factors influencing the equilibrium of the drug concentration include chemical degradation of the drug during the experimental episode, enzymatic degradation by the neuronal tissue, non-specific binding, and uptake of the drug by the tissue. Experiments done with the novel AChE inhibitors utilized bath application of the test compound into a volume of 1-2 ml. This should provide what is essentially an infinite reservoir of drug, compared to the volume of tissue. However, chemical degradation still can occur and complicate interpretation of neuronal network responses.

Neuronal networks consist of multiple interacting cell types expressing a wide variety of receptors. The accurate determination of binding strengths is dependent upon the measured response being mediated by a single receptor type. This may be possible if other drugs are used to block effects not specific to the receptor of interest. Knowledge of the drug mechanism and the ability to isolate the effect elicited by that mechanism either

pharmacologically or with suitable control experiments is a prerequisite. Quantification of the drug effect should be at a point where network activity has reached a stationary state. Drug applications often elicit responses that vary over time, with some compounds requiring several minutes to reach the full effect. Conversely, sometimes there is a recovery from the maximal effect a compound produces. This may represent mechanisms such as desensitization or internalization of the receptor, or homeostatic regulation of neuronal excitability that may occur on several time scales.

The primary goal for implementing large-scale pharmacological testing must become delineation of the response reliability of the neuronal networks to a wide range of known pharmacological compounds. This validation of the system is essential before testing of unknown drug candidates can be undertaken. The concomitant development of software to enable real-time multi-variate analysis of the large data streams inherent in the multi-channel environment will provide the tools necessary to ensure that neuronal networks can become reliable platforms for the evaluation of novel drug candidates.

CHAPTER 2

CHARACTERIZATION OF ACUTE NEUROTOXIC EFFECTS OF TRIMETHYLOLPROPANE PHOSPHATE VIA NEURONAL NETWORK BIOSENSORS

Summary

We have utilized cultured neuronal networks grown on microelectrode arrays to demonstrate rapid, reliable detection of a toxic compound, trimethylolpropane phosphate (TMPP). Initial experiments, which were performed blind, demonstrated rapid classification of the compound as a convulsant, a finding consistent with previous whole animal neurobehavioral studies. TMPP (2-200 µM) reorganized network spike activity into synchronous, quasi-periodic burst episodes. Integrated burst amplitudes invariably increased, reflecting higher spike frequencies within each burst. The variability of network burst parameters, quantified as coefficients of variation (CVs), was decreased. Mean CVs for burst duration, interburst interval, and burst rate were lowered by 42 ± 13, 58 ± 5.5, and 62 ± 1.8%, respectively (mean ± SEM, n=8 cultures, 197 channels). These changes in network activity paralleled the effects induced by bicuculline, a known disinhibitory and seizure-inducing drug, and confirmed classification of TMPP as a potential epileptogenic compound. Simple pharmacological tests permit exploration of mechanisms underlying observed activity shifts. The EC_{50} for GABA inhibition of network activity was increased from 2.8 to 7.0 µM by 20 µM TMPP and to 20.5 µM by 200 µM TMPP. Parallel dose response curves suggest that TMPP acts by a competitive

antagonism of GABA inhibition and are consistent with reported patch-clamp analysis of TMPP-induced reduction of inhibitory postsynaptic current amplitudes. The potency of TMPP in generating epileptiform activity *in vitro* was comparable to concentrations reported for *in vivo* studies. TMPP and bicuculline produced both increases and decreases in burst rate, depending on native spontaneous bursting levels. These results demonstrate a need for multivariate analysis of network activity changes to yield accurate predictions of compound effects.

Introduction

The ability to detect compounds with the capacity to affect neurophysiologic function is a major concern to civilian and military communities. Neuroactive compounds can alter performance and behavior of organisms in many different ways; from life-threatening catastrophic failure of organ systems that rely on neural input to subtle, but debilitating, changes in cognitive processes and motor coordination. Neuroactive compounds include neurotoxins, several of which are considered potential biological weapons, as well as neurotoxicants, where a risk may arise via environmental or occupational exposure. One such neurotoxicant, trimethylolpropane phosphate (TMPP), is an ethyl bicyclophosphate convulsant produced during the partial pyrolysis of certain synthetic, ester-based turbine lubricants supplemented with phosphate-based lubricity additives (Toia and Casida, 1987; Centers, 1992; Wyman *et al.*, 1987). Over the course of several years, it has been shown that acute exposure of rats to TMPP [0.05-1.0 mg/kg, intraperitoneal (ip)] induces electroencephalographic paroxysms, stereotypic behaviors, sub-clinical seizures, clinical convulsions, status epilepticus, or lethality in a dose-dependent manner (Bellet and Casida, 1973; Wyman et al., 1993; Lindsey et al., 1998). While there are no documented cases of human exposure to TMPP, it constitutes a potential human risk of dermal or inhalation exposure consequent to fires aboard military ships or both military and commercial aircraft (Wyman et al., 1987; Wyman et al., 1993).

Given the diversity of potential threats to neurophysiologic function, there is a need for sensor systems that rely on physiologic endpoints for detection. Moreover, the rapid introduction of new compounds by chemical and pharmaceutical industries, as well as academia, presents a significant challenge to neurotoxicologic screening efforts. To supplement current methods, which primarily rely on animal neurobehavioral testing, *in vitro* test systems using either cell lines or high-yield primary cell cultures, are receiving increased attention. Data accumulated so far indicates that *in vitro* systems are well suited for rapid, inexpensive, and quantitative screening of toxicants under highly controlled experimental conditions.

Recent advances in growing nerve cell networks on substrate-integrated, thin-film microelectrode arrays in cell culture have led to experimental systems in which the spontaneous electrical activity can be monitored by 32 to 64 electrodes for periods of time reaching several months (Gross, 1994). The large number of electrodes and stable cell-electrode coupling provide massive data on the internal dynamics of these nerve cell networks. These systems are accessible pharmacologically and have shown both a high sensitivity to neuroactive/toxic compounds and tissue-specific responses, i.e., the cultured networks share the profiles of pharmacological sensitivity of the parent tissue (Gross et al., 1997; Gramowski et al., 2000; Morefield et al., 2000). Clearly, subtle aspects of information processing, which are more dependent on circuit structure, cannot be duplicated in culture. Nevertheless, pharmacological responses are robust and highly reproducible (Gross and Kowalski, 1991; Gross et al., 1992; Gross, 1994; Rhoades and Gross, 1994; Gross et al., 1997). Such networks offer new assay and sensing systems

that lie between biochemistry and whole animal experiments and provide rapid, quantitative information on neurophysiological responses to chemicals.

TMPP originally was provided to the Center for Network Neuroscience at UNT as an unknown test substance. The compound was quickly identified as a potential convulsant, since it mimicked responses obtained with the $GABA_A$ antagonist bicuculline. With present equipment and methodologies, such a classification could be made in 10 to 30 min, depending on substance concentration. A reliable warning of potential debilitating neural changes often can be obtained in less than 3 min. This paper describes subsequent experiments designed to quantify acute neurophysiological effects of TMPP on spontaneously active primary neuronal cultures growing on substrate integrated microelectrode arrays. It aims to demonstrate that such systems can provide rapid, reliable warning of the presence of toxic substances and, from the manner in which the spontaneous activity changes, can provide information on the class of compound present and its potential physiological effects. This paper also demonstrates that simple pharmacological tests can provide valuable information on primary mechanisms involved in the altered neuronal network responses.

Methods

Techniques used to fabricate and prepare microelectrode arrays (MEAs) have been previously described (Gross, 1979; Gross et al., 1985; Gross and Kowalski, 1991). The hydrophobic surfaces of MEAs were activated by butane flaming through a stainless steel mask, followed by application of poly-D-lysine and laminin. Spinal and cortical tissues were harvested, respectively, from embryonic 14-15 and 16-18 day gestational age Hsd:ICR mice. The tissue was dissociated enzymatically (papain) and mechanically, seeded on the prepared areas of the MEAs, and maintained in either Minimum Essential Medium supplemented with 10% horse serum (MEM-10 for spinal cultures), or Dulbecco's Modified Minimal Essential Medium (DMEM) supplemented with 5% horse serum (for frontal cortex cultures), in a 90% air and 10% CO_2 atmosphere at 37^o C. No antibiotics/ antimitotics were used. Cultures were "fed" twice a week with 50% medium changes. Cultures maintained under these conditions can remain spontaneously active and pharmacologically responsive for more than six months (Gross, 1994). Figure 2.1 shows a typical research work station comprised of a Plexon MNAP system with two monitors (A) and recording chambers developed and fabricated by the CNNS (B). Fig. 2.1C depicts a monolayer network growing on an array of 64 ITO electrodes.

MEAs were placed in stainless steel recording chambers (Gross and Schwalm, 1994), and maintained at 37^oC on an inverted microscope stage (Fig. 2.1). The pH was stabilized at 7.4 by passing a stream of humidified 10% CO_2 (flow rate of 10-15 ml/min) in air through a cap featuring an ITO window heated to prevent condensation and thus

allow continual microscope observation. Neuronal activity was recorded with a two-stage, 64-channel amplifier system (Plexon Inc., Dallas, TX), and digitized simultaneously via a Dell 300 MHz computer (spike analysis) and a Masscomp 5700 computer (burst analysis). Total system gain used was typically 12,000. The neuronal activity was discriminated with a template-matching algorithm (Plexon Inc.) in real time to provide single unit spike rate data. Whole channel (multiple-units/channel) data was analyzed using custom programs for burst recognition and analysis.

The recording medium consisted of a 50/50 mixture of fresh DMEM or MEM and medium conditioned by culturing the respective tissues in flasks. Osmolarity was adjusted to 320 mOsmoles. TMPP was generously provided by the Naval Health Research Center/Toxicology Detachment (Wright Patterson Air Force Base, OH). All drugs were applied to a constant volume medium bath (1.0 or 2 ml). Stock concentrations were prepared so that sample volumes added never exceeded 2% of the total bath volume.

The experiments described lasted for several hours and, in some cases, for several days. During these experimental periods it was necessary to follow the evolution of activity with time and in response to test substances. We found bins of one minute to be adequate temporal windows for summarizing vast multichannel data without substantial phase delay. In these bins, activity variables such as spike and burst production remain numbers, whereas other variables such as burst duration, period, and integrated amplitude are averaged and form "minute means". Single unit activity per minute was averaged

across channels yielding mean network activity variables. These quantities were graphed as a function of time, providing a picture of the temporal evolution of activity and allowing a determination of stationary activity states (variations in burst and spike rates of <15%). An experimental episode mean was obtained from the minute values comprising the time period from the addition of a pharmacological substance to the next manipulation (wash or TMPP concentration increase). Control periods always were greater than 30 min., whereas experimental episodes ranged from 20-40 min. Within single experiments, significance of changes induced by drug application was tested with a paired Student's t-test, with $p<0.05$ accepted as significant. For pooled data, significance was tested with a one-way ANOVA followed by a post hoc Dunnett's test, $p<0.05$.

To derive bursts from spike data, the analog channel output was integrated, after rectification and filtering with low pass RC circuits with time constants of 50 ms. For display on chart recorders, pen inertia increased the time constant to approximately 200 ms. Fig. 2.2 shows whole channel, non-discriminated spike trains and the corresponding integrated profiles reflecting bursts. Such profiles allow a simple quantification of burst periods, durations, and burst amplitudes. The latter are influenced by the number of units recorded by an electrode, the spike amplitude, and the spike frequency in bursts. However, when the first two variables are constant (which is normally the case), the spike frequency dominates. This situation becomes simpler after spike discrimination in which the integrated profile represents only one selected unit. Clearly, toxic substances can change activity patterns as well as spike amplitudes and shapes, and a simultaneous monitoring of multiple variables is generally necessary.

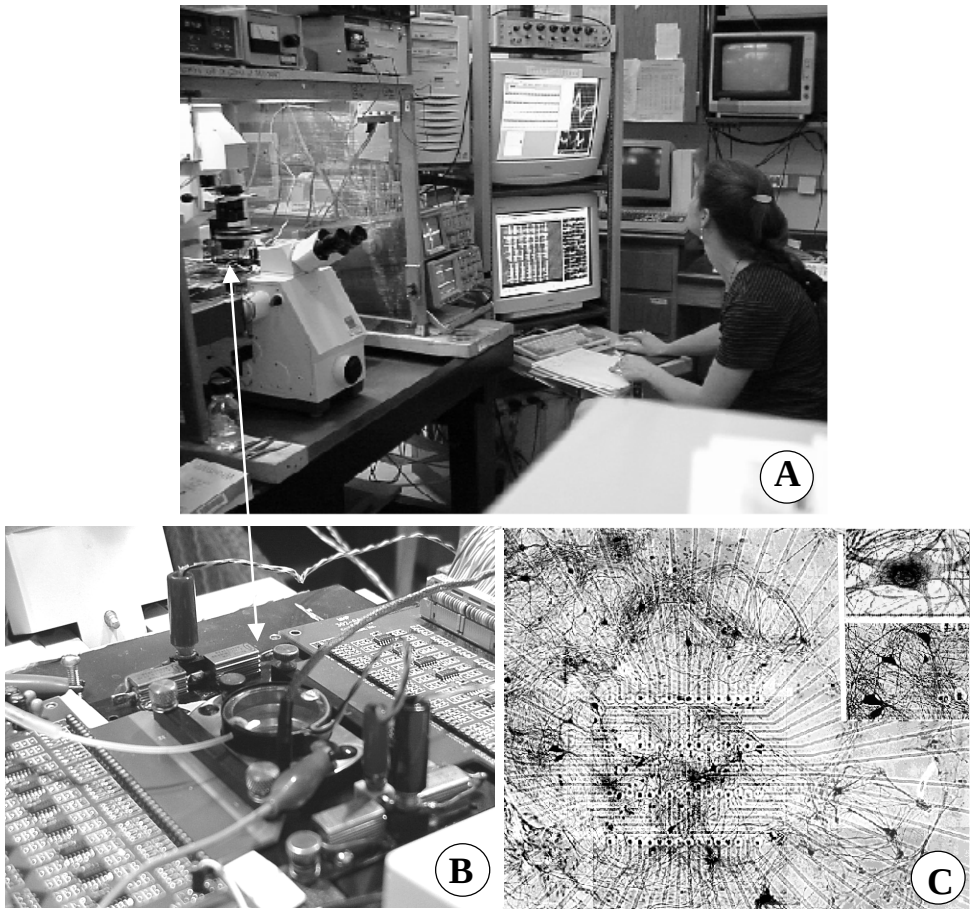

Figure 2.1. Experimental workstation. (A) Faraday cage with inverted microscope and culture life support accessories including DC power supplies for heating and gas metering equipment for providing 10% CO_2 in humidified air at 15 ml/min to maintain pH of the culture at 7.4. Oscilloscopes and two monitoring screens display data digitized by the Plexon multichannel data amplification and processing system. (B) recording chamber on microscope stage with Plexon preamplifiers attached. A cap with a heated window covers the medium bath and maintains a10% CO_2 atmosphere while allowing continual microscope observations. (C) Neuronal network on recording matrix of a 64-electrode array plate. Mouse embryonic spinal cord; age: 52 days in vitro.

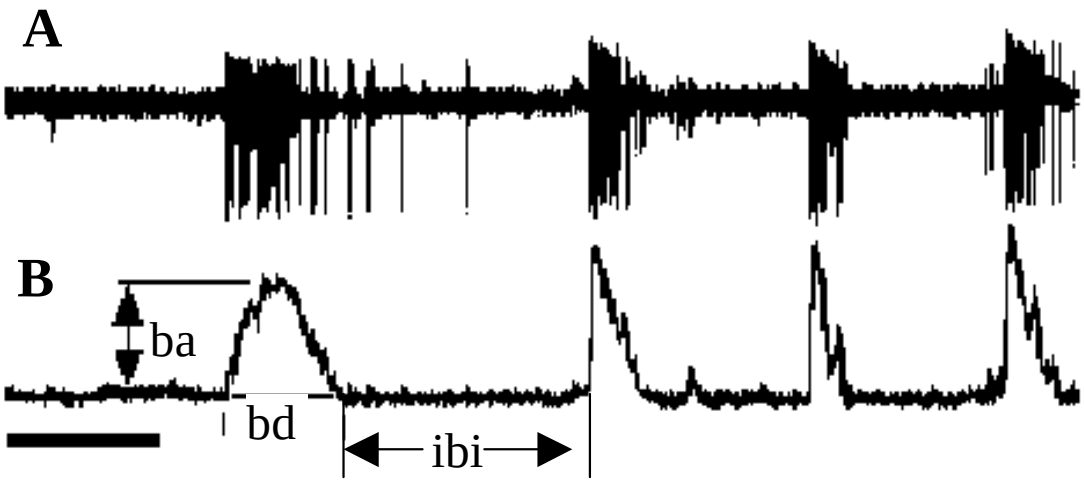

Figure 2.2 Analog integration of spike trains from all active units recorded by a single electrode. (A) Raw data displayed on oscilloscope, (B) the same data integrated with a time constant of 70 ms and displayed on chart recorder. Pen inertia increases the time constant to approximately 200 ms. Note the frequency dependence of integration, which responds only to bursts and ignores single spikes. Bar: 1 sec; ba: integrated burst amplitude; bd: burst duration; ibi: interburst interval.

Results

General Network Responses to TMPP

TMPP was evaluated initially as an unknown sample to determine the extent that the neuronal network sensor paradigm could be used for rapid classification of this neurotoxicant. Under control conditions, spontaneous activity from neuronal networks combined phasic and tonic spiking with bursts of variable durations into complex temporal patterns. Spikes were typically biphasic with duration of 0.5 to 1.0 ms and amplitude ranging from 200-1200 μV. Typical spontaneous baseline burst rates, averaged across the units recorded, ranged from 2-30 bursts per minute (bpm) and burst durations ranged from 80-300 ms (Fig.2.3A). Application of a low concentration of the unknown sample (2 μM) revealed an increase in the percentage of spikes found in bursts or by triggering bursting, if it is not present during the native spontaneous activity (Fig. 2.3B). In addition, the compound decreased the temporal variability of burst variables such as burst rate, burst duration, burst period, and integrated burst amplitude, and synchronized bursts on all channels. TMPP effects appeared to be "global", i.e. all monitored channels exhibited a similar response. At 2 μM, all channels reflected a reduction in the complexity of burst durations, and most channels showed an increase in burst amplitudes that, however, still revealed fluctuation in magnitude. At 100 μM TMPP, a substantial increase in burst amplitudes was observed, together with a remarkable decrease in the variability of amplitudes, burst rates, and burst durations (Fig. 2.3C & 2.3D). In this instance the response was more rapid (approximately 2 min), and regularization of burst

amplitude was immediately apparent. After 20 min, the network attained a highly regular pattern, with synchronized bursts of similar spike form and time course. These observations were completely consistent with the classification of the unknown compound as an antagonist of inhibitory transmission with strong similarity to other compounds capable of inducing convulsant activity, such as the $GABA_A$ receptor inhibitor bicuculline. Subsequent experiments were performed to explore the utility of network parameters and coefficients of variation as metrics for neuronal network performance using both TMPP and bicuculline. In addition, we determined changes in network behavior resulting from TMPP exposure after pharmacological modulation of neurotransmitter pathways, including cholinergic and GABAergic types A and B.

Figure 2.3

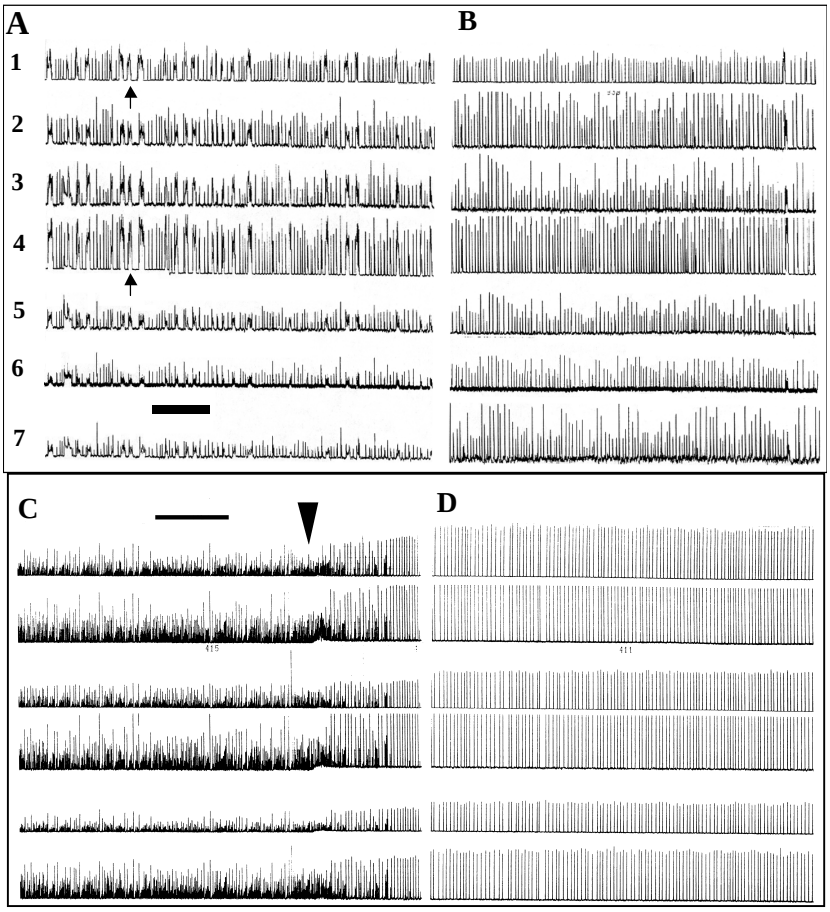

Figure 2.3 Burst pattern changes in response to TMPP shown with integrated spike data as displayed on a chart recorder. (A) Native activity showing bursts of short and long durations, with irregular burst amplitudes. (B) The same channels 20 min after application of 2 μM TMPP. Burst durations have regularized with the disappearance of long duration bursts (arrows), and burst amplitudes have increased on most channels (especially Ch 2 and 7). (C & D) Responses of a different network to 100 μM TMPP applied at the arrow. Within 3 minutes, the activity transitions from irregular, partially coordinated bursting to a much more regular and synchronized pattern. (D) 20 min after TMPP application, the network has reached a quasi-periodic oscillatory state. Each bar represents 1 min. Arrows indicate time of TMPP addition. Amplitude of traces is proportional to spike frequencies within bursts.

The restructuring of network spike patterns by TMPP is demonstrated in Fig. 2.4. The evolution of activity in terms of the variables burst rate and spike rate (per min) is shown for a 150 min time period (Fig. 2.4A). The network responded to 20 μM TMPP with a small increase in spike production (25 ± 1.9%, mean ± SEM, n=41 units), but with a very large increase in burst production; the burst rate significantly rose from a control level of 3 ± 1.1 bpm (n=14 channels) to 30 ± 0.8 bpm after exposure to TMPP. No further statistically significant changes were observed in either spike or burst rate with subsequent increases of the TMPP concentrations to 40 and 80 μM, suggesting that receptor saturation is reached near 20 μM. As shown in the raster display (Fig. 2.4B), the native activity consists of spontaneous spiking with minimal coordinated bursting. In this network, TMPP generated network bursting that is coordinated among channels, without causing a major change in spike production (Fig. 2.4C).

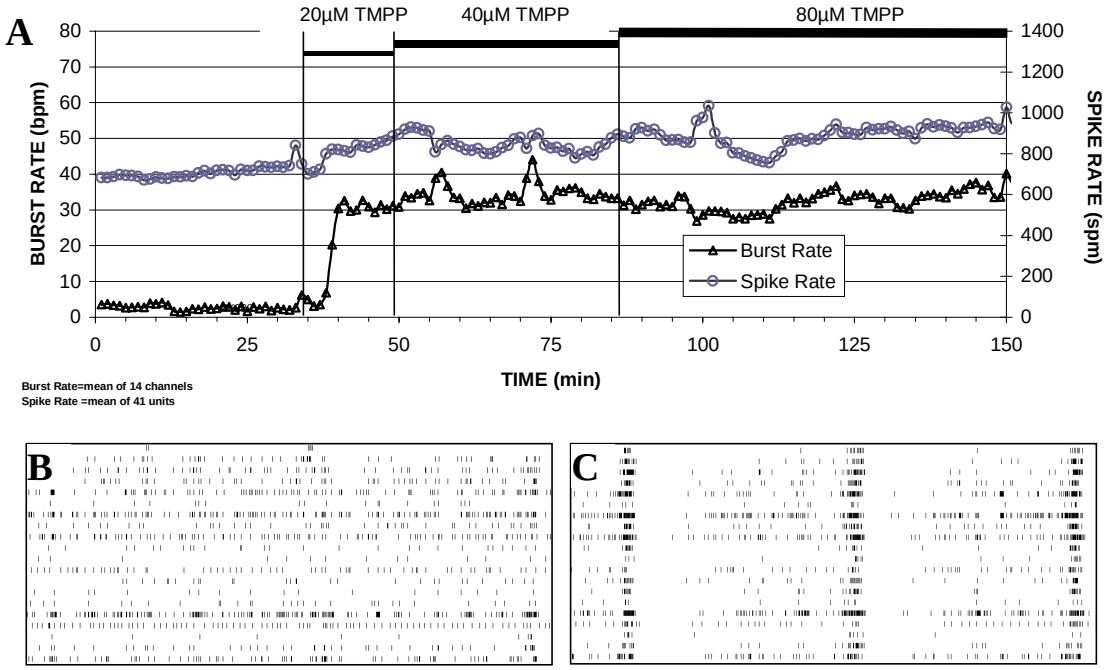

Figure 2.4 (A) Temporal evolution of burst and spike rate of a frontal cortex culture subjected to three concentrations of TMPP. The spike production per minute (circles) is minimally affected by the addition of 20 µM TMPP, but the burst rate increases from 2 to 30 bpm about 5 min after this addition. Subsequent increases of TMPP to 40 and 80 µM produce no further increases. (B) Spike raster display of activity at the 25 min mark in A. Note the lack of bursting and activity coordination among the 20 channels depicted. (C) The same channels at the 45 min mark in A. Burst organization and channel coordination can be seen. Both panels represent 5 sec of data.

TMPP decreased the variability of network bursting, as summarized in Fig. 2.5, for burst duration, interburst interval (the interburst interval extends from the end of one burst to the beginning of the next burst), and burst rate. The mean coefficients of variation (CVs) are plotted from 8 experiments (197 total channels) for both control and TMPP-treated conditions. In each case, the CVs were markedly decreased in a statistically significant manner after exposure to TMPP. Such increases in the reliability of burst events, concomitant with increased neuronal synchronization and increased spike

frequencies within each burst, are characteristic of compounds with known epileptogenic properties.

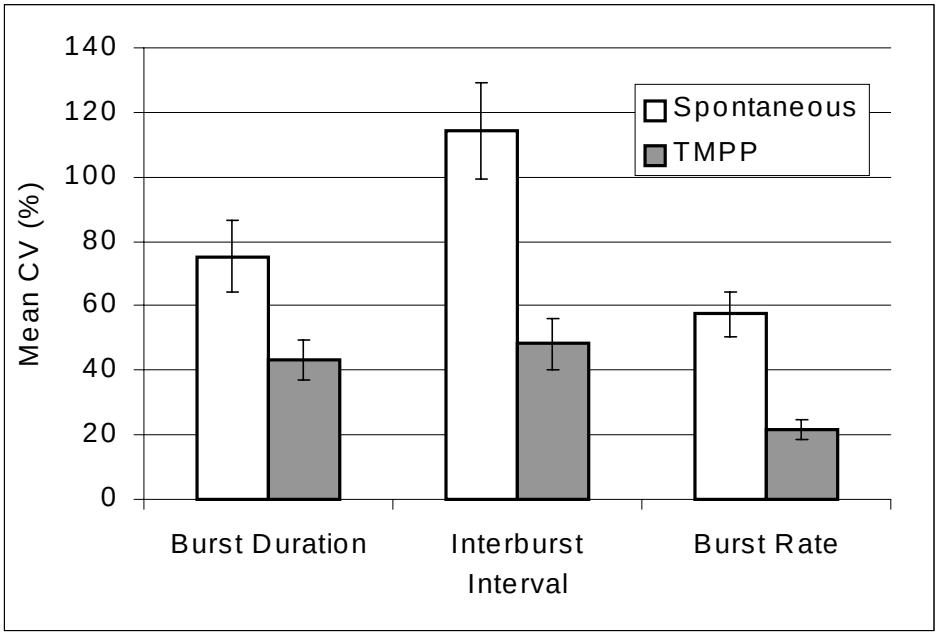

Figure 2.5 Mean coefficients of variation for burst duration, interburst interval, and burst rate during spontaneous activity (clear bars) and in the presence of TMPP (20-100μM, solid bars) calculated for 8 separate cultures (197 channels). 20 min segments of activity for each experimental condition (episode) in individual experiments were used to calculate mean and standard deviations of each burst variable for individual channels. Episode CVs for each channel were calculated, and a mean network CV was obtained from all channel CVs. TMPP decreases the temporal variability of these burst variables. Error bars represent SEM. All changes are statistically significant (ANOVA, $p<0.05$).

Although pattern changes to TMPP influences can be determined unmistakably by visual inspection (cf Fig. 2.4), a simple relationship between burst rates and TMPP concentration does not exist because of a dependence on the native activity of the test culture. As shown in Fig. 2.6, burst rates increased when initial burst activity was relatively low but decreased when the native activity was high. Healthy cultures often can exhibit a wide range of native bursting activity and can yield mean activity values not unlike data depicted in Figs. 2.6A and 2.6B. Data from two experiments (Fig. 2.6C), in which the difference between TMPP and native activity is plotted against the native activity, show an approximately linear relationship with a crossing of the zero line at 16 bpm. These data imply that cultures with native burst rates near 16 bpm will show little change in burst rate with application of TMPP. However, other variables, such as burst amplitudes and the associated CVs of the burst variables, will change dramatically.

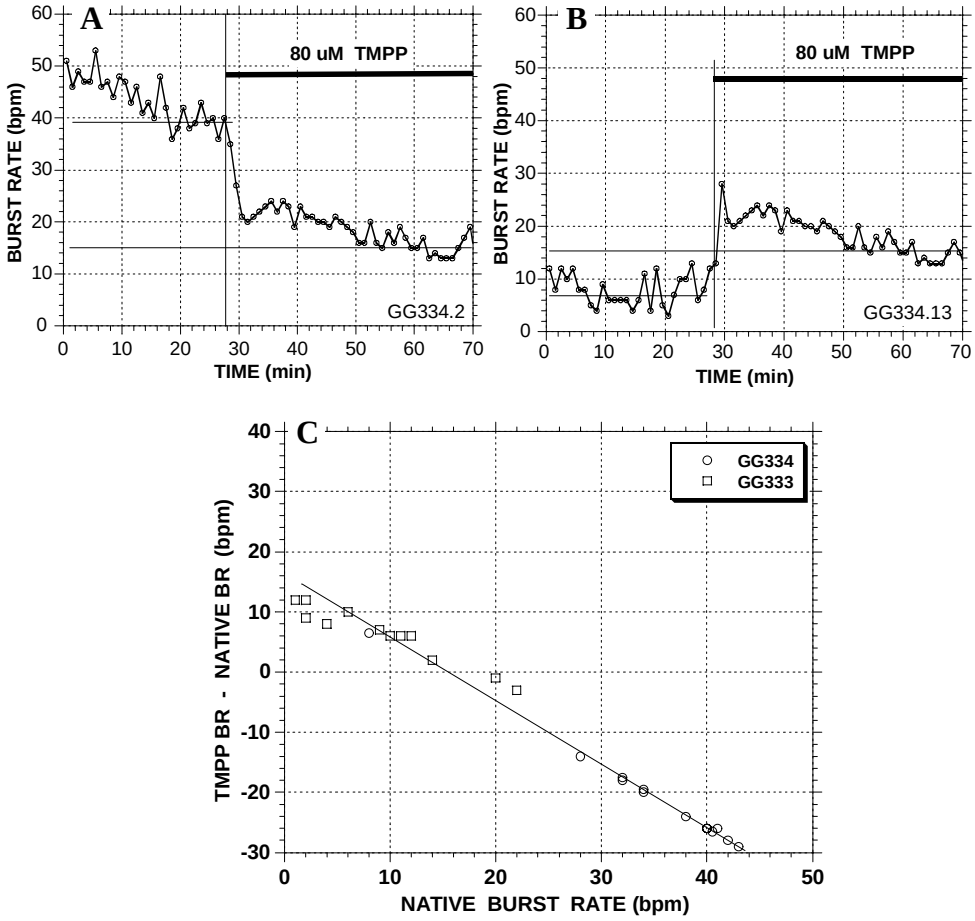

Figure 2.6 Dependence of TMPP burst rates on native activity states. (A, B) Single channel profiles of burst rate changes upon addition of TMPP. High native burst rates are reduced by TMPP, whereas low initial rates are increased. Panel C shows data from two networks (27 channels total) plotted as the difference between TMPP and native burst rates against the native burst rate. The crossover occurs at approximately 16 bpm.

Comparison with Bicuculline

The pattern changes induced by TMPP were very similar to what is seen after application of bicuculline methiodide. Despite the dramatic effect on bursting, network synchronization, and variability of burst parameters shown by both compounds, neither compound exerted a consistent effect on spike shape or spike amplitude (Fig. 2.7). Fig. 2.8A shows such a bicuculline response on three channels from a slow speed chart recording. Increases in burst amplitude and cross-channel synchronization comparable to those changes evoked by administration of TMPP (Fig. 2.3) were observed. Like TMPP, bicuculline burst rates also depended on the initial network activities (Fig. 2.8B).

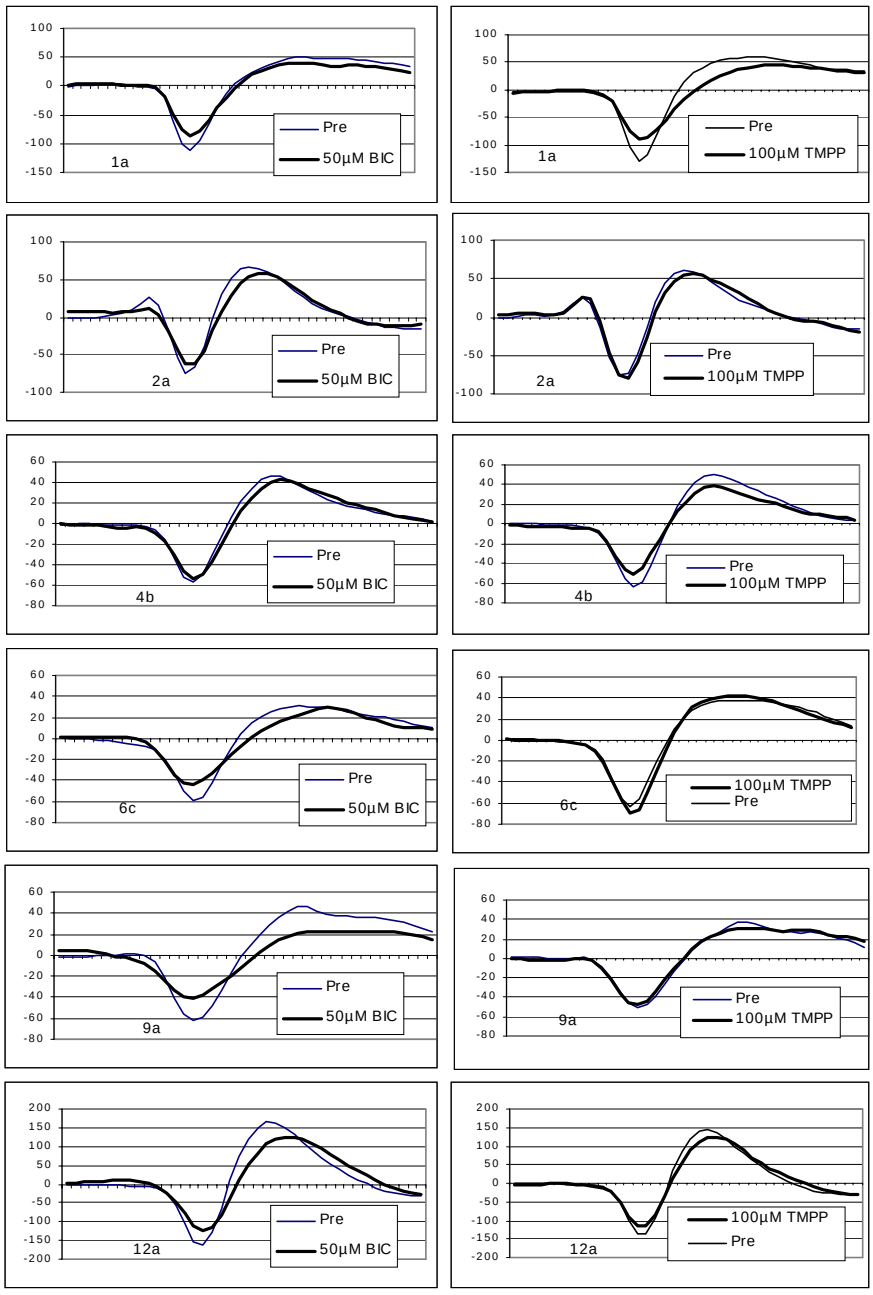

Figure 2.7 Effects of bicuculline and TMPP on waveform shapes. Each line represents the mean of 50 consecutive action potentials. There are no consistent changes induced by either drug. Window width is 1ms. Amplitudes are µV.

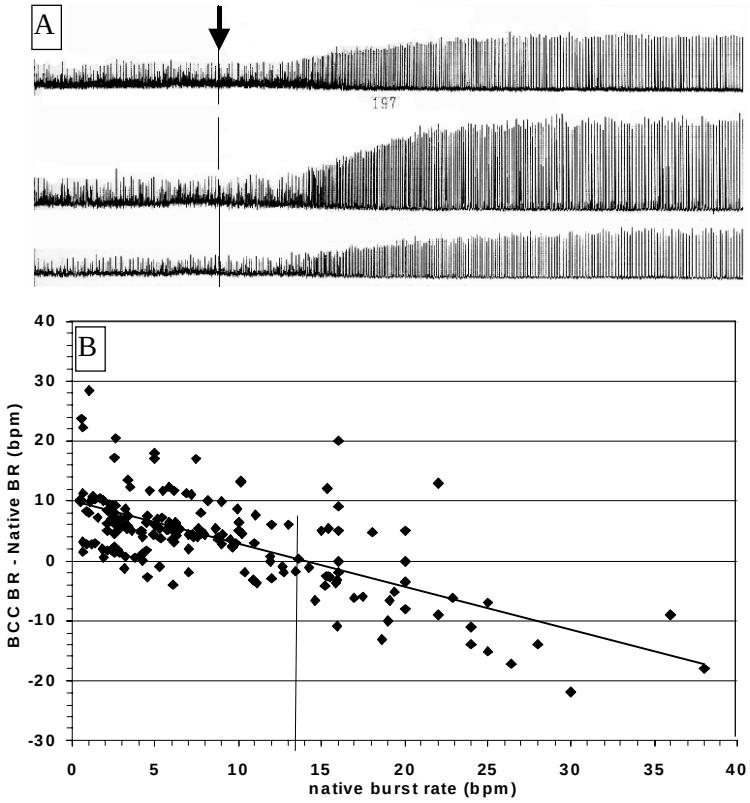

Figure 2.8 Network responses to 40µM bicuculline added at arrow. (A) Integrated burst data from a slow speed chart recording showing a transition from native bursting to a disinhibited activity state characterized by increases of spike frequencies within burst (increased integrated burst amplitudes), regularization of burst amplitudes, and activity coordination among channels. (B) The burst rates established under bicuculline are a function of the initial activity. Low initial BR are increased, whereas high initial BR are decreased. The crossover occurs at approximately 16 bpm (13 experiments, 160 channels total).

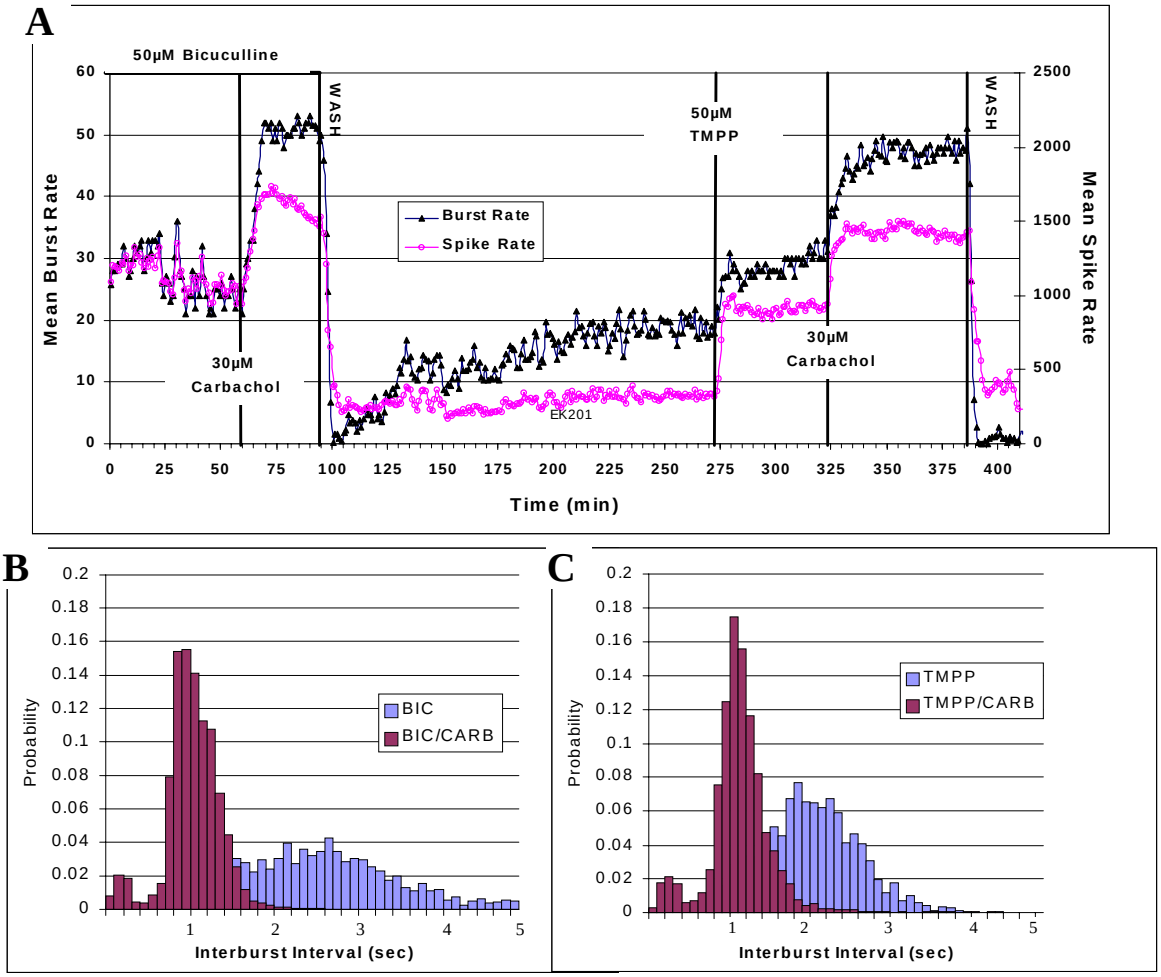

Figure 2.9 (A) Evolution of activity under 50µM bicuculline and 50µM TMPP showing similar burst and spike rates. Subsequent additions of 30µM carbachol also produced almost identical effects. (B and C) Burst interval distributions for the conditions shown in A also reveal a highly similar shift to shorter intervals with distribution modes at approximately 1 sec.

Fig. 2.9A illustrates network responses to co-application of bicuculline and carbachol, a drug combination used to elicit hippocampal theta oscillations *in vitro* (Lukatch and MacIver, 1997; Psarropoulos and Dallaire, 1998; Williams and Kauer, 1997). As expected, immediate increases in both burst and spike rates were produced after the administration of carbachol (30 µM). After washout, the network activity recovered to a stationary state. The experiment then was repeated with TMPP substituted

for bicuculline. The similar response profiles of bursting and spiking to both combination of compounds suggest that TMPP and bicuculline share common mechanisms. Figs. 2.9B and 2.9C shows histograms of interburst intervals constructed from the data shown in Fig. 2.9A. The distribution under 50 µM TMPP is narrower than that under 50µM bicuculline, reflecting a more stable oscillation during the TMPP episode. Nevertheless, bicuculline/carbachol and TMPP/carbachol produced nearly identical interval distributions.

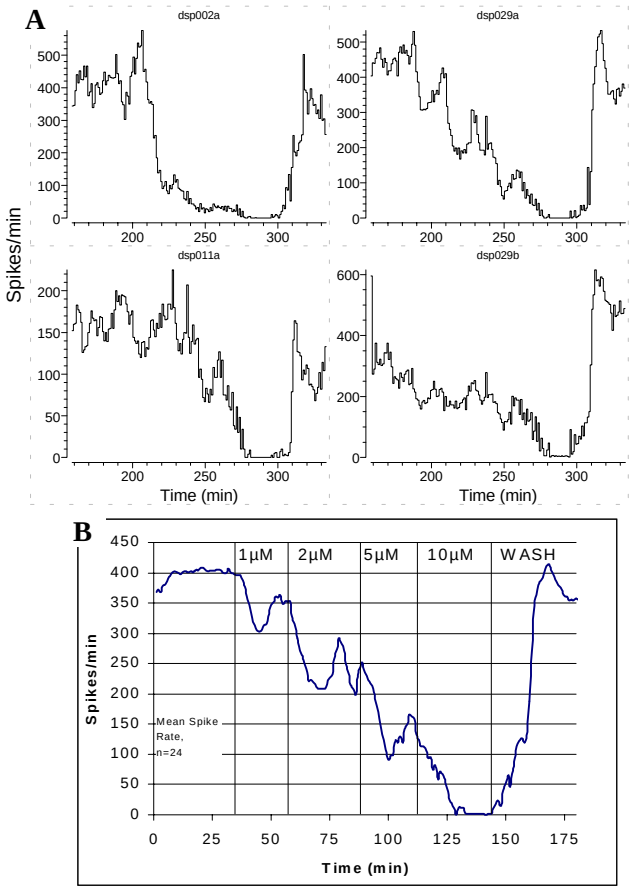

Figure 2.10 Bath application of GABA inhibits spiking in a dose dependent, reversible fashion. (A) Responses of a sample of 4 out of 24 channels as GABA was titrated from 1 - 10 µM, followed by two complete medium changes, which restored spiking to near initial levels of activity. (B) Mean spike rate graph constructed from 24 separate channels from the experiment shown in A. Vertical lines mark the times when GABA concentrations were raised to the concentration indicated.

Mechanism of Action of TMPP

To test the hypothesis that TMPP and bicuculline share a common mechanism of action, we examined the competitive interactions of GABA and TMPP. All neuronal tissues in culture responded to GABA. Spinal monolayer cultures were shown to terminate bursting at 18 ± 5.0 μM (mean ± SD, n = 12 cultures, Jordan, 1995). Frontal cortex tissue may be more sensitive and terminates bursting and spiking between 10 and 15 μM. Spike rate responses of 24 discriminated units from a frontal cortex culture were acquired (Fig. 2.10A), and a mean spike rate of all identified units as a function of time and GABA concentration was derived (Fig. 2.10B). Bath application of GABA inhibited spontaneous activity in a reversible, concentration-dependent manner. All spiking was abolished at 10 μM, with a single medium change restoring the activity to control levels.

Figure 2.11

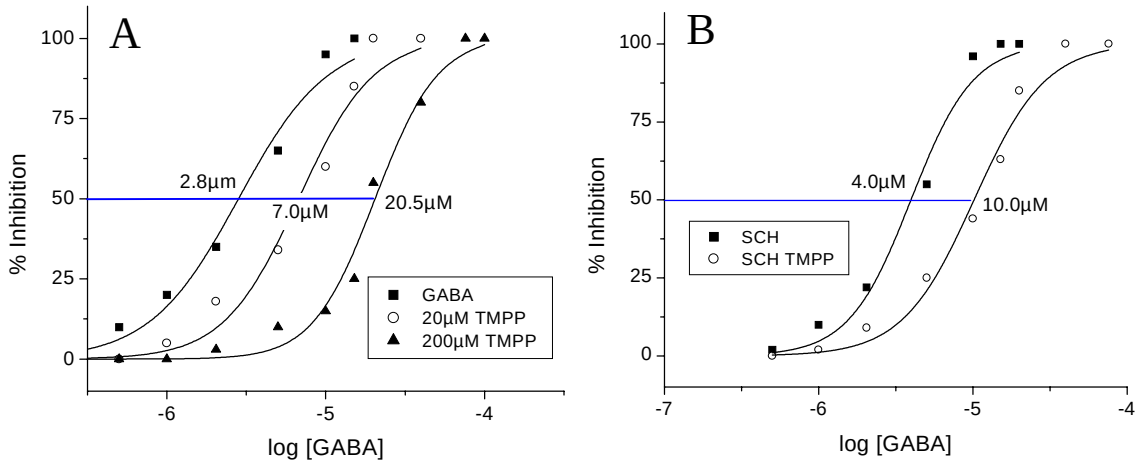

Figure 2.11 TMPP is a competitive antagonist of GABA inhibition of spiking activity. (A) Dose response curves for GABA inhibition of spontaneous spiking under three conditions, GABA only, in the presence of 20 μM TMPP, and in the presence of 200 μM TMPP. EC_{50}s were 2.8, 7.0 and 20.5 μM, respectively. (B) GABA titration repeated with the competitive $GABA_B$ receptor antagonist SCH50911 (50 μM), limiting effects to those mediated by the $GABA_A$ receptor, resulted in an EC_{50} of 4.0 μM. With both 50 μM SCH50911 and 20 μM TMPP, the curve was shifted to the right, with an EC_{50} of 10.0 μM. The effects of the two antagonists are additive, possibly indicating separate sites of action.

Dose response curves were calculated from the mean spike rate graphs generated by each network (Fig. 2.11). The EC_{50} for inhibition of spontaneous spike rate by GABA was 2.8 μM (2 cultures, n=48 channels). Repeating the experiment in the presence of 20μM TMPP (2 cultures, n= 56 channels) shifted the dose-response curve to the right, with an EC_{50} of 7.0 μM. A further increase in TMPP concentration to 200 μM (1 culture, n=20) resulted in an EC_{50} for GABA inhibition of 20.5μM. The similar shapes of the dose-response curves, with nearly parallel center segments of the curves, and the maintained GABA efficacy in the presence of 20 or 200μM TMPP implies competitive antagonism by TMPP.

Kao et al. (1999) reported that 5μM TMPP decreased both amplitude and frequency of spontaneous inhibitory postsynaptic currents (sIPSCs). The decrease in amplitude was consistent with an antagonistic effect at the $GABA_A$ receptor. The mechanism underlying the decrease in sIPSC frequency, which implies a presynaptic locus, is unexplained. A possible explanation could be action at the $GABA_B$ receptor, which has been shown to decrease release of both glutamate and GABA (Capogna et al.,

1996; Poncer et al., 2000; Stevens et al., 1999). To test the possible interaction of TMPP with the $GABA_B$ receptor, we first titrated GABA in the presence of the competitive $GABA_B$ antagonist, SCH50911 (Fig. 2.11B). With the $GABA_B$ receptors blocked, GABA inhibited spiking with an EC_{50} of 4.0 µM (n=12), which is significantly different from the EC_{50} of 2.8 µM for GABA action through both $GABA_A$ and $GABA_B$ receptors (Fig. 10, $p<0.05$). This indicates a contribution of $GABA_B$ receptors to the inhibition of spontaneous spiking by bath applied GABA. However, when GABA was titrated in the presence of SCH50911 (50 µM) and 20 µM TMPP, an EC_{50} of 10.0 µM (n=12 channels) was obtained. The inhibition of spiking, with both GABA receptors blocked, was significantly different from GABA inhibition in the presence of only TMPP. This result shows that the effects of TMPP and SCH50911 are additive in antagonizing GABA inhibition of spiking and imply that the effect of TMPP on sIPSC frequency is not $GABA_B$ mediated.

Discussion

The present study has demonstrated the utility of neuronal networks for detection and classification of a model neurotoxicant, TMPP. TMPP-induced changes in network properties were evident within minutes of administration, such that TMPP could be quickly classified as a convulsant. Detailed analysis of spike and burst parameters, in particular the CVs, revealed that TMPP has a profile similar to network disinhibitors, such as bicuculline, a well-known antagonist of the $GABA_A$ receptor. These findings are consistent with TMPP studies that span from whole animal neurobehavioral and EEG measurements (Lin et al., 1998; Lindsey et al., 1998) to studies at the molecular level focusing on $GABA_A$ receptor function (Higgins and Gardier, 1990; Kao et al., 1999).

Previous studies have shown that the effects of TMPP are rapid and do not depend on a metabolite of the compound (Rossi et al., 1998). Binding assays have revealed that TMPP binds to the $GABA_A$-benzodiazepine receptor complex with greater affinity than does picrotoxin (Bowery et al., 1976; Casida *et al.*, 1976; Higgins and Gardier, 1990), but with no apparent binding affinity for $GABA_B$, noradrenergic, dopaminergic, or cholinergic receptors (Jung et al., 1995). Past work examining ion flux (Higgins and Gardier, 1990), receptor binding (Bowery *et al.*, 1976; Casida *et al.*, 1976; Toia and Casida, 1987), and membrane currents (Kao *et al*., 1999) have demonstrated that $GABA_A$ receptor function in dissociated neural cells can be affected by TMPP. The results presented here confirm these findings: Competitive inhibition of GABA and a lack of

influence on the $GABA_B$ receptor were demonstrated by the dose response curves of Fig. 2.11.

TMPP is not an "excitatory" substance as is glutamate, NMDA, or even ACh. Rather, its responses are classically "disinhibitory". Whereas excitation increases spike production without generating organized patterns, disinhibition causes highly regular, synchronized burst patterns. Although an increase in spike production often is associated with this change, it is not the salient feature. TMPP fits unmistakably in the category of the disinhibitory agents studied so far, and its actions closely resemble the effects of bicuculline.

The results presented also demonstrate that the monitoring of a single activity variable is not sufficient for reliable detection of convulsion-inducing compounds. This is seen in Fig. 4, in which application of 20-80 µM TMPP elicited only minor changes in spike rates, but produced a dramatic reorganization of the network activity into synchronous, quasi-periodic burst episodes. Burst rate changes also have a “blind spot”. This phenomenon also is evident in Figs. 6 and 7, which demonstrate that the burst rates resulting from disinhibition with either TMPP or bicuculline depend upon the native burst rates of the network. Networks with spontaneous native activity ranging from 14 –18 bpm may not show the presence of a burst-inducing compound, if only this one variable is observed. However, burst durations, spike frequencies within bursts, coordination among channels, and, especially, the regularity of all activity variables change noticeably upon addition of TMPP.

The native burst rate at which a disinhibitory compound elicits only minor burst rate changes (near the cross-over points of Figs. 6 and 7) may be tissue- or compound-specific. Although the mechanism is not clearly understood, it probably is linked to burst after-hyperpolarization. As TMPP and bicuculline increase spike frequencies in bursts, the burst duration variability is lessened, and the burst duration generally increases. Small, short-duration bursts are eliminated from the pattern. Consequently, for a network bursting above 20 bpm, application of a disinhibitor causes a reduction in burst rate. Networks with slow initial activity have large interburst intervals that can accommodate increases in burst rates and durations, without encountering AHP limiting effects. These examples highlight the need for a multivariate analysis approach to provide reliable quantification of compound responses.

It is important to emphasize that the concentrations at which networks respond correlate with those used *in vivo*. This was shown for trimethyltin chloride (Gramowski et al., 2000) and for the cannabinoid mimetic anandamide (Morefield et al., 2000). With regard to the relevance of the concentrations used in the present study, it has been demonstrated that IP injection of TMPP into adult Sprague-Dawley rats causes partial kindling of electroencephalographic paroxysms at ≥0.1 mg/kg, subclinical seizures at ≥0.2 mg/kg, clinical seizures at ≥0.4 mg/kg, *status epilepticus* at ≥0.6 mg/kg, and death at >0.7 mg/kg (Psarropoulou and Dallaire,1998). It recently has been shown that a single IP injection of 0.075 mg of TMPP induces a peak blood concentration of 1.5 μg/ml (Rossi et al., 1998). If we assume a rat of average mass (250 g) blood volume (64 ml/kg), then 0.3

mg/kg corresponds to approximately 1 μM TMPP. This crude approximation, which assumes no binding to blood proteins, suggests that the concentrations used *in vitro* are consistent with the TMPP dosage range associated with neurobehavioral alterations.

Neurons, by virtue of intrinsic, electrophysiological mechanisms, represent efficient transducers that report dynamics of cell death, receptor-ligand interactions, alterations in metabolism, and generic membrane perforation processes. However, single neurons are vulnerable and unreliable, and only networks of neurons form robust, fault-tolerant, spontaneously active dynamic systems with high sensitivity to their chemical environment and reproducible reactions (Gross et al, 1997, Morefield at al., 2000). Networks in culture generate response profiles that are concentration and substance-specific and react to a broad range of compounds (Gross and Kowalski, 1991; Gross et al., 1992; Gross, 1994; Rhoades and Gross, 1994; Gross et al., 1997). Additionally, changes in action potential patterns and action potential shape often can be detected before irreversible cell damage occurs. These reversible changes provide rapid warning and the opportunity for cycling varying concentrations of toxins through the same network.

Before *in vitro* systems can be used effectively, reliable data must be established on intra- and interculture repeatability, response sensitivity, and substance-specific response patterns. These include highly reproducible generation of test cultures, optimization of substance application protocols, and development of data analysis procedures that can

provide key data in real time. Thereafter, a new, powerful test system should emerge with the potential of making substantial contributions to the rapid screening of new compounds and the establishment of concentrations limits at which reversible and irreversible toxic effects commence. In light of the demonstrated longevity of neurons in culture (6-9 months, Gross, 1994; Kamioka et al., 1996), such test systems also will allow chronic exposure studies and investigations of developmental influences. Preliminary data suggests this concept is viable and that responses will be obtained from all substances able to stop or alter nervous system activity, as well as from general metabolic toxins.

Additional Considerations for the Use of Neuronal Networks in Toxicology

This work demonstrates the utility of neuronal networks as detectors of compounds possessing neural activity. It is likely that neuronal networks are capable of reporting the presence of most neurally active compounds that: a) bind to receptors, b) bind to or are solublized in the neuronal membrane, c) can be internalized, with subsequent effects on intracellular processes, including gene expression or metabolic processes; d) alter the function of ion channels, or e) change the intrinsic excitability of the neurons. The concentrations at which the networks react are usually within the ranges shown to produce physiological changes in whole animals. Thus, the promise of neuronal networks as biosensors is supported by a rapidly growing body of data. If this promise is realized, neuronal networks could fill a void that exists in current methodologies for human risk assessment in areas contaminated with pollutants, pathogens, or other agents. This is evidenced by a general inability to: a) simultaneously detect large numbers of possible threats, especially unknown or unanticipated ones, b) characterize the functionality of known agents that have been identified using conventional techniques, and c) predict human performance decrements caused by low levels of agents or synergistic effects of environmental toxicants.

This work also demonstrates how a novel compound, once detected, can be classified according to its action in changing the activity of the networks. The effects of TMPP on organization of activity into bursts and in increasing the frequency of spikes

within those bursts were comparable to those seen with bicuculline, and allowed the classification of TMPP as a disinhibitory substance. By accumulating a database of model compounds that produce different effects on neuronal network behavior, it is hoped these effects can be separated into distinct categories. One simple classification scheme might have three categories: Excitatory, Inhibitory, and Disinhibitory. Examples of compounds that might be considered representative of each category are respectively: a) glutamate, b) GABA, and c) bicuculline. All of these produce reliable network responses at narrow concentration ranges, which is a prerequisite for the use of a potential compound in the construction of a response template. Comparison of responses elicited by novel compounds with these templates will allow this novel compound to be categorized.

Conventional methods for detecting environmental threats are based primarily on chemical, antibody- or nucleic acid-based assays, which rely on chemical properties or molecular recognition to identify a particular agent. These methods can precisely identify compounds for which they are specifically tailored, but cannot detect compounds lacking that known molecular signature expected by the detector. Neuronal networks, on the other hand, respond to such a wide variety of substances that the identification of an unknown compound is problematical. The difficulty is exacerbated by the fact that rarely, if ever, will the absolute concentration of the compound be known. It may be feasible to construct floating dose-response curves, in which the concentration of the unknown can be varied relative to the concentration that first elicited an effect, but this methodology has not been proven. It is possible that an expert-based system, with a large library of

neuronal-network response profiles and utilizing algorithms similar to those used by speech-recognition software, could be developed to enable unknown identification.

If the goal of using neuronal networks as biosensors in civilian areas such as water monitoring or in military applications for real-time warning of chemical or biological attacks is to be attained, advancements in current laboratory-based technology must be made.

Needed advancements include:

- Implementation of large-scale production of cultures with reproducible responses to a wide range of neuroactive substances,
- Production of a system to maintain a stable artificial environment, with automated measurements of temperature, pH, osmolarity, glucose, amino acids, neurotransmitters, etc. from microliter-size volumes on a continual basis, to ensure that changes in network activity reflect modulation by potential threats and not variations in the network environment
- Development of a methodology to validate data generated from the cultures, so that false-positives can be minimized, as well as a method to interrogate the network, and ensure that it remains functionally responsive,
- Design of a system for automatic determination of the meaning data gathered, so that an alarm can be generated appropriate for the detected threat, and

- Determination of the set of network activity variables providing the most robust visualization of activity changes elicited by environmental threats, enabling compounds to be "fingerprinted" according to the changes they produce.

Each of these advancements presents unique challenges. The realization of all of them will require an interdisciplinary effort combining tissue-culture, computer science, statistics, fluid mechanics, physical chemistry, and neuroscience. The goal of implementing neuronal cultures as biosensors always must be driven by the cultures themselves, however. Without healthy, spontaneously active networks, all other efforts are wasted.

CHAPTER 3

NMDA RECEPTOR DEPENDENT PERIODIC OSCILLATIONS IN CULTURED SPINAL CORD NETWORKS

Summary

Cultured spinal cord networks grown on microelectrode arrays display complex patterns of spontaneous burst and spike activity. During disinhibition with bicuculline and strychnine, synchronized burst patterns emerge routinely. However, the variability of both intra- and interculture burst periods and durations are typically large under these conditions. As a further step in simplification of synaptic interactions, we blocked excitatory AMPA synapses with NBQX, resulting in network activity mediated through the NMDA receptor ($NMDA_{ONLY}$). This activity was abolished by APV, an NMDA receptor antagonist. The oscillation under $NMDA_{ONLY}$ conditions at 37 ^{0}C was characterized by a period of 2.9 ± 0.3 s (16 separate cultures). Over 98% of all neurons recorded participated in this highly rhythmic activity. The temporal coefficients of variation, reflecting the rhythmic nature of the oscillation, were 3.7, 4.7, and 4.9 % for burst rate, burst duration, and inter-burst interval, respectively (mean CVs for 16 cultures). The oscillation persisted for at least 12 hrs without change (maximum observation time). Once established, it was not perturbed by agents that block mGlu receptors, $GABA_B$ receptors, cholinergic receptors, purinergic receptors, tachykinin receptors, 5-HT receptors, dopamine receptors, electrical synapses, burst afterhyperpolarization, NMDA receptor desensitization, or the hyperpolarization-

activated current. However, the oscillation was destroyed by bath application of NMDA (20-50μM). These results suggest a presynaptic mechanism underlying this periodic rhythm that is solely dependent upon the NMDA synapse. When the AMPA/kainate synapse was the sole driving force (n=6), the resulting burst patterns showed much higher variability and did not develop the highly periodic, synchronized nature of the $NMDA_{ONLY}$ activity. Network size or age did not appear to influence the reliability of expression of the $NMDA_{ONLY}$ activity pattern. For this reason, we suggest that the $NMDA_{ONLY}$ condition unmasks a fundamental rhythmogenic mechanism of possible functional importance during periods of NMDA receptor dominated activity, such as embryonic and early postnatal development.

Introduction

The mechanisms driving the spontaneous activity of neuronal ensembles and their generation of spatio-temporal spike and burst patterns are difficult to study quantitatively *in vivo* because simultaneous monitoring of neurons in small ensembles is technically extremely difficult. However, neuronal networks grown in culture provide simpler systems in which a quasi-monolayer architecture can be coupled to planar microelectrode arrays that allow ensemble recording over long periods of time. We used murine spinal cord networks growing on such microelectrode arrays (Droge et al., 1986; Gross, 1994) to obtain long-term, multisite recording of spontaneous and pharmacologically modified activity (Fig.1.1). The chemical environment can be controlled with precision and specific activity states can be maintained and investigated for many hours, a time period usually not achievable *in vivo.* Although this provides a unique opportunity to investigate basic cellular and ensemble mechanisms related to the observed activity states, networks in culture still represent the interactions of multiple synaptic driving forces, resulting in complex spike and burst patterns.

In mammalian development, there is a short period during which neuronal networks are connected by purely excitatory synapses (Habets et al., 1987; Jackson et al., 1982). Throughout this developmental window, or when inhibitory synapses are blocked in more mature tissue, networks exhibit bursts of action potentials that are roughly synchronized across the population. It is suggested these synchronous population bursts are important in pruning and sculpting neuronal circuits during development (Tosney and

Landmesser, 1985). However, the mechanisms that initiate and terminate such bursting are unclear, especially in the absence of inhibitory circuitry.

Disinhibition of cultured networks, organotypic spinal cord cultures, and acute spinal cord preparations with inhibitory neurotransmitter antagonists reliably induces oscillatory behavior consisting of bursts of action potentials concomitant with intracellular Ca^{+2} oscillations (Lawrie et al., 1993; Rhoades and Gross,1994; Robinson et al., 1993; Wallen and Grillner, 1987; Wang and Gruenstein, 1997). Similar results also have been obtained by increasing excitability with ionic manipulations, such as low Mg^{+2} or increased extracellular K^{+}. Fictive locomotion can be elicited in intact spinal cord preparations, with burst patterns alternating between the right and left sides of the cord, by application of 5-HT, NMDA, or 5-HT and NMDA in combination or by elevated extracellular K^{+} (Bracci et al., 1998; MacLean et al., 1998; Wallen and Grillner, 1987). These studies have shown that inhibitory conductances are not essential for rhythmogenesis, but the relative contributions of cellular versus network properties in the production of rhythmic motor output are unresolved.

In order to study burst patterns in excitatory-only coupled networks, we pharmacologically reduced the inhibitory and excitatory neurotransmitter systems that drive spontaneous activity in cultured murine spinal cord networks to one dominated by NMDA receptor activation, a situation reminiscent of that found during the embryonic/early postnatal period (Scheetz and Constantine-Paton, 1994). The resulting activity (termed "$NMDA_{ONLY}$") is characterized by (1) a highly regular burst oscillation,

as evidenced by the low CV values for population burst variables, (2) burst synchronization among units in the network, and (3) a stationary burst rate of 21.0 ± 2.0 bpm (mean ± SD, n = 16 cultures), which is independent of the initial activity state. Blocking NMDA receptors in the presence of bicuculline (BCC) and strychnine (STR), which left the AMPA/kainate glutamate receptor subtypes as the sole driving force (n=6), produced network oscillations at a much lower level of organization as that seen during $NMDA_{ONLY}$ activity.. It appears that the NMDA receptor may be uniquely suited for production of the highly stable and uniform burst oscillations.

We explored burst termination mechanisms with potential contribution to $NMDA_{ONLY}$ activity. These include afterhyperpolarization (AHP), receptor desensitization, and depression of neurotransmitter release (O'Donovan, 1999). Blocking both AHP and NMDA receptor desensitization did not affect established $NMDA_{ONLY}$ oscillations. Synaptic depression, possibly resulting from exhaustion of the readily releasable pool (RRP) of excitatory neurotransmitter vesicles, has been observed in disinhibited whole spinal cord and spinal cord slices (Bracci et al., 1996a; Streit, 1993). CA3 population activity can be dominated by vesicle depletion and the time required to refill the RRP (Staley et al., 1998). Our results suggest that strong synaptic depression caused by the depletion of the RRP could serve as burst termination mechanism during $NMDA_{ONLY}$ activity, with the time needed to refill the pool setting the period of the oscillation.

Methods

Cell Culture

Cell culture procedures were identical to those described in Chapter 2 for spinal cord cultures.

Drugs and Solutions

Apamin, atropine, bicuculline, $CaCl_2$, charybdotoxin, curare, Evan's blue, glycine, KCl, $MgCl_2$, norepinephrine, and strychnine were purchased from Sigma Chemical Co., St. Louis, MO. APV, haloperidol, L-733,060, MCPG, NBQX, and SCH 50911 were purchased from Tocris Cookson, Ballwin, MD. Carbenoxolone was purchased from ICN, Costa Mesa, CA. Methysergide maleate was obtained from RBI, Natick, MA.

Extracellular Recording Procedures and Data Analysis

MEAs were placed into constant-bath recording chambers (Gross and Schwalm, 1994; Gross, 1994) and maintained at 37°C on a microscope stage. The pH was maintained at 7.4 with a continuous stream of filtered, humidified, 10% $C0_2$. Stainless steel chamber components were sterilized via autoclaving before each experiment. Neuronal activity was recorded with a two-stage, 64-channel amplifier system (Plexon Inc., Dallas), and digitized simultaneously via a Dell 410 workstation (spike analysis) and a Masscomp 5700 computer (burst analysis). Total system gain used was normally 12K. Spike identification and separation were accomplished with a template-matching algorithm (Plexon Inc.) in real time to provide single unit spike rate data. In addition, whole channel (multiple-units/ channel) data were analyzed offline using custom

programs for burst recognition and analysis. Burst patterns derived from spike integration (τ = 200ms) provided a high signal-to-noise feature extraction that has been shown to reveal modes of neuronal network behavior (Gross et al., 1994). From this approach, burst rate, duration, and interburst interval were readily quantified from individual recording sites.

Statistics

Statistical significance was determined using two sample Student's *t*-test with $P<0.05$ considered as significant. In order to quantify the periodicity of the bursting, as well as the synchronization of the neuronal population participating in each burst event, we calculated the coefficient of variation (CV) across time and across the network after 15-30 min stabilization periods to allow the networks to reach a steady activity state after pharmacological manipulation. Figure 3.1 summarizes the calculation of CVs. CV_{time} reflects the periodic character of the activity pattern (Bracci et al., 1996a). $CV_{network}$ reflects the synchronization between different neurons. CV_{time} was obtained from minute means of each channel by averaging over the experimental episode. The episode CVs per channel then were averaged to yield temporal network means. $CV_{network}$ was obtained by averaging values in 60-sec bins, followed another average across channels that yielded a $CV_{network}$ for each minute. These CVs were averaged for each experimental episode. The CVs were calculated for different burst variables: burst rate (BR), burst duration (BD), and interburst interval (IBI) during different experimental episodes (spontaneous, partial disinhibition with bicuculline, and $NMDA_{ONLY}$). Large CVs imply a wide range of variability in the activity of the networks across both time and the neurons recorded.

Hence, if a population was synchronized, but fluctuated together, low $CV_{network}$ and high CV_{time} were obtained. Conversely, a non-synchronized network with several regular (periodic) patterns yielded high $CV_{network}$ with low CV_{time}.

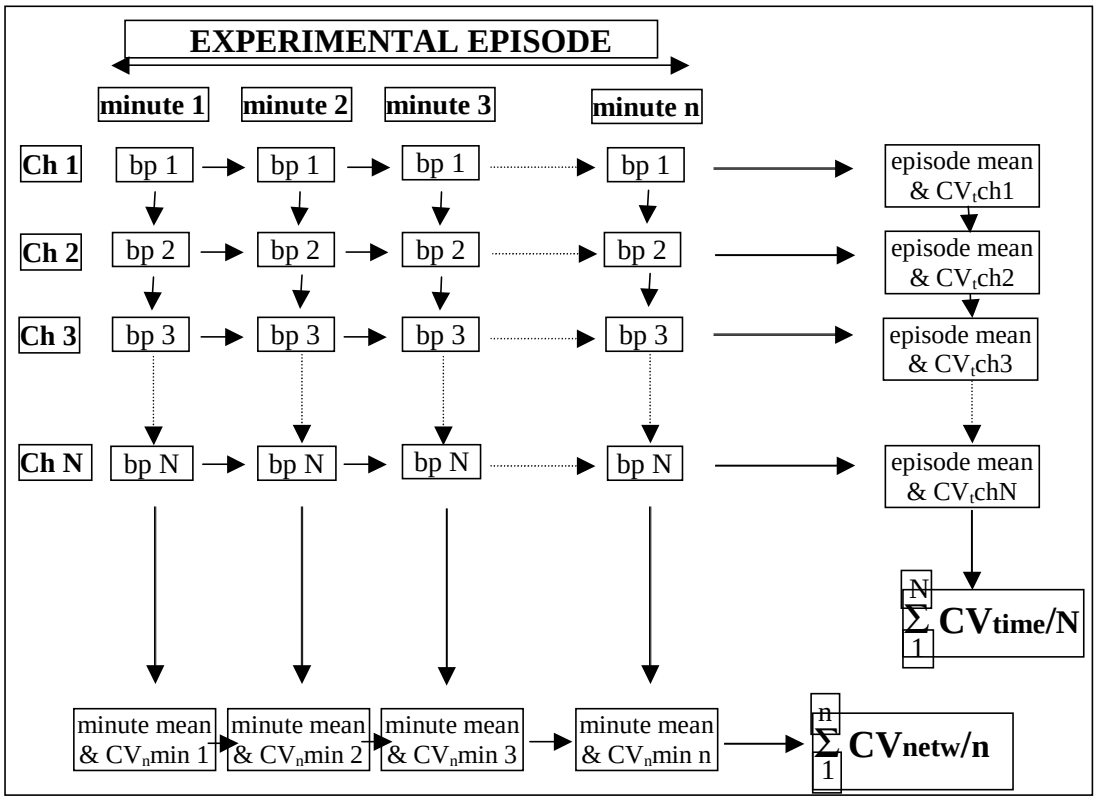

Figure 3.1 Determination of temporal regularity and network synchronization using coefficients of variation (CV). All calculations are based on one minute bins during which a specific burst parameter (bp) either is logged as a number for burst rate or averaged for burst duration and inter-burst interval. These values are used to obtain episode means with CVs for experimental episodes (left/right), or minute means for each minute of the experimental episode (top to bottom). The episode CVs (CV_{time}) for each channel represent a measure of temporal pattern fluctuation for that channel. Averaged across the network, CV_{time} reflect pattern regularity even if several patterns exist and even if they are not synchronized. Conversely, the CVs obtained by averaging minute values across channels ($CV_{network}$) represent channel coordination. Averaged across the experimental episode, $CV_{network}$ reflect the degree of network synchronization, even if the pattern fluctuates in time.

Results

In their original medium (native state), spinal cord networks typically exhibited multiple patterns of activity (Fig 3.2a). Disinhibition with the $GABA_A$ receptor antagonist BCC (40µM) elicited robust bursting activity that was synchronized across the network (Fig 3.2b). However, under BCC, the temporal variation in the burst period still was high. Further disinhibition by the blocking of glycine receptors using 1 µM STR did not reduce the variability of the burst period. When AMPA/kainate receptors were subsequently blocked with 10 µM NBQX, the networks were entrained to one common, highly periodic burst pattern activity (Fig 3.2c). This unique activity state persisted for up to 12 hrs without change in regularity (Fig. 3.2d).

Data presented in this report were obtained from 16 separate cultures. In a subset of 8 experiments, the oscillations with a period of 2.8 ± 0.2 s (mean ± SD), began almost immediately after the addition of NBQX, which followed the sequential addition of BCC and STR. This oscillation period was associated with high spatial and temporal burst pattern regularity. The eight remaining networks established longer burst periods after NBQX addition (4.3- 3.8 s) with less regularity of the bursts, suggesting that additional inhibitory mechanisms, such as $GABA_B$ receptor inhibition of vesicle release (Isaacson and Hille, 1997), might have prevented the establishment of the unique 2.8 s oscillation. Indeed, the addition of 50 µM SCH 50911 (a soluble $GABA_B$ antagonist) decreased the burst period in 5 out of 8 networks to 3.0 ± 0.3 s (mean ± SD).

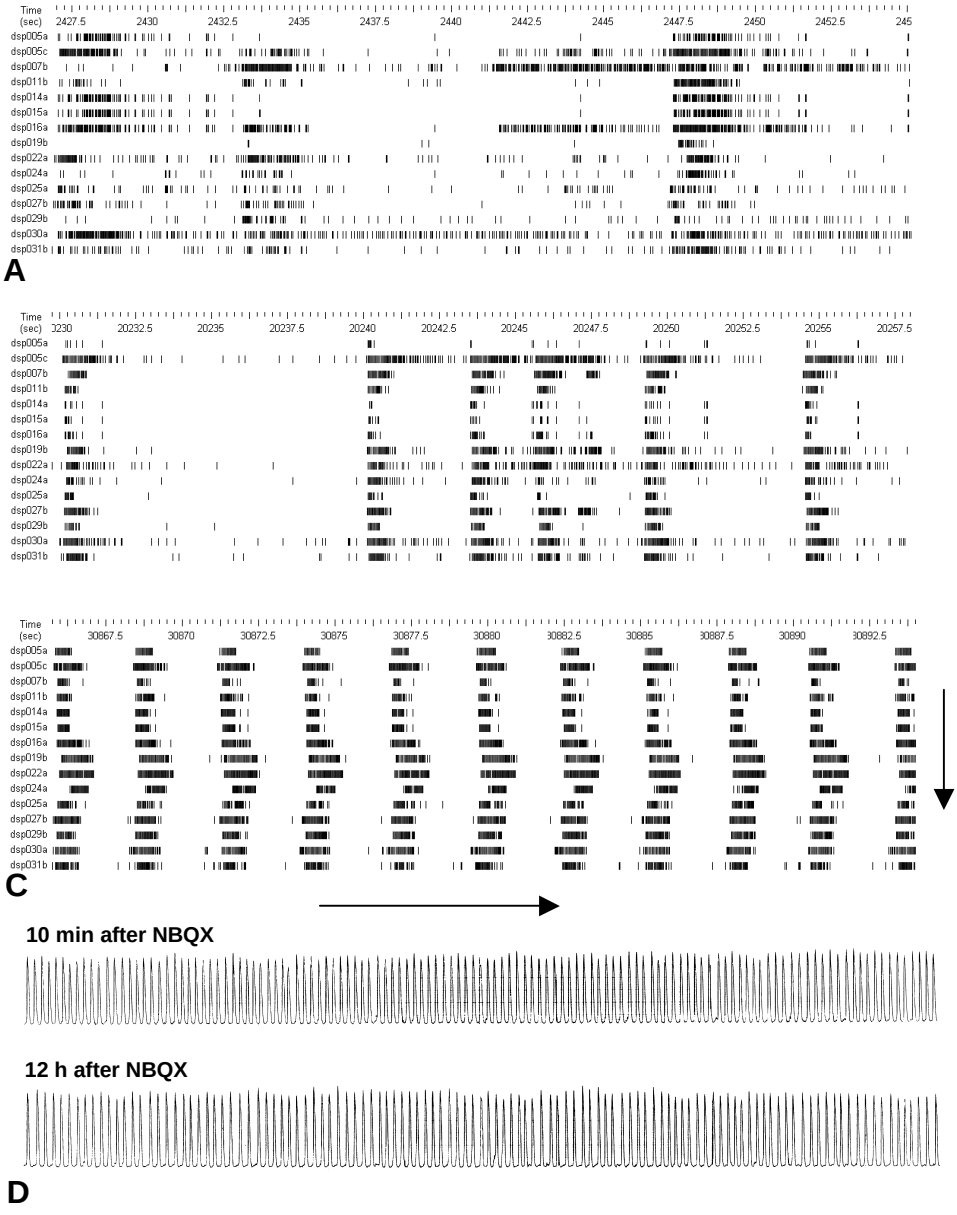

Figure 3.2 A, B, C: Simultaneous spike trains from 15 discriminated neurons during different experimental episodes (25 s samples). A: Spontaneous native activity displaying tonic and phasic firing with occasional coordinated bursting. B: 40µM bicuculline transforms the activity into a bursting pattern that is coordinated across neurons but with a high degree of variability in the interburst intervals (IBI) and burst durations (BD). C: $NMDA_{ONLY}$ activity consists of a synchronized periodic burst pattern. Two coefficients of variation CV_{time} and $CV_{network}$ are obtained from the temporal sequence (horizontal arrows) and the channel sequence (vertical arrows), respectively. CV_{time} provides a measure of the temporal variation of a specific network activity variable (e.g. BR, BD, IBI). $CV_{network}$ reflects the degree to which activity is coordinated among recorded neurons within the network. D: The long-term stability of the $NMDA_{ONLY}$ burst oscillation is demonstrated with chart recorder trace of integrated activity (τ = 0.7s) from a single channel at 5 min and after 12 hours of continuous NBQX exposure.

In the three remaining networks, the sequential application of 40 µM norepinephrine (NE), in addition to the above four compounds, led promptly to the adjustment of the burst oscillation to a regular, periodic burst period of 2.8 ± 0.2 sec (mean ± SD). NE is known to affect NMDA receptor desensitization and the slow burst afterhyperpolarization, two other potentially inhibitory mechanisms (Legendre et al., 1993; Madison and Nicoll, 1986; Tong and Jahr, 1994; Tong et al., 1995). It is important to emphasize that SCH 50911 and/or NE had no effect if they were added after the $NMDA_{ONLY}$ oscillation was established. These results indicate that $GABA_B$ receptor mediated inhibition of neurotransmitter release, or mechanisms sensitive to NE were sometimes sufficient to prevent the characteristic $NMDA_{ONLY}$ pattern from developing but were not necessary for its maintenance. It is also important to note that the low CVs characterizing the $NMDA_{ONLY}$ activity pattern were not obtained if the network burst rate following BCC/STR/NBQX was lower than 17 bpm. High pattern regularity and the characteristic 2.8s oscillation period were always linked.

The mean periods with associated SDs of all three pharmacological manipulations (1) BCC/ STR/ NBQX, (2) BCC/STR/NBQX/SCH, and (3)BCC/STR/NBQX/SCH/NE were not significantly different ($p>0.05$, t-test for two samples), and thus data from all 16 experiments were pooled for subsequent analysis. In order to quantify the periodicity of the bursting, as well as the synchronization of the neuronal population participating in each burst event, we calculated the coefficients of variation for several burst variables across time and across the network. All calculations were done with binned data from 1 min time intervals. The results of the CV calculations for three different burst variables

(burst rate (BR), burst duration (BD) and interburst interval (IBI)) under three different conditions, (spontaneous, disinhibited with 40 µM bicuculline, and under $NMDA_{ONLY}$) are summarized in Figure 3.3. During native conditions, the CVs are large, implying a wide range of variability in the activity of the networks across time and between the neurons recorded. 40 µM bicuculline reliably reduced the CVs of all three burst parameters, showing that disinhibition has a stabilizing effect on network oscillations. However, reducing the synaptic driving forces to one mediated through the NMDA receptor only produced CV_{time} of 2.6-5% (Fig. 3.3a) and entrained virtually all recorded neurons (n=678, 16 experiments), as evidenced by the global $CV_{network}$ for burst rate of 2.8%. The dependency of the oscillation on the NMDA receptor was demonstrated with 40-100 µM APV, which abolished activity in all cases (n=7).

Figure 3.3

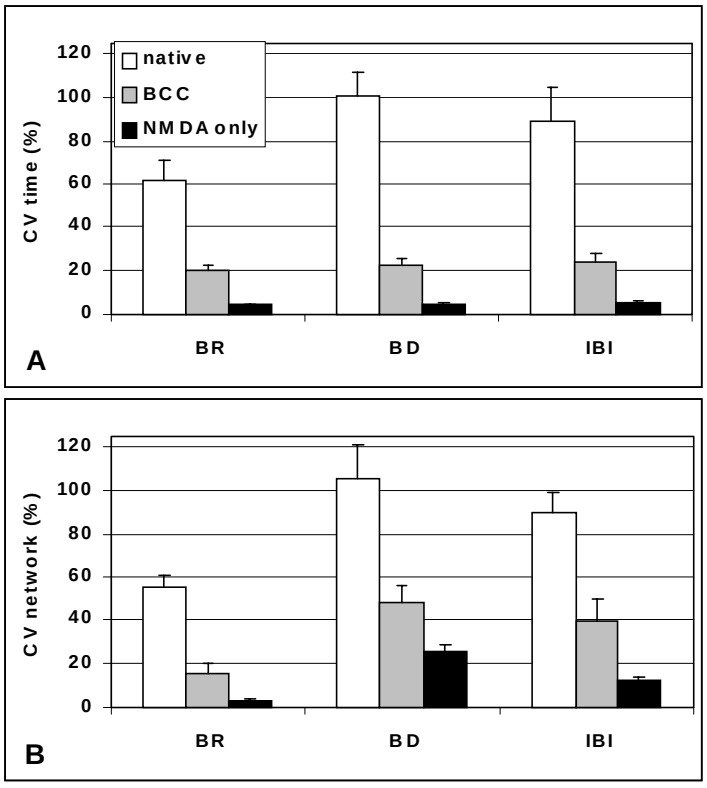

Figure 3.3 Mean coefficients of variation (16 experiments) for three experimental episodes: native, under 40µM bicuculline, and $NMDA_{ONLY}$ (number of channels 185, 185, 87 respectively). (A) CV_{time} for three different burst variables: burst rate (BR), burst duration (BD), and interburst interval (IBI). CV_{time} reflects periodic behavior of the burst variable during a particular experimental episode. Large CV_{time} during the native episodes are due to the complex interaction of multiple neurotransmitter systems. (B) $CV_{network}$ for the same three burst variables. $CV_{network}$ reflects the inter-neuron synchronization across the network. When the $GABA_A$ antagonist bicuculline is applied, both $CV_{network}$ and CV_{time} decrease for all variables to a range of 15-45%. When the activity is mediated solely by NMDA receptors, a further decrease in all CVs occurs (range 2.6-23%), with a concomitant reduction of the standard errors (error bars) obtained from global CVs of 16 different networks. All CVs in the two categories (time and network) are significantly different between experimental episodes for all burst variables ($p< 0.05$).

In a series of six experiments, we applied BCC, STR, and 100 µM APV to examine whether AMPA receptors were able to produce the precise oscillation. In three of those six experiments, we also applied SCH50911 and NE. In no case did the resulting activity approach the precision of the $NMDA_{ONLY}$ condition. For example, the mean CV_{time} for all six experiments was 13.5 (BR), 15.5(BD), and 22.4 % (IBI). While these values indicate a relatively stable oscillatory structure when the activity was driven solely by AMPA receptors, it did not match the degree of regularity and synchronization of the $NMDA_{ONLY}$ activity (Fig. 3.4). These results indicate that NMDA receptor activation is suited uniquely to provide extremely regular population burst oscillations.

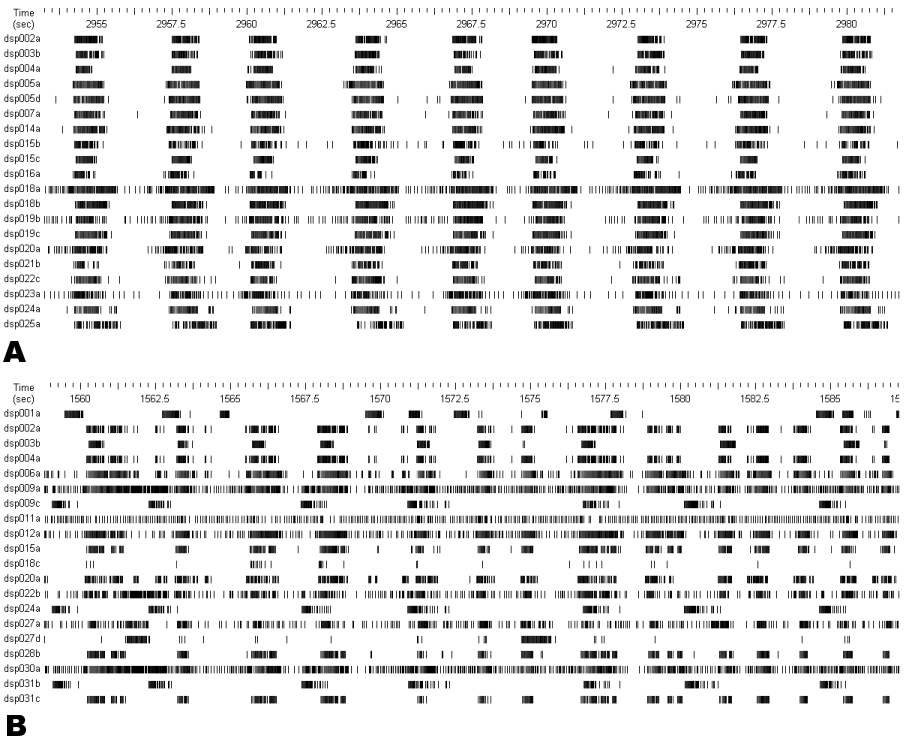

Figure 3.4 The highly periodic nature of the $NMDA_{ONLY}$ activity (A) is not approached when synaptic interactions are limited to those mediated by AMPA receptors (B).

Figure 3.5 illustrates the evolution of activity with sequential addition of BCC, STR, and NBQX to the culture bath, culminating in the $NMDA_{ONLY}$ activity pattern. The period of spontaneous activity shows low rates of bursting and spiking. Addition of 40 µM BCC produces an increase in both activity variables within 5 minutes of application. However, the minute-to-minute variation in both variables still is quite large. Addition of 1 µM STR to remove the second set of inhibitory circuits elicits a further increase in burst and spike rates, accompanied by an increase in the temporal variability. The subsequent application of 10 µM NBQX results in a decrease in both burst and spike rates from the totally disinhibited activity. Both measures stabilized at near constant levels after about 20 minutes. The thirty minutes following establishment of stable

$NMDA_{ONLY}$ activity had CV_{time} for BR, BD and IBI of 2.1, 4.1, and 2.9 % respectively. The dependence of the stationary activity on NMDA receptor mediated events is shown by the application of 100 µM APV at 412 min, which resulted in cessation of all bursting within 10 minutes.

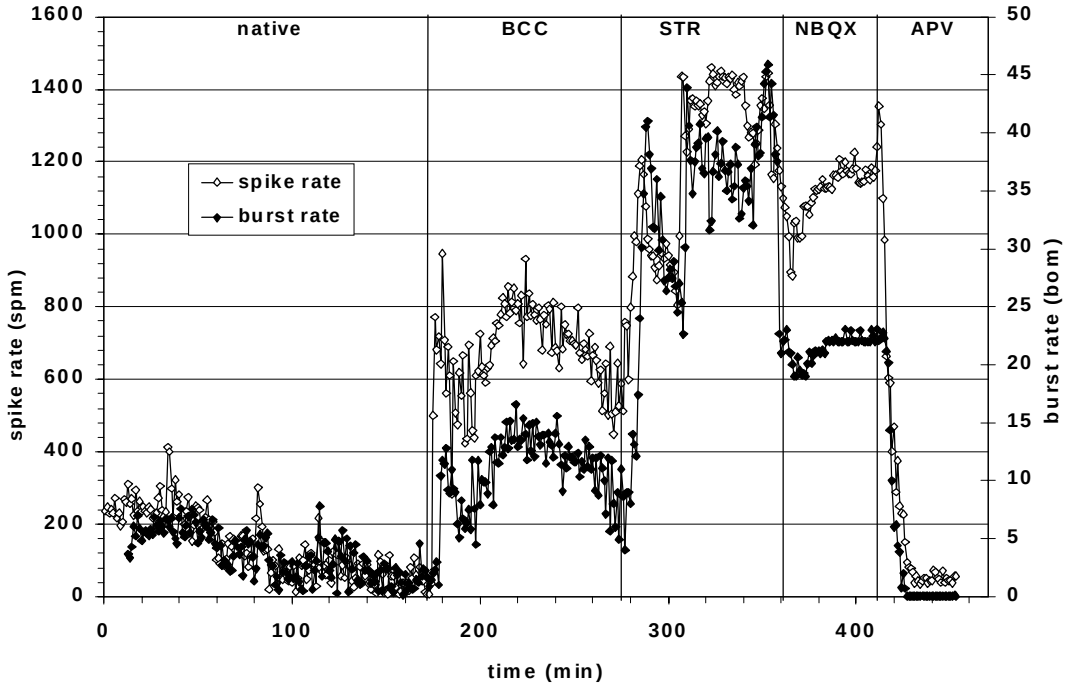

Figure 3.5 Changes in spontaneous spike rate (●) and burst rate (◆) induced by sequential addition of 40µM bicuculline (BCC), 1µM strychnine (STR), 10µM NBQX, and 100µM APV. Each symbol represents the mean of 27 neurons (spike rate) and 14 channels (burst rate). Vertical lines indicate times of drug application. Spontaneous activity increases within three minutes of bicuculline application at 170 minutes. Strychnine application at 270 minutes induces a further increase in both bursting and spiking accompanied by an increase in temporal variability. Blocking AMPA receptors with NBQX at 360 minutes reduces both bursting and spiking to levels intermediate to BCC and STR. Note the greatly reduced activity fluctuation within 20 min after NBQX application. APV abolishes all bursting and most spiking within 10 minutes of application, demonstrating the dependence of the activity on the NMDA receptor.

During $NMDA_{ONLY}$ activity, spinal cord networks consistently oscillated within a very narrow range of burst rates. This activity was apparently independent of network age or neuronal density, as the 16 cultures from which the data was gathered ranged in age from 18-113 d.i.v. and were seeded at concentrations of 0.2-0.5 $x10^6$ cells/ml. Averaging burst rates from all 178 channels resulted in a mean global burst rate of 21.0 ± 2.0 bpm.

For each channel, the $NMDA_{ONLY}$ burst rate essentially was independent of the initial (native) burst rate. The distribution of burst rates for all 16 cultures (178 channels) under three different conditions is shown in Figure 3.6. Native activity prior to any pharmacological additions (Panel A), ranged from 3 to 27 bpm. When BCC (40 µM) was added to block $GABA_A$ mediated inhibition, the burst rate distribution was broadened, ranging from 3-36 bpm (Panel B). A peak in the distribution at 12-15 bpm indicates that the disinhibited network state has some preferential activity modes, but the typical BCC response varies between cultures. Panel C, which shows the $NMDA_{ONLY}$ activity distributed from 18-24 bpm, demonstrates the reliability of expression of the oscillation in all cultures (n=16).

Mechanisms Controlling Burst Oscillations

Possible mechanisms that contribute to the unique characteristics of the $NMDA_{ONLY}$ activity were explored using a battery of pharmacological agents summarized in Table 3.1. These agents may be divided roughly into (1) compounds that affect neurotransmitter release, (2) compounds that affect receptor desensitization, (3)

compounds that affect burst and spike afterhypolarization (AHP), and (4) antagonists of neurotransmitter receptors.

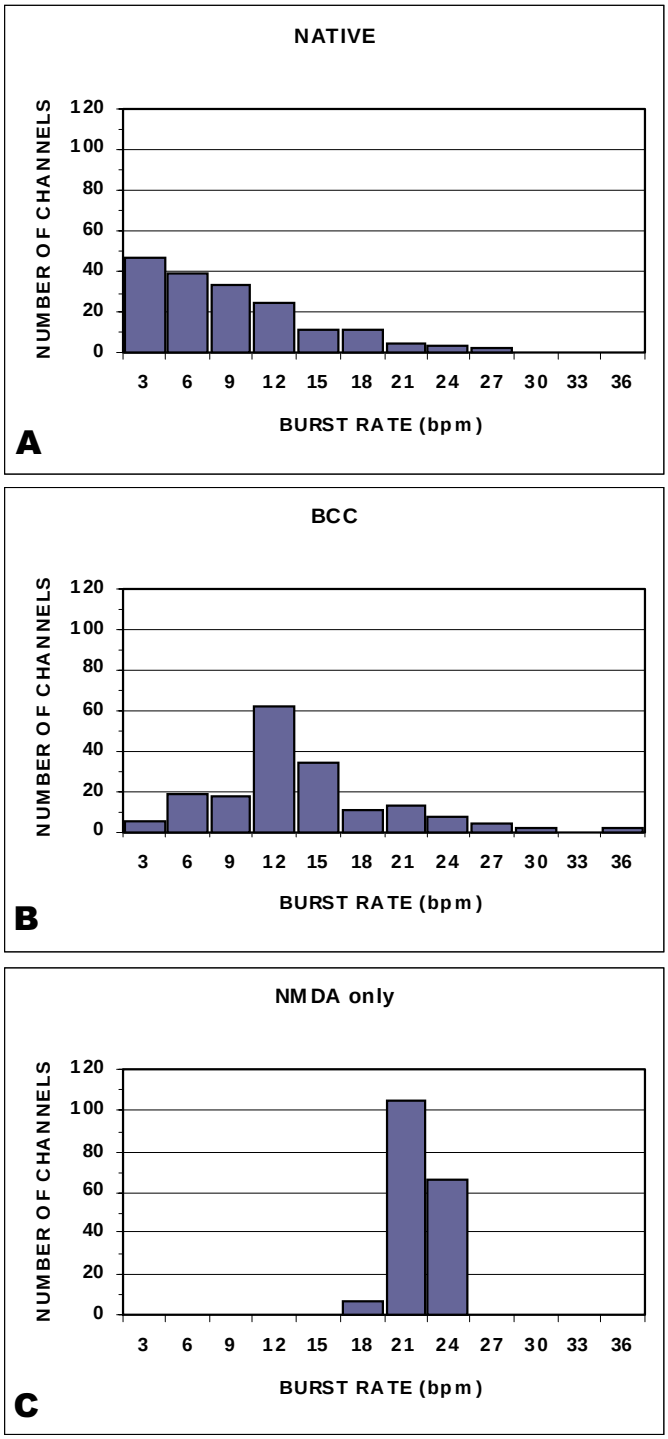

Figure 3.6 Burst rate distributions under 3 different conditions. A: Native activity of 16 cultures ranges from 3-27 bpm. B: Disinhibition with 40µM bicuculline results in a wider range (3-36 bpm), with a small peak at 12-15 bpm, indicating a preference for certain activity states, but with relatively low reliability of expression. C: $NMDA_{ONLY}$ activity ranges from 18-24 bpm. The narrow distribution shows the inter-culture reproducibility of the oscillation. Mean burst rates for 60 min intervals under each condition were calculated on a per-channel basis (n=178 channels).

TABLE 3.1: List of Pharmacological Agents Tested

Active Agent[μM]	Mode of Action
Apamin [1]	Antagonist, small conductance (SK) Ca^{+2} activated K^+ channels
APV [5-100]	NMDA receptor antagonist
Atropine [10-30]	Cholinergic muscarinic antagonist
Bicuculline [40]	$GABA_A$ antagonist
Ca^{+2} [1200-5000]	facilitation of neurotransmitter release
Carbenoxolone [50-100]	Gap junction blocker
Charybdotoxin [0.015]	Antagonist, large conductance (BK) Ca^{+2} activated K^+ channels
Curare [10-20]	Cholinergic nicotinic antagonist
Evan's Blue [50]	P2X receptor antagonist (adenosine)
Glycine [10]	Prevents glycine-dependent NMDA receptor desensitization (strychnine insensitive glycine site)
Haloperidol [0.002]	Dopamine receptor antagonist
K^+ [5400-10000]	enhancer of neuronal excitability
L-733,060 [0.002]	NK_1 receptor antagonist (sub. P)
MCPG [100-200]	Metabotropic glutamate receptor antagonist
Methysergide [20]	Serotonin receptor antagonist
Mg^{+2} [0-6000]	inhibitor of neurotransmitter release, NMDA receptor blocker
NBQX [10-20]	AMPA/kainate antagonist
NMDA [50]	Selective agonist
Norepinephrine [40-50]	PKA activator (β-adrenergic receptor mediated), blocks burst after hyperpolarization, also counteracts Ca^{+2}-dependent NMDA receptor desensitization
SCH 50911 [50-100]	$GABA_B$ antagonist
Strychnine [1]	Glycine receptor antagonist
ZD7288 [50]	Hyperpolarization activated cationic conductance blocker (I_h current)

Compounds affecting neurotransmitter release

As previously described, when the main synaptic driving force had been reduced to $NMDA_{ONLY}$ and network activity had stabilized to a highly periodic burst rate of 21.0 ± 2.0 bpm, the $GABA_B$ receptor antagonist SCH 50911 (50 µM) was without effect. However, in 8 experiments the combination of BCC/STR/NBQX resulted in a burst rate of less than 17 bpm. The variability in the burst parameters also was significantly higher than in the 8 experiments that responded with precise burst oscillations immediately after application of NBQX. In 5/8 of these cultures, SCH50911 increased the burst rate to 18-24 bpm and established a highly periodic pattern of activity. Thus, it appears that in our preparation, inhibition of neurotransmitter release through activation of $GABA_B$ receptors by endogenous GABA is sometimes sufficient to prevent the characteristic $NMDA_{ONLY}$ pattern of activity from developing. These network specific effects may reflect fluctuations in network structure that are revealed by pharmacological manipulations.

In three experiments, after $NMDA_{ONLY}$ activity had been established, we titrated the Ca^{+2} concentration from 1.3 to 8.0 mM (Fig. 3.7). Ca^{+2} suppressed mean burst durations from 600ms at 3 mM Ca^{+2} to 300ms at 8 mM Ca^{+2} but did not affect the burst rate significantly. In two of these experiments, we subsequently raised K^+ concentrations from the basal level of 5.4 mM to 8.5 mM. K^+ increases both the level of neuronal excitability and the level of Ca^{+2} influx at the presynaptic terminal. The effect of elevated K^+ under these conditions was to increase the burst rate consistent with an increase in neuronal excitability (Fig. 3.7). 8.5 mM K^+ only slightly decreased burst durations. After

the extensive pharmacological manipulations, it is significant that the network responded to elevated K^+ concentrations in a predictable manner (Rhoades and Gross, 1994).

The contribution of metabotropic glutamate receptors (mGluR) to neurotransmitter release was examined with the non-selective group I/II antagonist MCPG (200 µM). The compound demonstrated no measurable effect in 5 experiments, indicating mGluR activation was not a significant factor in the control of glutamate release in our cultures. This finding is in accord with those of von Gersdorff et al. (1997), who showed that mGluR activation apparently contributes to approximately 10% of the EPSC depression induced by afferent stimulation at the calyx of Held in the rat brainstem.

Figure 3.7

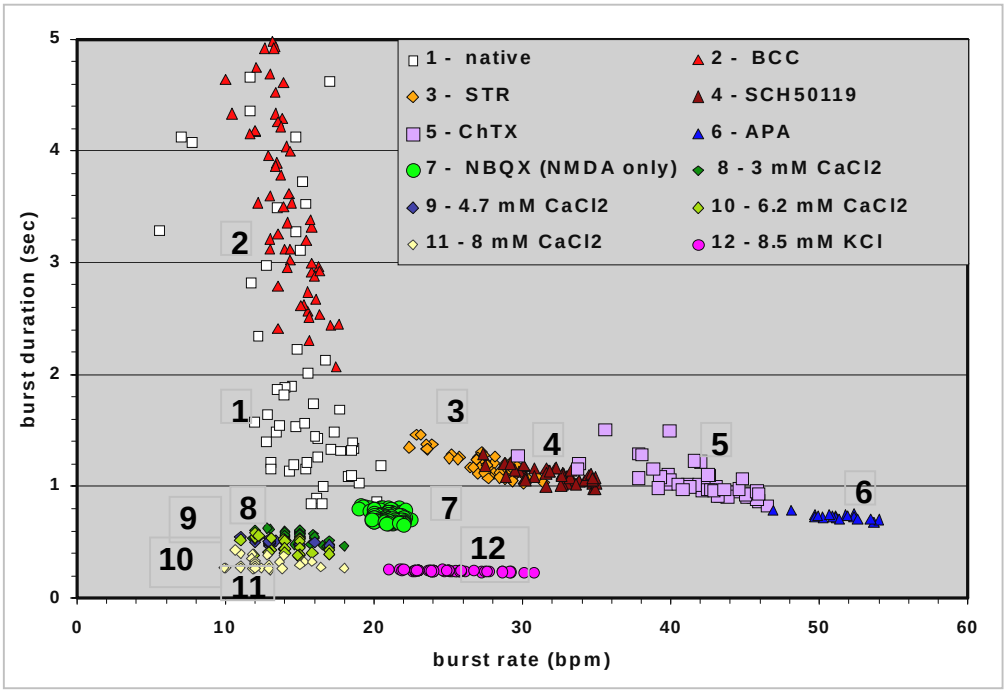

Figure 3.7 Changes in burst duration and burst rate elicited by pharmacological manipulation of synaptic driving forces and burst ignition and termination mechanisms (minute means from 14 channels, single experiment). The extremely low variability of the $NMDA_{ONLY}$ activity is indicated by the tight cluster after addition of 10µM NBQX (7). Further manipulation by titration of Ca^{+2} decreases both duration and rate, while raising K^{+} to 8.5mM increases the burst rate.

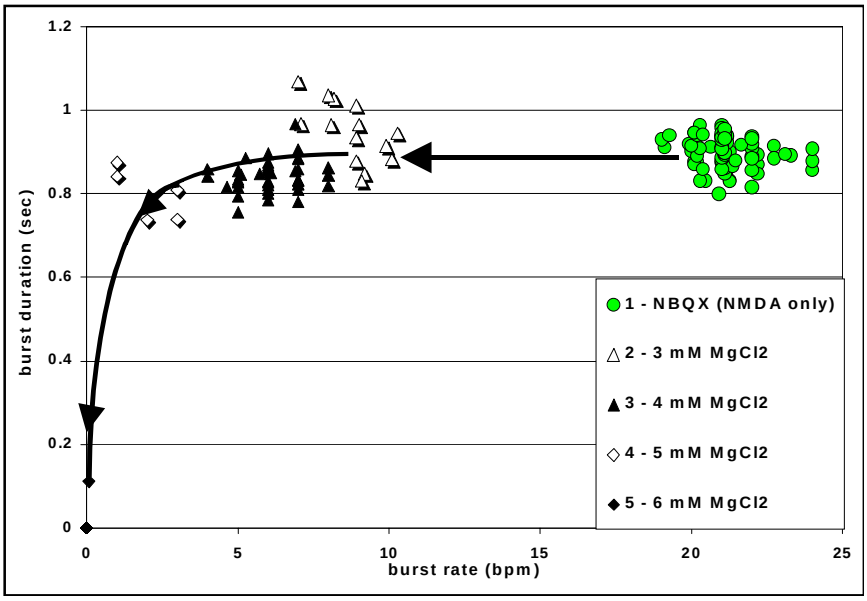

Figure 3.8 Effect of increasing Mg^{+2} concentration on burst rate and burst duration. Raising Mg^{+2} from the basal 0.8mM under $NMDA_{ONLY}$ conditions caused a progressive decrease in burst rates without affecting burst durations until 4-5mM Mg^{+2}. A catastrophic loss of all activity occurred at 6mM Mg^{+2}. Points represent the minute means of 14 channels under each pharmacological condition.

Titrating the extracellular Mg^{+2} from the normal 0.8 mM to a maximum of 6 mM after establishment of $NMDA_{ONLY}$ activity resulted in a dose-dependent reduction in the burst rate without affecting the burst duration, except at the higher concentrations immediately prior to network failure (Fig. 3.8). Like Ca^{+2}, Mg^{+2} has multiple sites of action. It inhibits neurotransmitter release and blocks the NMDA channel in a voltage-

dependent fashion. Increasing the concentration of Mg^{+2} raises the threshold for relief of the voltage dependent blockade. Mg^{+2} also is implicated in suppression of spontaneous activity by charge screening of voltage-sensitive Na^{+} channels (Guth and Drescher, 1990).

Compounds affecting receptor desensitization

NMDA receptors undergo different forms of desensitization that potentially could contribute to the activity pattern. Glycine dependent desensitization of NMDA receptor mediated currents has been reported in cultured hippocampal neurons (Mayer et al 1989; Vyklicky et al., 1990). Both groups found that 3µM glycine was sufficient to alleviate a strong depression of such currents. To test the hypothesis that glycine-dependent NMDA receptor desensitization influenced the neuronal network activity under $NMDA_{ONLY}$ conditions, we added 10 µM glycine to counteract desensitization (n=3). The glycine was without measurable effect, indicating that glycine-dependent desensitization did not play a role in generating $NMDA_{ONLY}$ oscillations.

. In addition, the NMDA receptor undergoes a Ca^{+2} dependent form of desensitization that is mediated by the phosphatase calcineurin (Legendre et al., 1993; Tong and Jahr, 1994; Tong et al., 1995). Raman et al. (1996) showed that NE increases PKA activity through a β-adrenergic dependent process, which is sufficient to counteract the phosphatase actions of calcineurin and to prevent NMDA receptor desensitization. In three experiments, application of 40 µM NE increased burst rates and stabilized IBI at $NMDA_{ONLY}$ levels. When NE was applied subsequent to establishment of a stable

$NMDA_{ONLY}$ pattern, it was without effect. However, NE also inhibits the slow afterhyperpolarization (sAHP) that may serve to terminate bursting (Madison and Nicoll, 1986). Therefore, it is unclear whether the effects produced by NE were a result of blocking receptor desensitization or the sAHP. In either case, the $NMDA_{ONLY}$ pattern of activity, once established, was not dependent upon a mechanism sensitive to NE.

Compounds affecting afterhyperpolarization

Action potentials in many excitable cells are followed by a prolonged afterhyperpolarization that modulates repetitive firing. Apamin has been shown to inhibit the Ca^{+2} dependent S(K) current that is responsible for this afterhyperpolarization (Sah and McLachlan, 1992). In our hands, 1 μM apamin (n=4) increased burst rates when it was applied prior to blocking AMPA/kainate receptors (Fig. 3.7). When apamin was applied after the $NMDA_{ONLY}$ activity was established (n=3), it was without effect. This indicates that the apamin-sensitive AHP does not affect $NMDA_{ONLY}$ oscillations.

A transient AHP was identified in hippocampal slices (Alger and Williamson, 1988) that were sensitive to charybdotoxin (ChTX), indicating its mediation by B(K) K^+ channels. We performed experiments with 20 nM ChTX before (n=3) and after (n=3) network activity was reduced to $NMDA_{ONLY}$. ChTX increased burst rates when it was applied before blockade of AMPA/kainate receptors (Fig. 3.7) but was without effect when applied after NBQX. These results indicate that the Ca^{+2} activated B(K) channel does not dominate $NMDA_{ONLY}$ oscillations.

Neurotransmitter receptor antagonists

After the $NMDA_{ONLY}$ activity was established, we used atropine (muscarinic receptor antagonist, 1-30 µM, n=3), curare (nicotinic receptor antagonist, 10- 20 µM, n=3), haloperidol (dopamine receptor antagonist, 2 nM, n=2), methysergide ($5\text{-}HT_{1/2}$ receptor antagonist, 20 µM, n=2), Evan's blue (P2X receptor antagonist, 50 µM, n=2), and L-733,060 (tachykinin receptor antagonist, 2 nM, n=2). None of these compounds exhibited measurable effects on previously established $NMDA_{ONLY}$ oscillations.

Involvement of electrical synapses and I_h currents

The functional contribution of gap junctions was investigated with carbenoxolone (50-100 µM, n=3). No measurable effect was demonstrated on the $NMDA_{ONLY}$ activity, indicating that gap junction coupling played no significant role in these oscillations. ZD7288 (50 µM, n=3) was used to test for the contribution of the hyperpolarization-activated cationic conductance (I_h) to $NMDA_{ONLY}$ activity. This agent also was ineffective.

Pre- vs post-synaptic control mechanisms

The addition of 20-50 µM NMDA to the experimental culture medium after the $NMDA_{ONLY}$ activity was established resulted in increased spike production and a disruption of the periodic nature of the activity (Fig. 3.9, n=2). CV_{time} for burst rate was 58% in one network and 71% in the other, indicating that the regular oscillations no longer were present. The disruption of the pattern can be demonstrated in the spike frequency domain with Fourier analysis of spike intervals from the same identified units.

Figs. 3.9 b and d reveal a drastic alteration in the spike interval structure. While the $NMDA_{ONLY}$ activity peaks at 0.34 Hz (b), the addition of NMDA to the medium (d) obliterates the interval organization.

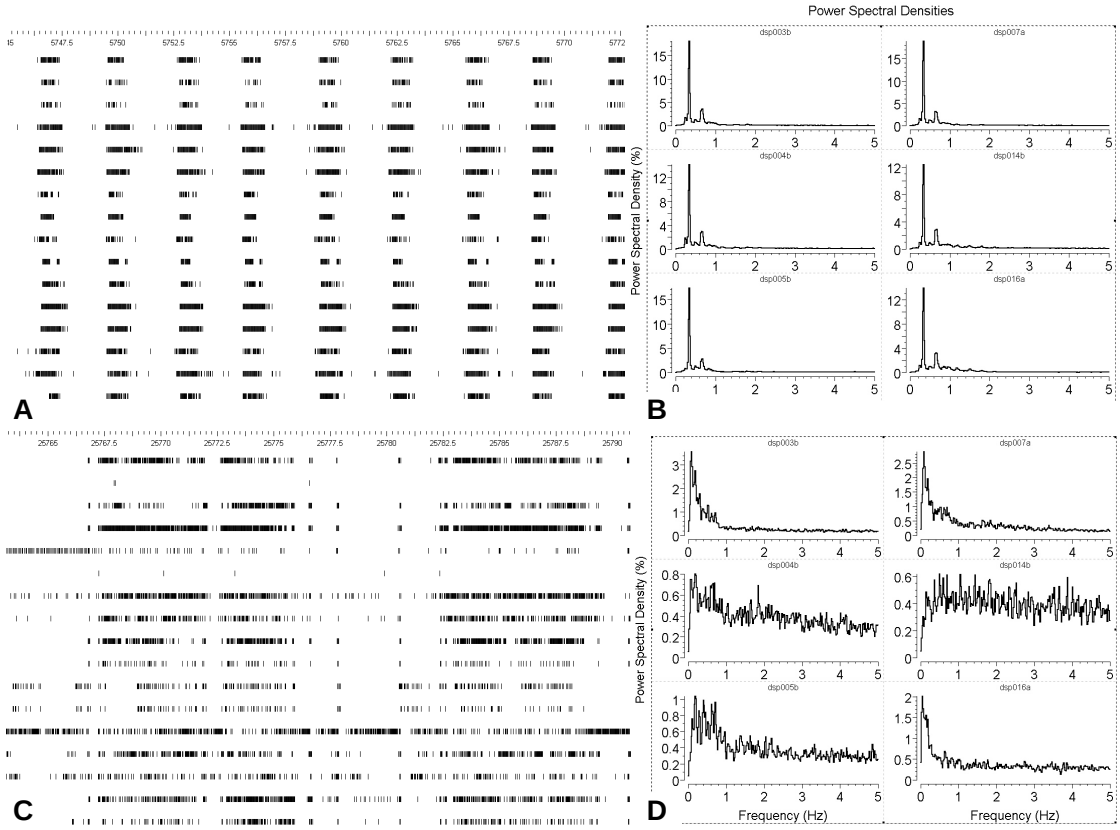

Figure 3.9 Uncoupling of presynaptic influences by bath application of 50µM NMDA destroys the periodic nature of $NMDA_{ONLY}$ oscillations. A: 25 s of activity of 16 neurons under $NMDA_{ONLY}$ conditions. B: The period of the $NMDA_{ONLY}$ burst oscillation is reflected in the large peak in the power spectra at 0.34Hz (2.94 s period) calculated for a sample of 6 of the neurons shown in Panel A. C: The same 16 neurons 5 min after 50 µM NMDA was added to the experimental bath. The periodic and synchronized nature of the $NMDA_{ONLY}$ activity is destroyed. D: Power spectra calculated for the same neurons as in B after NMDA addition.

The NMDA receptor channel possesses a unique voltage dependent Mg^{+2} block that has been shown to induce oscillations in several preparations (Hu and Bourque, 1999, Rioult-Pedotti, MS, 1997; Wallen and Grillner, 1987). This oscillation is elicited by NMDA receptor activation in the presence of physiological levels of Mg^{+2} and apparently is due to the negative slope in the current-voltage relation of the NMDA synapse. Wallen and Grillner (1987) showed that NMDA application produced TTX-resistant oscillations in membrane potential, indicating an intrinsic cellular property. Because bath application of NMDA directly activates the receptors independent of vesicle release, essentially uncoupling the NMDA synapses from presynaptic influences, the loss of regular oscillations strongly suggests that the periodicity under $NMDA_{ONLY}$ conditions is not induced on the receptor level only.

Discussion

Independent of spontaneous activity or age, 16 spinal cord cultures were entrained to a remarkably stable, highly periodic burst pattern of 21.0 ± 2.0 bpm under $NMDA_{ONLY}$ conditions. This pattern of activity persisted for up to 12 hours (maximum observation time, Fig.3.2d) and more than 98% of all recorded neurons participated (40-85 neurons per experiment). NMDA receptor activation was necessary for generation of this unique, highly periodic activity pattern, since it was abolished by 40-100 μM APV. However, tonic NMDA receptor activation was not sufficient to maintain the periodicity, implying that control of the period may originate at the presynaptic level. Additionally, disinhibition with BCC and STR and blocking NMDA receptors with APV, leaving only the AMPA/kainate synapse as the sole driving force, did not produce the characteristic oscillation.

Mechanisms underlying intrinsic burst generation have been explored in several different cell types (Azouz et al., 1996; Bracci et al., 1996b; Ballerini et al., 1999; Llinas, R.R., 1988; Streit, J., 1993; Traub et al., 1994). Generally, these investigations have analyzed burst phenomena one cell at a time, although population studies using Ca^{+2} imaging (Lawrie et al., 1993; Robinson et al., 1993; Wang and Gruenstein, 1997) or extracellular field potentials (Staley et al., 1998) have provided insights into network bursting. Acutely isolated intact spinal cords, acute spinal cord slices, and organotypic slice preparations have been used to study the mechanisms of fictive locomotion and putative central pattern generators. For example, elevated extracellular K^+ resulted in

increased neuronal excitability leading to rhythmic, synchronized oscillations in organotypic rat spinal cord slices (Ballerini et al., 1999). These oscillations were network dependent as they were blocked by TTX and low Ca^{+2}/high Mg^{+2} solutions. Comparable oscillations also were seen in isolated spinal cord preparations (Bracci et al., 1998).

Interestingly, the burst oscillations reported in these other preparations typically show a high degree of variability when compared to our N DA_{ONLY} oscillations. For example, Ballerini et al. (1999) reported in one experiment a persistent, network-dependent, rhythmic burst oscillation in ventral horn interneurons with a period of 2.8 ± 1.5 sec under elevated (6-7 mM) extracellular K^+ (a period close to the 2.9 ± 0.3 sec that we observed during $NMDA_{ONLY}$ activity). However, in the Ballerini study, the CV of the burst period was 20 ± 5% within that one experiment. In contrast, the mean CV for burst period in 16 separate experiments we performed was only 3.4% using one-minute bins (range 1.4-4.8%). Thus, the $NMDA_{ONLY}$ activity was characterized not only by remarkable temporal and spatial stability of all burst parameters within individual experiments but also by high inter-experiment reproducibility with networks that varied widely in age and cell density. This suggests the $NMDA_{ONLY}$ network state may be unmasking a fundamental cellular mechanism, rather than a circuit-specific network property.

CA3 network activity can be dominated by strong synaptic depression, presumably induced by depletion of a finite supply of releasable glutamate (Staley et al., 1998). They suggested that the period of the population bursts was determined by the

rate of refilling of this pool. Recent investigations have provided insights into the dynamics of neurotransmitter vesicle pools (Goda and Stevens, 1998; Ryan et al, 1993; Ryan et al., 1996). The RRP in central neurons has been shown to contain from 5-20 vesicles (Dobrunz and Stevens, 1997; Stevens and Tsujimoto, 1995). This pool refills with a time constant of 5-12 seconds (Rosenmund and Stevens, 1996). High frequency stimulation of presynaptic terminals with trains of 100-300 Hz significantly enhances the rate of refilling compared to square wave depolarizing input (Wang and Kaczmarek, 1998). Stevens and Wesseling (1998) reported that the synaptic recovery period was reduced from 6 sec to 3 sec when focal hyperosmotic conditions were paired with presynaptic 10 Hz stimulation. The recovery time for CA1 synapses depleted by 10 Hz stimulation in hippocampal slices was 2.8 ± 2.0 sec (Dobrunz and Stevens, 1997), a time remarkably similar to our $NMDA_{ONLY}$ period. By comparison, the $NMDA_{ONLY}$ bursts in our studies produced long plateaus (0.2-0.4 s) at spike frequencies of 200-250 Hz. The close agreement between the $NMDA_{ONLY}$ oscillation period of 2.9 ± 0.3 sec, and the time constants reported for refilling of the RRP during electrical stimulation, in conjunction with the results of our pharmacological manipulations implying a presynaptic control of the $NMDA_{ONLY}$ activity, suggest the vesicle depletion/refilling cycle is a good candidate for controlling the period of the unique burst oscillations observed.

Although presynaptic mechanisms may underlie the unique $NMDA_{ONLY}$ oscillations, it also is necessary to survey postsynaptic responses that can influence spike frequencies in bursts as well as burst durations. NMDA receptor activation is associated with Ca^{+2} conductances supporting plateau potentials with effects on burst mechanisms

that are not seen with AMPA receptor activation (MacLean et al., 1997). Calton et al. (2000) showed that single stimulation pulses were sufficient to elicit Ca^{+2} spikes through activation of voltage-dependent calcium channels (VDCCs) in pyramidal cells of rat amygdala slices. AMPA receptor-mediated depolarization was unable to elicit these spikes, despite providing a greater depolarizing current. Schiller et al. (1998) showed that pairing of glutamate application with postsynaptic action potential firing resulted in a threefold increase of Ca^{+2} entry through the NMDA receptor compared to glutamate alone. In cultured cortical neurons, Robinson et al. (1993) found that Ca^{+2} oscillations concomitant with action potential burst firing were dependent upon NMDA receptor activation in low Mg^{+2} medium. Bacci et al. (1999) established that NMDA receptors, along with VDCCs, provide a long-lasting depolarization necessary for support of action potential burst firing in cultured hippocampal neurons. These results all highlight the unique relationship of the NMDA receptor to intracellular Ca^{+2} dynamics. Hence, NMDA receptor dependent Ca^{+2} influx is likely to influence the character of the burst generated, which, in turn, influences the degree of vesicle depletion at the presynaptic terminal.

In the lamprey, NMDA application induces a robust fictive swimming rhythm that is dependent upon NMDA induced Ca^{+2} currents and Ca^{+2}-dependent K^{+} currents in pacemaker cells (Brodin et al., 1991). Rat spinal neurons exhibit membrane potential oscillations in response to NMDA application, which are TTX resistant but are dependent upon serotonin (Hochman et al., 1994a; 1994b; MacLean et al., 1998). These membrane potential oscillations have been hypothesized to contribute to phasic population activity occurring during fictive locomotion, allowing the expression of a precise oscillation

period by filtering temporally dispersed synaptic activity (Hochman et al., 1994b). While our experiments certainly do not preclude this mechanism from contributing to the oscillatory nature of the $NMDA_{ONLY}$ activity, the disruption of the periodicity of pre-existing oscillations by application of NMDA indicate that the receptor alone is not sufficient to drive the bursting with great precision.

Staley et al. (1998) speculated that depletion of the excitatory neurotransmitter vesicle pool might be necessary for burst termination, with other mechanisms such as inhibitory conductances and AHP acting to modulate the postsynaptic effect of glutamate. It is of interest that early in postnatal development, GABA application depolarizes neurons (Ben-Ari et al., 1997; Menedez de la Prida and Sanchez-Andres, 1999). During this period, bursting patterns of coordinated activity occur (Habets et al., 1987; Jackson et al., 1982). This coordinated activity selectively activates subsets of synapses and functions as an important mechanism for sculpting circuitry preserved in the adult animal (Landmesser and Pilar, 1978; Tosney and Landmesser, 1985). During the period when GABA is depolarizing, mechanisms other than fast synaptic inhibition must serve to terminate bursting. Strong synaptic depression induced by vesicle depletion would allow the coordination of phasic activity between recurrently connected neurons, permitting the expression of fundamental motor patterns such as the respiratory rhythm prior to establishment of mature synaptic circuitry.

Few neuronal systems can be forced into specific dynamic states with high reliability and remain entrained for many hours. The availability of such a stable dynamic

system provides a tool for studies of structure/function relationships controlling network behavior, excitotoxicity, quantitative assessment of functional synaptic deficits, and therapeutic measures designed to restore synaptic efficacy. $NMDA_{ONLY}$ activity represents a simplification of synaptic driving forces, which will allow the study of excitatory-coupled network dynamics and basic burst mechanisms, providing insight into the complex interactions of cellular and network properties.

Additional Considerations for the use of Cultured Neuronal Networks in Basic Neuroscience

Many investigators have found that NMDA receptor activation is necessary for expression of rhythmic motor drivers in a variety of preparations (Smith and Feldman, 1987; Daw et al., 1993; Douglas et al., 1993). Application of exogenous NMDA has been used to induce rhythmic bursting in intact rat spinal cord (MacLean et al., 1997), in medullary slices containing nucleus solitarius neurons (Vincent et al., 1996), in rat spinal interneurons (Kiehn et al., 1996), and in cholinergic nucleus basalis neurons (Khateb et al., 1995). In the work reported here, the activation of the NMDA receptor by endogenous glutamate in the absence of any inhibitory transmission resulted in the expression of a remarkably periodic oscillation that was reproduced within networks composed of highly variable neuronal numbers with, presumably, equally variable neuronal connectivity. The regularity of this NMDA receptor mediated bursting was destroyed by bath application of NMDA (Fig. 3.9), in contrast to results of the studies cited above. These observations suggest a fundamental mechanism that operates predominately on the presynaptic side to produce the observed periodic behavior.

Of course, cultured neuronal networks lack afferent input and make no efferent connections. The spontaneous activity that arises within such networks may be considered a result of self-excitation within a massively recurrently connected system. Under these conditions, isolating presynaptic from postsynaptic contributions to network

activity is difficult, as the architecture of the network dictates a continual feedback from the postsynaptic to the presynaptic side. We have developed a model to explain the unique characteristics of the NMDA receptor mediated activity. This model incorporates the special relationship between NMDA receptor activation and Ca^{+2} entry, which has been characterized by a number of investigators (Bacci et al. 1999; MacLean et al., 1997; Robinson et al. 1993; Schiller et al., 1998). Even if our model is incorrect in some details, it suggests a number of experiments that will help uncover the mechanisms producing the highly regular pattern of activity.

Model

Under conditions of NMDA receptor mediated activity, influx of Ca^{+2} is maximized, through both the NMDA receptor channel and through voltage-dependent Ca^{+2} channels (Calton et al., 2000). The kinetics of NMDA receptor activation/deactivation promotes a longer average open time compared to AMPA receptor mediated events. The combination of increased Ca^{+2} conductance and longer open time leads to an intracellular Ca^{+2} concentration that is larger in magnitude and more persistent than that seen under other pharmacological conditions. This Ca^{+2} "plateau potential" in turn supports a more depolarized membrane potential than normal. The absence of inhibitory conductances prevents repolarization of the neuronal membrane, allowing prolonged, high frequency burst firing. It is this relatively long period of intense bursting (plateau frequencies of 200-225 Hz for periods of 200-400 ms) that promotes complete depletion of the readily-releasable neurotransmitter pool by each burst. The high intensity bursting efficiently recruits most of the neurons in the network to

participate in each burst episode. With each burst resulting in complete depletion of the readily-releasable pool of glutamate, the kinetics of the vesicular recycling mechanism become the determining factor in the control of network activity. Under this scenario, initiation of new bursts is dependent upon 1) the recovery of the readily releasable pool to a level that supports a reasonable probability of release, and 2) the amount of depolarizing input to the network needed to enable the voltage-dependent Mg^{+2} block of the NMDA receptor pore complex to be relieved.

The time constant of recovery for the readily releasable pool has been defined in several systems (Dobrunz et al., 1997; Rosemund et al., 1996; Staley et al., 1998; Wang and Kacmarek, 1998). If this time is smaller than that required for complete buffering of the large intracellular Ca^{+2} transients elicited by NMDA receptor activation, then average membrane potential will be effectively clamped at a sufficiently depolarized level to allow initiation of the next population burst as the number of spontaneous EPSPs recovers to a threshold level. Experiments to perform Ca^{+2} imaging in parallel with recording of population bursting under several different pharmacological conditions could provide an indication of the relative intracellular Ca^{+2} concentrations reached during each condition. Recording of intracellular potentials concomitant with the multichannel electrophysiology could provide an indication of the number of EPSPs occurring before and after each population burst. Depletion of the readily releasable pool is correlated with loss of EPSPs, and recovery of the pool is signaled by an exponential increase in the number of EPSPs (Dobrunz et al., 1997; Rosemund et al., 1996). Experiments might be performed to manipulate the vesicular recycling process, such as

with bafilomycin A, a compound that reversibly inhibits the vesicular ATPase responsible for reacidification of the vesicle lumen after endocytosis. This should lead to a smaller number of vesicles competent to release neurotransmitter in the readily releasable pool. Additional experiments to manipulate the exocytotic machinery with Botulinum toxin have been initiated. Such experiments are anticipated to provide valuable insights into the mechanisms underlying the highly periodic nature of the NMDA receptor dependent activity.

It is hoped that this work provides clear evidence of some of the contributions cultured networks can make in areas of basic research. Bursting occurs spontaneously or can be elicited in many different preparations by a wide variety of pharmacological and electrophysiological stimuli. Cultured networks are ideally suited to study burst mechanisms, as they permit long-term simultaneous monitoring of large numbers of neurons. Extensive pharmacological manipulations are easily performed, as this work clearly demonstrates. Future studies of the contributions individual neurons make to population behavior will be greatly facilitated by combining techniques such as laser cell surgery with the electrophysiology. Various neurodegenerative and neuropathological diseases can be studied in these preparations, which permit simultaneous optical and electrophysiological monitoring of cellular and network health and performance. The facility with which neuronal behavior may be studied is unmatched by any other preparation.

RECOMMENDATIONS FOR FUTURE RESEARCH

Multi-channel recording of electrical activity from cultured neuronal networks offers a tool for rapid assessment and detection of a wide variety of chemical and biological compounds. This tool, if properly exploited, will benefit applied research in areas including drug discovery, toxicological evaluation of environmental contaminants, and detection of biological and chemical warfare agents. The examples presented here demonstrate the utility of neuronal networks for detecting neurally active compounds and for discriminating physiological effects induced by minor molecular differences of structurally related compounds. Future work will involve testing and defining a large number of substances based on the effects they produce on neuronal network activity, and the creation of a library of substance "fingerprints". When fully implemented, this will allow identification of an unknown compound by comparison of the effects it induces to the library of previously tested substances. This study will help define the parameters of that library.

The effect induced by bath application of a substance on the electrical activity of a particular cell embedded in a neuronal network, is an integration of the effects mediated by the receptor population that cell expresses, together with the effects produced via chemical and electrical synaptic inputs from all other cells that make contact with the neuron in question. This integration complicates analysis of mechanisms of action of a particular substance, but allows prediction of the functional consequences of a specific

compound on a behaving animal. Analyzing responses to neuroactive agents may be done on the single cell or the network level. Such analyses may report changes in excitability with rate histograms, changes in patterns of action potentials with inter-spike intervals, or changes in network coordination with cross-correlograms. The level of analysis (single cell or network) and the set of parameters used for analysis are substance and experiment specific. Simply reporting that a compound has caused a cessation of all activity at a particular reproducible concentration is valuable information in the screening for neurally active drugs. Examination of the single cell dynamics of that global inhibition may be necessary for understanding the mechanism of the effect.

Healthy neuronal networks express a population of receptors that can be addressed by a wide variety of pharmacological agents. When a specific receptor type binds an appropriate ligand, the effects that receptor mediates on neuronal excitability may be observed. Reliable dose-response curves may be produced for a wide variety of compounds, so long as data from the test period are normalized relative to an experimentally determined reference period of activity. The concentration required to elicit a particular effect in the neuronal networks may be different from that observed in other preparations but in many cases the direction of that effect in the other preparations may be accurately predicted from the neuronal network data. For example, a compound that causes synchronized, high frequency oscillations in a neuronal network almost certainly will be epileptogenic in an *in vivo* preparation, or a compound that totally inhibits network activity without causing cytotoxicity can be predicted to produce catatonia *in vivo.* Of course, if this inhibition occurs in the medulla to the extent that it

adversely impacts respiration, death may also result. In either case, the network responses can be qualitatively related to the *in vivo* effects.

Analysis and interpretation of data obtained from multiple, simultaneous spike trains is an emerging area of science. The work in this lab in the past has focused on the analysis of integrated data, which minimizes the contributions of single action potentials, but does allow the quantification of multiple burst parameters from the simplified dataset. Current technology has evolved to the point that acquisition and analysis of high rate, large data files is routine. This makes the analysis of single spike data feasible. However, the problem becomes one of selecting the parameters necessary to capture the essence of the neuronal network activity changes while providing an easily interpretable analysis of effects induced by experimental manipulation.

It is likely that future data analysis techniques will incorporate a multivariate approach, with different activity parameters plotted orthogonally to yield cluster plots of network activity states under various condition (see for example Fig. 3.8). Dynamics of the clusters as network activity evolves in response to an experimental manipulation will provide a *Gestalt* of network behavior. This approach should allow neuronal network analysis capabilities to include actual identification of unknown substances. The relative changes of the different activity variables elicited by a particular compound will provide insights into the mechanisms being affected.

Initial attempts at performing such a multivariate analysis have proved fruitful. In collaboration with Alexandra Gramowski, a series of experiments were performed to characterize the effects of 40 μM bicuculline applied both singly (n=23) and in combination with 1 μM strychnine (n=27) on spinal cord networks. Two subsequent experiments were performed in which bicuculline and the bicuculline/strychnine combination were applied in a blind test. An analysis of 13 different measures of network activity, which then were compared to the response database, allowed the correct identification of the test substances. All analyses were performed off-line in a labor-intensive manner. These analytic approaches, and more sophisticated ones such as the cluster plots discussed above, should be implemented in real time, allowing the experimenter to adjust conditions to maximize information obtained from a particular experiment.

Several future uses for neuronal networks will rely on the ability to simultaneously process a large number of different samples. For example, cell-based drug screening of thousands of compounds requires separate cell cultures, usually contained in 96- or 384-well plastic containers conducive to assay using optical approaches. Clearly, the number of assays that can be performed with a single culture of cells on microelectrode array will be relatively low. The viability of many cell types, especially neurons, depends on the continuous availability of soluble factors, which would be depleted as the cells are exposed to samples instead of culture media. Even if complex engineering methods were to be employed to mitigate the dilution of culture media, continuous exposure of a single cell population to a series of environmental

samples would still be necessary. This would seriously complicate the interpretation of any single assay.

One approach to this problem would be construction of a massively parallel version of the microelectrode arrays across a set of separate, miniature culture wells. This would allow each culture to be used for a single assay, obviating problems associated with the loss of soluble factors and the interpretation of results. Thus, the throughput of the system could be increased in proportion to the number of miniaturized culture wells that contain microelectrodes.

Multi-network arrays will find application in the biosensor arena, as well. The anticipated design would allow administration of environmental samples (after necessary concentration and pre-treatment) to a test network, while one network remains isolated from outside influences. Thus, should the activity of the test network be altered markedly by the environmental sample and the control network activity remain stable, the cause of the change in test network activity can be ascribed with a high level of confidence to the presence of a neurally active compound in the environment. Alternatively, should both of the networks exhibit parallel changes in activity, problems with environmental control systems must be suspected. Incorporating more than two networks in the biosensor would permit redundancy in the detection process. Of course, each increase in the number of networks will require a corresponding increase in the complexity of the programming necessary to permit the biosensor to operate autonomously.

Currently, neuronal networks are not yet ready for field deployment. However, meaningful physiological information now can be obtained from neuronal networks. The most significant hurdle that remains is that the cells themselves are not comparably "stable," compared to other sensing elements such as antibodies or nucleic acid probes, meaning that a continual supply of replacement cultures must be available. Under laboratory standard cell culture conditions, the lifetime of neuronal networks can exceed 300 days (Gross 1994). Presently, cryopreservation of intact neural networks for long-term storage has not been demonstrated, although spontaneously active networks have been grown from cells cryopreserved for periods of up to six months at -80^{o} C. These cells formed networks of neurons and glia that were morphologically indistinguishable from those formed from unfrozen cells. Pharmacological tests revealed normal responses to most common neurotransmitters, such as GABA, glycine, glutamate, and ACh. However, there seemed to be deficiency in the expression of the NMDA receptor (unpublished observations). These results are promising enough to encourage further experimentation. An approach that encourages stabilization of the cellular cytoskeleton with compounds such as taxol, in combination with improvements in the cryopreservative medium, may prove productive in attempts to cryopreserve intact neuronal networks.

Experimental Problems

During the past three-and-one-half years, I have performed approximately 300 experiments with cultured neuronal networks. This experience has provided some insights into the limitations of this preparation in its present form. A list of the problems include but certainly are not limited to: a) variability in activity between cultures, b) tissue-specificity of receptor expression, c) systematic experimenter errors in areas such as drug concentrations and application trauma, and d) difficulty of testing non-water soluble compounds. Each of these factors can produce highly variable results from culture to culture and between different experimenters. However, understanding the sources of this variability often can allow appropriate compensations to be made and enable valuable data to be salvaged.

Activity Variability

Experience has shown that the dynamic range of spontaneous activity within separate cultures can be from zero to over 60 bursts/min, and mean spike frequency variability is even greater. This disparity in the spontaneous activity virtually requires that comparisons of responses elicited by a particular compound be performed using normalized values. In this way, data generated by different networks can be pooled, and mean and standard deviations of the response can be calculated. Of course, for testing an unknown compound, it would seem that a culture with spontaneous rates somewhere in the middle of the dynamic range would be the most reliable detector. Thus, if a substance is inhibitory, the activity can be suppressed. If excitatory, the activity can increase

without exceeding the physiological limits of the neurons. Often, if the spontaneous network activity is low, application of a disinhibitory compound such as bicuculline, or an excitatory compound, such as glutamate, can elicit increased spiking and bursting. If it is undesirable to interfere with a neurotransmitter system, elevations in the external K^+ concentration can produce a generalized excitation. At the other extreme, cultures that are overly active may be slowed by increasing external Mg^{+2}, which both decreases neurotransmitter release probability and increases the threshold for NMDA receptor activation. Manipulations such as these can increase the value of the data gathered from a particular network.

Tissue Specificity

Cultured neurons retain the pharmacological responsiveness of the tissue from which they were obtained. Thus, a culture grown from tissue harvested from the spinal cord responds to application of glycine or to the glycinergic antagonist strychnine. Frontal cortex cultures on the other hand, show much weaker responses to glycine or strychnine. An application of 10 μM ACh to frontal cortex will produce robust increases in both bursting and spiking, whereas the spinal cord does not respond to ACh until the concentration is raised to 100-150 μM. Medulla cultures reliably increase spiking activity in the presence of as little as 1 μM ACh. However, of the three tissues, only the frontal cortex cultures seem to possess functional cholinergic synapses, since AChE inhibitors, such as eserine, cause changes in spontaneous activity that parallel those caused by application of exogenous ACh. Results such as these demonstrate the preservation of tissue-specific receptor and neurotransmitter expression in cell culture. This specificity

can cause confounding results. Depending upon the mechanisms a specific test compound affects, it may be essentially invisible to one tissue, yet produce robust responses in another tissue type.

Experimenter Errors

Working with neuronal networks requires a facility with certain laboratory practices. For example, a common experimental paradigm when testing pharmacological compounds requires the culture to be "washed," meaning that the medium containing the test substance is exchanged with fresh medium. The number of washes required to reverse the effects elicited by the test compounds is a function of several variables, including concentration applied, solubility, and the intrinsic reversibility of the compound. In the open chamber configuration used in all the experiments described in this work, the experimenter must manually remove the medium with a pipette or syringe, and immediately replace it. The sudden change in medium can have several detrimental effects on neuronal networks. The open chamber allows constant evaporation from the experimental bath, which permits the osmolarity of the medium to gradually increase with time. If the experimenter neglects to maintain the osmolarity with periodic additions of distilled water, a medium change can result in a sudden osmotic shock that will disrupt the network activity. If the osmotic change is too great, neuronal swelling and synaptic disruption may occur. The changes in cellular morphology may be observed through the microscope. Network activity may also be disrupted by the physical shock of a medium change if the experimenter carelessly applies the fresh medium at too fast a rate or directly to the neuronal culture. The network may be killed if the experimenter is too

slow to replace the medium and the network dries out. Network activity also will be disrupted if the pH of the fresh medium is not adjusted to a physiological range of 7.3-7.4. Other experimenter errors may occur in the application of test substances. Stock solutions should be of a sufficient concentration to minimize the volume added to the experimental bath. Sudden additions of large drug volumes may be as osmotically disruptive as those caused by sudden medium changes.

The experimenter must be careful to ensure that the concentration of the drugs added is calculated correctly. The stability of the compound must also be considered. The sensitivity of the neuronal networks means they can easily detect degradation of test substances with time. If an experimental response to a calculated drug concentration is depressed as compared to the response seen in previous experiments, a fresh stock solution should be tested. This often will restore the network responsiveness.

Solubility

Neuronal networks are bathed in an aqueous medium, a factor that complicates analysis of some test substances. Many of the cannabimimetic agents for example, are only moderately to relatively insoluble in water. The degree of solubility varies with the size of the molecule in question and the number of double bonds it contains. Compounds such as the military grade jet fuels JP-4, JP-5, and JP-8 have been tested with the networks. These hydrocarbon compounds are virtually insoluble in water. Various strategies have been employed to compensate for some of these properties. In the case of the cannabimimetics, addition of a carrier molecule such as bovine serum albumin (BSA)

is sometimes useful. Sonication for extended periods often can yield a relatively clear test solution. The aircraft fuels were tested by creating micelles, produced by sonicating a mixture of BSA, water, and fuel. This allowed the test substance to be introduced into the experimental bath, but the concentration that actually dissolved into the bath remained unknown. In the case of the cannabimimetics anandamide, methanandamide, and a related molecule palmitoyl ethanolamide, post-experimentation comparison of calculated concentrations with actual concentrations using gas chromatography/mass spectrometry revealed that the calculated concentrations were as much as 70 times higher than the concentration delivered to the neuronal network (Morefield et al., 2000). Obviously, errors of this magnitude must be resolved before responses observed in the network can be compared to those generated with other preparations.

Some compounds are soluble only in liquids such as ethanol or DMSO. For substances that must be administered in these carriers, care must be taken to minimize the amount of solvent to which the network is exposed. This means that stock solutions must be made at the highest concentration possible. Control studies must be performed to determine the response of the networks to equi-volume amounts of solvent without the test compound. Experience has shown that additions of less than 0.5% v/v DMSO or 0.3% v/v ethanol produces very little effect on network activity. For lipophilic compounds such as the cannabimimetics, reversibility of the effects may be problematic, as the compound can incorporate directly into the neuronal membrane, effectively stabilizing the concentration at an undetermined level. For experiments in which exact

quantitative data are required, as the construction of dose-response curves, this characteristic can limit the number of drug applications possible with a single network.

Additional Considerations

This work has demonstrated applications of neuronal networks in three different areas of neuroscience. As the technology for acquiring and analyzing the large data sets generated by multichannel recording matures and decreases in cost, neuronal network uses will inevitably spread beyond this laboratory. As the sophistication of life support systems and drug administration increase, the reliability of data generated by neuronal network research will also increase. The availability of a library of compound responses will allow rapid determination of novel drug mechanisms by comparing response profiles and facilitate the deployment of neuronal networks as autonomous biosensors for military and strategic protection uses. Recent work reporting the synergistic effects of the common agricultural chemicals maneb and paraquat in producing Parkinson-like symptoms in mice (Thiruchelvam et al., 2000) signals a burgeoning area of toxin evaluation that will require new, rapid approaches such as those possible with neuronal networks. The list of potential toxins is long and diverse, including the obvious, such as organophosphate pesticides, and the more elusive, such as microbial defense toxins. The potential for neuronal network applications is only beginning to be appreciated. Works such as this will help define the problems for which neuronal networks are best suited, and will highlight the limitations that current technology and experimental practices place on their immediate use outside of a laboratory setting. The most powerful demonstration of neuronal network capabilities will arise from supplementing the multichannel

electrophysiology with other techniques, including intracellular recording, Ca^{+2} imaging, and analysis of changes in expression levels induced by experimental manipulations. With adjunct methods such as these providing converging lines of evidence, neuronal networks will realize their full potential.

REFERENCES

Alger BE, Williamson A (1988) A transient calcium-dependent potassium component of the epileptiform burst after-hyperpolarization in rat hippocampus. J Physiol 399: 191-205.

Arvidsson U, Riedl M, Elde R, Meister B (1997) Vesicular acetylcholine transporter (VAChT) protein: a novel and unique marker for cholinergic neurons in the central and peripheral nervous systems. J Comp Neurol 378:454-467.

Azouz R, Jensen MS, Yaari Y (1996) Ionic basis of spike after-depolarization and burst generation in adult rat hippocampal CA1 pyramidal cells. J Physiol 492: 211-223.

Bacci A, Verderio C, Pravettoni E, Matteoll M (1999) Synaptic and intrinsic mechanisms shape synchronous oscillations in hippocampal neurons in culture. Eur J Neurosci 11: 389-397.

Ballerini L, Galante M, Grandolfo M, Nistri A (1999) Generation of rhythmic patterns of activity by ventral interneurones in rat organotypic spinal slice culture. J Physiol 517: 459-475.

Bellet, EM, Casida, E, (1973) Bicyclic phosphorus esters: high toxicity without cholinesterase inhibition, Science 182:1135-1136.

Ben-Ari Y, Khazipov R, Leinekugel X, Caillard O, Gaiarsa J (1997) GABAA, NMDA, and AMPA receptors: a developmentally regulated "menage a trios" TINS 20: 523-529.

Bowery, NG, Collins, JF, Hill, RG, (1976) Bicyclic phosphorus esters that are potent convulsants and GABA antagonists. Nature 261: 601-603.

Bracci E, Ballerini L, Nistri A (1996a) Spontaneous rhythmic bursts induced by pharmacological block of inhibition in lumbar motoneurons of the neonatal rat spinal cord. J Neurophysiol 75: 640-647.

Bracci E, Ballerini L, Nistri A (1996b) Localization of rhythmogenic networks responsible for spontaneous burst induced by strychnine and bicuculline in the rat isolated spinal cord. J Neurosci 16: 7063-7076.

Bracci E, Beato M, Nistri A (1998) Extracellular K+ induces locomotor-like patterns in the rat spinal cord in vitro: comparison with NMDA or 5-HT induced activity. J Neurophysiol 79: 2643-2652.

Brodin L, Traven HG, Lansner A, Wallen P, Ekeberg O, Grillner S (1991) Computer simulations of N-methyl-D-aspartate receptor-induced membrane properties in a neuron model. J Neurophysiol 66: 473-484.

Calton JL, Kang M-H, Wilson WA, Moore SD (2000) NMDA-receptor-dependent synaptic activation of voltage-dependent calcium channels in basolateral amygdala. J Neurophysiol 83: 685-692.

Capogna M, Gahwiler BH, Thompson SM (1996) Presynaptic inhibition of calcium-dependent and independent release with ionomycin, gadolinium, and alpha-latrotoxin in the hippocampus. J Neurophysiol. 75: 2017-28.

Casida, JE, Eto, M, Moscioni, AD, Engel, JL, Milbrath, DS, Verkade, JG (1976) Structure-toxicity relationships of 2,6,7-trioxabicyclo[2.2.2]-octanes and related compounds. Toxicol. Appl. Pharmacol. 36: 261-279

Centers, PW, (1992) Potential neurotoxin formation in thermally degraded synthetic ester turbine lubricants. Arch. Toxicol 66: 69-680.

Chapin JK, Moxon KA, Markowitz RS, Nicolelis MAL (1999) Real time control of a robotic arm using simultaneously recorded neurons in the motor cortex. Nat Neurosci 2: 664-670.

Cossette P, Umbriaco D, Zamar N, Hamel E, Descarries L (1993) Recovery of choline acetyltransferase activity without sprouting of the residual acetylcholine innervation in adult rat cerebral cortex after lesion of the nucleus basalis. Brain Res 630:195-206.

Daw NW, Stein PS, Fox K, (1993) The role of NMDA receptors in information processing. Annu Rev Neurosci 16: 207-222.

Dobrunz LE, Stevens CF (1997) Heterogeneity of release probability, facilitation, and depletion at central synapses. Neuron 18: 995-1008.

Douglas JR, Noga BR, Dai X, Jordan LM (1993) The effects of intrathecal administration of excitatory amino acid agonists and antagonists on the initiation of locomotion in the adult cat. J Neurosci 13: 990-1000.

Droge MH, Gross GW, Hightower MH, Czisny LE (1986) Multielectrode analysis of coordinated, rhythmic bursting in cultured CNS monolayer networks. J Neurosci 6: 1583-1592.

Dudel J, Schramm M, Franke C, Ratner E, Parnas H (1999) Block of quantal end-plate currents of mouse muscle by physostigmine and procaine. J Neurophysiol 81:2386-2397.

Edelman GM (1987) Neural Darwinism. Basic Books Inc. N. Y.

Emanuel PA, Dang J, Gebhardt JS, Aldrich J, Garber EA, Kulaga H, Stopa P, Valdez JJ, Dion-Schultz (2000) Recombinant antibodies: a new reagent for biological detection. Biosens Bioelectron 14: 751-759

Georgopoulos AP, Schwartz AB, Ketter RE (1986) Neuronal population coding of movement direction. Science 233: 1416-1419.

Goda Y, Stevens CF (1998) Readily releasable pool size changes associated with long term depression. Proc Natl Acad Sci USA 95: 1283-1288.

Gramowski, A, Schiffmann, D, Gross, GW (2000) Quantification of acute neurotoxic effects of trimethyltin using neuronal networks cultured on microlectrode arays. NeuroToxicology 21: 331-342.

Grillner S, Cangiano L, Hu G.-Y., Thompson R, Hill R, Wallen P (2000) The intrinsic function of a motor system: from ion channels to networks and behavior. Brain Res. 886: 224-236.

Gross GW (1979) Simultaneous single unit recording in vitro with photoetched, laser-deinsulated, gold multimicroelectrode surface. IEEE Trans Biomed Eng 26: 273-279.

Gross GW (1994) Internal dynamics of randomized mammalian neuronal networks in culture. In: Enabling Technologies for Cultured Neural Networks, Stenger, D.A. and McKenna, T.M., eds. (Academic, New York), pp. 277-317.

Gross GW, Azzazy HME, Wu M-C, Rhoades BK (1995) The use of neuronal networks on multielectrode arrays as biosensors. Biosensors and Bioelectronics 10: 553 - 567.

Gross GW, Harsch A, Rhoades BK, Göpel W (1997a) Odor, drug and toxin analysis with neuronal networks in vitro: extracellular array recording of network responses. Biosensors and Bioelectronics 12: 373 - 393.

Gross GW, Kowalski JM (1991) Experimental and theoretical analysis of random nerve cell network dynamics. In: Neural Networks, Concepts, Application and Implementation. Vol.4, Antognetti,P., and Milutinovic, V., eds. (Prentice Hall, New Jersey), pp. 47-110.

Gross GW, Norton S, Gopal K, Schiffmann D, Gramowski A (1997b) Nerve cell network in vitro: Applications to neurotoxicology, drug development, and biosensors. In: The Neuro-Electronic Interface. Cellular Engineering 2: 138-147.

Gross GW, Schwalm FU (1994) A closed chamber for long-term electrophysiological and microscopical monitoring of monolayer neuronal networks. J Neurosci Meth 42: 73-85.

Gross GW, Wen W, Lin J (1985) Transparent indium-tin oxide patterns for extracellular, multisite recording in neuronal cultures. J Neurosc Meth 15: 243-252.

Gross, GW, Norton, S, Gopal, K, Schiffmann, D., Gramowski, A (1997) Neuronal networks in vitro: applications to neurotoxicology, drug development and biosensors. Cellular Engineering 2: 138-147.

Gross, GW, Rhoades, BK, Jordan, RJ, (1992) Neuronal networks for biochemical sensing. Sensors and Actuators 6: 1-8.

Guth SL, Drescher DG (1990) Effects of divalent cations on the frequency of spontaneous action potentials from the lateral line organ of Xenopus laevis. Brain Res 508: 76-84.

Habets AM, Van Dongen AM, Van Huizen F, Corner MA (1987) Spontaneous neuronal firing patterns in fetal rat cortical networks during development in vitro: a quantitative analysis. Exp Brain Res 69: 43-52.

Harsch A, Ziegler C, Gopel W (1997) Strychnine analysis with neuronal networks in vitro: extracellular array recording of network response. Biosens Bioelectron 12: 827-835

Higgins, GM, Gardier, RW, (1990) γ-Aminobutyric acid antagonism produced by an organophosphate-containing combustion product. Toxicol Appl Pharma 105: 103-112.

Hochman S, Jordan LM, MacDonald JF (1994a) N-methyl-D-aspartate receptor-mediated voltage oscillations in neurons surrounding the central canal in slices of rat spinal cord. J Neurophysiol 72: 565-577.

Hochman S, Jordan LM, Schmidt BJ (1994b) TTX-resistant NMDA receptor-mediated voltage oscillations in mammalian lumbar motoneurons. J Neurophysiol 72: 2559-2562.

Hu B, Bourque CW (1999) NMDA receptor-mediated rhythmic bursting activity in rat supraoptic nucleus neurones in vitro. J Physiol 458: 667-687.

Isaacson JS, Hille B (1997) GABAB-mediated presynaptic inhibition of excitatory transmission and synaptic vesicle dynamics in cultured hippocampal neurons. Neuron 18: 143-152.

Jackson MB, Lecar H, Brenneman DE, Fitzgerald S, Nelson PE (1982) Electrical development in spinal cord cell culture J Neurosci 2: 1052-1061.

Johnston MV, McKinney M, Coyle JT (1981) Neocortical cholinergic innervation: a description of extrinsic and intrinsic components in the rat. Exp Brain Res 43:159-172.

Jordan, RS, (1992) Investigations of inhibitory influences in neuronal monolayer networks cultured from mouse spinal cord. MS Thesis, University of North Texas, Denton, TX.

Jung, AE, Narayanan, TK, Rossi III, J, Ritchie, GD, Valenti, P J (1995) Anatomical disposition, receptor binding and clearance of the neuroconvulsant trimethylolpropane phosphate (TMPP). The Toxicologist 15 :18-34.

Kamioka, H, Maeda, E, Jimbo, Y, Robinson, HPC, Kawana, A (1996) Spontaneous periodic synchronized bursting during formation of mature patterns of connections in cortical cultures. Neuroscience Letters 206: 109-112.

Kao, WY, Liu QY, Ma, W, Ritchie, GD, Lin, J, Nordholm, AF, Rossi III, J, Barker, JL, Stenger DA, Pancrazio JJ (1999) Inhibition of spontaneous GABAergic transmission by trimethylolpropane phosphate. Neurotoxicology 20: 843-849.

Khateb A, Fort P, Serfin M, Jones, BF, Mulethaler M (1995) Rhythmical bursts induced by NMDA in guinea-pig cholinergic basalis neurons in vitro. J Physiol 487: 623-638.

Kiehn O, Johnson BR, Rastaad M (1996) Plateau properties in mammalian spinal interneurons during transmitter-induced locomotor activity. Neuroscience 75: 263-273.

Krupka RM, Laidler KJ (1961) Molecular mechanisms for hydrolytic enzyme action: Apparent non-competitive inhibition, with special reference to acetylcholinesterase. J Am Chem Soc 83: 1445-1447.

Landmesser L, Pilar G (1978) Interactions between neurons and their targets during in vivo synaptogenesis. Fed Proc 37: 2016-22.

Lawrie AM, Graham ME, Thorn P, Gallacher DV, Burgoyne RD (1993) Synchronous calcium oscillations in cerebral granule cells in culture mediated by NMDA receptors. Neuroreport 4: 539-542.

Legendre P, Rosenmund C, Westbrook GL (1993) Inactivation of NMDA channels in cultured hippocampal neurons by intracellular calcium. J Neurosci 13: 674-684.

Lin J, Cassell J, Ritchie GD, Rossi III J (1998) Repeated exposure to trimethylol-propane phosphate induces central nervous system sensitization and facilitates electrical kindling. Physiol. Behav. 65: 51-58.

Lindsey JW, Prues SL, Alva C, Ritchie GD, Rossi III J, (1998) Trimethylolpropane phosphate (TMPP) perfusion into nucleus accumbens of the rat: electroencephalographic, behavioral and neurochemical correlates. Neurotoxicology 19: 215-226.

Llinas RR (1988) The intrinsic electrophysiological properties of mammalian neurons: insights into central nervous system function. Science 242: 1654-1664.

Lukatch HS, MacIver MB, (1997) Physiology, pharmacology, and topography of cholinergic neocortical oscillations in vitro. J Neurophysiol 77: 2427-45.

MacLean JN, Cowley KC, Schmidt BJ (1998) NMDA receptor-mediated oscillatory activity in the neonatal rat spinal cord is serotonin dependent. J Neurophysiol 79: 2804-2808.

MacLean JN, Schmidt BJ, Hochman S (1997) NMDA receptor activation triggers voltage oscillations, plateau potentials and bursting in neonatal rat lumbar motoneurons in vitro. Eur J Neurosci 9: 2702-2711.

Madison DV, Nicoll RA (1986) Actions of noradrenaline recorded intracellularly in rat hippocampal CA1 pyramidal neurones, in vitro. J Physiology 372: 221-244.

Marchi M, Raiteri M (1996) Nicotinic autoreceptors mediating enhancement of acetylcholine release become operative in conditions of "impaired" cholinergic presynaptic function. J Neurochem 67:1974-81.

Mayer ML, Vyklicky Jr L, Clements J (1989) Regulation of NMDA receptor desensitization in mouse hippocampal neurons by glycine. Nature 338: 425-427.

McGehee DS, Role LW (1996) Presynaptic ionotropic receptors. Curr Opin Neuro 1996 6: 342-349.

Menendez de la Prida L, Sanchez-Andres JV (1999) Nonlinear frequency-dependent synchronization in the developing hippocampus. J Neurophysiol 82: 202-208.

Morefield SI, Keefer EW, Chapman KD, Gross GW (2000) Drug evaluations using neuronal networks cultured on microelectrode arrays. Characteristic effects of cannabinoid agonists anandamide and methanandamide on cortical and spinal cultures. Biosens and Bioelec 15: 383-396.

O'Donovan MJ, (1999) The origin of spontaneous activity in developing networks of the vertebrate nervous system. Curr Opinion Neurobiol 9: 94-104.

Poncer JC, McKinney RA, Gahwiler BH, Thompson SM (2000) Differential control of GABA release at synapses from distinct interneurons in rat hippocampus. J Physiol 528: 123-130.

Psarropoulou C, Dallaire F (1998) Activation of muscarinic receptors during blockade of GABA(A)-mediated inhibition induces synchronous epileptiform activity in immature rat hippocampus. Neuroscience 82: 1067-77.

Raman IM, Tong G, Jahr CE (1996) β-adrenergic regulation of synaptic NMDA receptors by cAMP-dependent protein kinase. Neuron 16: 415-421.

Ransom BR, Neale E, Henkart M, Bullock PN, Nelson PG (1977) Mouse spinal cord in cell culture. J Neurophysiol 40: 1132-1150.

Rhoades BK, Gross GW (1994) Potassium and calcium channel dependence of bursting in cultured neuronal networks. Brain Res 18: 310-318.

Rioult-Pedotti MS (1997) Intrinsic NMDA-induced oscillations in motoneurons of an adult vertebrate spinal cord are masked by inhibition. J Neurophysiol 77: 717-730.

Robinson HPC, Kawahara M, Jimbo Y, Torimitsu K, Kuroda Y, Kawana A (1993) Periodic synchronized bursting and intracellular calcium transients elicited by low magnesium in cultured cortical neurons. J Neurophysiol 70: 1606-1616.

Rosenmund C, Stevens CF (1996) Definition of the readily releasable pool of vesicles at hippocampal synapses. Neuron 16: 1197-1207.

Rossi III, J, Jung, AE, Ritchie, GD, Lindsey, JW, Nordholm, AF, (1998) Tissue distribution, metabolism, and clearance of the convulsant trimethylolpropane phosphate (TMPP) in rats. Drug Metabol Dispos 26: 1058-1062.

Rouse ST, Thomas, TM, Levy, AI (1997) Muscarinic acetylcholine receptor subtype, m2: diverse functional implications of differential synaptic localization. Life Science 60:1031-1038.

Ryan TA, Reuter H, Wendland B, Schweizer FE, Tsien RW, Smith SJ (1993) The kinetics of synaptic vesicle recycling measured at single presynaptic boutons. Neuron 11: 713-724.

Ryan TA, Smith SJ, Reuter H (1996) The timing of synaptic vesicle endocytosis. Proc Natl Acad Sci USA 93: 5567-5571.

Sah P, McLachlan EM (1992) Potassium currents contributing to action potential repolarization and the afterhyperpolarization in rat vagal motoneurons. J Neurophysiol 68: 1834-1841.

Scheetz AJ, Constantine-Paton M (1994) Modulation of NMDA receptor function: implications for vertebrate neural development. FASEB J 8: 745-52.

Schiller J, Schiller Y, Clapham DE (1998) NMDA receptors amplify calcium influx into dendritic spines during associative pre- and postsynaptic activation. Nat Neurosci 1: 114-118.

Schwartz AB (1994) Direct cortical representation of drawing. Science 265: 540-542.

Smith JC, Feldman BJ (1987) In vitro brainstem-spinal cord preparations for study of motor systems for mammalian respiration and locomotion. J Neurosci Methods 21: 321-333.

Smith JC, Ellenberger HH, Ballanyi K, Richter DW, Feldman JL (1991) Pre-botzinger complex: a brainstem region that may generate respiratory activity in mammals Science 254: 726-729.

Staley KJ, Longacher M, Bains JS, Yee A (1998) Presynaptic modulation of CA3 network activity. Nature Neurosci 1: 201-209.

Stenger, DA, Pancrazio, JJ (1999) Inhibition of spontaneous GABAergic transmission by trimethylolpropane phosphate. Neurotoxicol. 20: 843-850.

Stevens CF, Tsujimoto T (1995) Estimates for the pool size of releasable quanta at a single central synapse and for the time required to refill the pool. Neurobiol 92: 846-849.

Stevens CF, Wesseling JF (1998) Activity-dependent modulation of the rate at which synaptic vesicles become available to undergo exocytosis. Neuron 21: 415-424.

Stevens DR, Kuramasu A, Haas HL (1999) GABAB-receptor-mediated control of GABAergic inhibition in rat histaminergic neurons in vitro. Eur J Neurosci 11: 114-54.

Streit, J (1993) Regular oscillations of synaptic activity in spinal networks in vitro. J Neurophysiol 70: 871-878.

Thiruchelvan M, Richfield EK, Baggs RB, Tank AW, Cory-Slechta D (2000) The nigrostriatal dopaminergic system as a preferential target of repeated exposures to combined paraquat and maneb: implications for Parkinson's disease. J Neurosci 20: 9207-9214.

Toia, RF and Casida, JE (1987) Probicyclophosphates as novel GABA antagonists. Act Mol 3: 465-468.

Tong G, Jahr CE (1994) Regulation of glycine-insensitive desensitization of the NMDA receptor in outside-out patches. J Neurophysiol 2: 754-761.

Tong G, Shepherd D, Jahr CE (1995) Synaptic desensitization of NMDA receptors by calcineurin. Science 267: 1510-1512.

Tosney KW, Landmesser LT (1985) Specificity of early motoneuron growth cone outgrowth in the chick embryo. J Neurosci 5:2336-2344.

Traub RD, Jefferys JG, Whittington MA (1994) Enhanced NMDA conductance can account for epileptiform activity induced by low Mg2+ in the rat hippocampal slice. J Physiol 478: 379-393.

Trouth CO, Millis RM, Bernard DG, Pan Y, Whittaker JA, Archer PW (1993) Cholinergic-opioid interactions at the brainstem respiratory chemosensitive areas in cats. Neurotoxicology. 14: 45-467.

van den Beukel I, van Kleef RG, Oortigiesen M (1998) Differential effects of physostigmine and organophosphates on nicotinic receptors in neuronal cells of different species. Neurotoxicology 19: 777-787.

Vincent A, Jean A, Tell F (1996) Developmental study of N-methyl-D-aspartate induced firing activity and whole-cell currents in nucleus tractus solitarii neurons. Eur J Neurosci 8: 2748-2752.

Vizi ES, Kobayashi O, Torocsik A, Kinjo M, Nagashima H, Manabe N, Goldiner PL, Potter PE, Foldes FF (1989) Heterogeneity of presynaptic muscarinic receptors involved in modulation of transmitter release. Neuroscience 31: 259-67.

von Gersdorff H, Schneggenburger R, Weis S, Neher E (1997) Presynaptic depression at a calyx synapse: the small contribution of metabotropic glutamate receptors. J Neurosci 17: 8137-8146.

Vyklicky Jr L, Benveniste M, Mayer ML (1990) Modulation of N-methyl-D-aspartic acid receptor desensitization by glycine in mouse cultured hippocampal neurons. J Physiol 428: 313-331.

Wallen P, Grillner S (1987) N-methyl-D-aspartate receptor-induced, inherent oscillatory activity in neurons active during fictive locomotion in the lamprey. J Neurosci 7: 2745-2755.

Wang L-Y, Kaczmarek, LK (1998) High-frequency firing helps replenish the readily releasable pool of synaptic vesicles. Nature 394: 384-388.

Wang X-S, Gruenstein EI (1997) Mechanism of synchronized Ca2+ oscillations in cortical neurons. Brain Res 767: 239-249.